CENTRO DE INVESTIGACION Y DE ESTUDIOS
AVANZADOS DEL INSTITUTO POLITECNICO
NACIONAL

UNIDAD ZACATENCO

Departamento de Control Automático

Análisis sísmico bidireccional y control estructural

Tesis que presenta:

M. en C. Satyam Paul[1]

Para obtener el grado de
Doctor en Ciencias

En la Especialidad de
Control Automático

Director de Tesis:
Dr. Wen Yu Liu

CENTER FOR RESEARCH AND ADVANCED STUDIES OF THE NATIONAL POLYTECHNIC INSTITUTE

UNIDAD ZACATENCO

Department of Automatic Control

Bidirectional seismic analysis and structural control

Thesis submitted by:

Satyam Paul

A thesis submitted in the fulfillment for the degree of:
Doctor of Philosophy

In the specialization of
Automatic Control

Thesis supervisor:
Dr. Wen Yu Liu

Mexico City   **November 2017**

Resumen

La protección de las estructuras civiles muy grandes y sus habitantes de desastres naturales como un terremoto es importante desde el punto de vista de la investigación y ha sido vista con gran interés a través de los años. La motivación general de este trabajo es el diseño y la validación de un sistema de control activo de vibración para estructuras civiles bajo el efecto del terremoto bidireccional, también el análisis de la velocidad del sistema.

Las entradas sísmicas bidireccionales en los edificios inducirán vibraciones acopladas a la torsión de la traducción en los edificios que son más graves con graves daños estructurales y deben tenerse en cuenta. Es un aspecto importante del sistema de control estructural detectar la respuesta de la estructura continuamente y actuar superiormente para mitigar la vibración causada por las ondas sísmicas. Un criterio más importante al diseñar un controlador es su estabilidad. Todas estas cuestiones son el factor motivador de este trabajo. La primera parte de la tesis se centra en el modelado y control de retroalimentación de estructuras de construcción inelástica. Nuestra primera contribución es el diseño del algoritmo de control PD / PID. Es el control más simple y mejor, ya que se realiza eficazmente sin el conocimiento del modelo. En la segunda parte, combinamos las clásicas técnicas de control difuso PD / PID (Proporcional-Integral-Derivativo) y tipo-2 para compensar las incertidumbres presentes en el edificio. La metodología para ajustar las ganancias de PD / PID se obtiene utilizando el teorema de estabilidad de Lyapunov y se verifica la estabilidad del sistema. El diseño de control establecido requiere cierto conocimiento del sistema para afinar las ganancias PD / PID. Así que en la parte final, sugerimos un controlador de modo deslizante discreto (FDSMC) que no necesita los parámetros del sistema. Generalmente, el control de tiempo discreto o control de muestreo es el más adecuado para el control estructural. La estabilidad del controlador propuesto se verifica utilizando el candidato de Lyapunov. La parte más crucial de nuestro trabajo es la capacidad de manejar la incertidumbre estructural mediante el esquema de adopción en línea. Como criterio importante, la estabilidad en lazo cerrado de nuestra metodología propuesta se expresa teóricamente. También hemos probado nuestros controladores para excitaciones sísmicas bidireccionales. La otra contribución de este trabajo de tesis es el desarrollo de un actuador torsional (TA) para mitigar la vibración torsional.

En el marco de este estudio, se estableció una disposición de mesa de sacudidas de dos ejes en el Departamento Control Automático de CINVESTAV-IPN. El rendimiento del controlador se valida experimentalmente en función de las características estructurales específicas de la excitación y construcción, y de las incertidumbres. Se utiliza un amortiguador de masa activa (AMD) y el actuador de torsión (TA) para generar la fuerza requerida para minimizar las vibraciones. Se usaron señales de terremoto para excitar el prototipo del laboratorio. En el estudio experimental, los controladores propuestos proporcionaron supresión significativa de la vibración.

Abstract

Safeguard of large civil structures and human residents from natural hazards such as earthquakes is very important from the research point of view andhave been seen with great interest over the years. The mainmotivation of this workis the designing and validation of anactive vibration control system for building structuresunder the effect of the bidirectional earthquake and to perform its stability analysis.

The bidirectional seismic inputs in buildings will induce translation-torsion coupled vibrations in buildings which are more severe with severe structural damage and should be taken into consideration. It is an important aspect of the structural control system to sense the response of the structure continuously and performs superiorly to mitigate the vibration caused by seismic waves. One more important criterion while designing a controller is its stability. All these issues are the motivating factor of this work. The first part of the thesis focuses on the modeling and feedback control of inelastic building structures. Our first contribution is the design of the PD/PID control algorithm. It is simple and finest control as it performs effectively without the knowledge of the model. In the second part, we combine the classic PD/PID (Proportional-Integral-Derivative) and type-2 fuzzy control techniques to compensate the uncertainties present in the building. The methodology for tuning the gains of PD/PID is obtained using Lyapunov stability theorem and the stability of the system is verified. The stated control design requires some knowledge of the system in order to tune the PD/PID gains. So in the final part, we suggested a discrete sliding mode controller (FDSMC) which does not need the system parameters. Generally, discrete-time control or sampling control is most suited for the structural control. The stability of the proposed controller is verified using Lyapunov candidate. The most crucial part of our work is the ability to deal structural uncertainty using on-line adoption scheme. As an important criterion, the closed-loop stability of our proposed methodology is expressed theoretically. Also we have tested our controllers for bidirectional seismic excitations. The other contribution of this thesis work is the development of a torsional actuator (TA) in order to mitigate the torsional vibration.

Within the framework of this study, a two-axis shake table setup was established in the Control Automatic Department of CINVESTAV-IPN. The controller performance is experimentally validated based on the specific excitation and building structural characteristics, and uncertainties. An active mass damper (AMD) and the torsional actuator (TA) are used to generate the force required to minimize the vibrations. Earthquake signals were used to excite the lab prototype. In the experimental study, the proposed controllers provided significant vibration suppression.

This thesis is dedicated to my father, mother and wife
For their endless love, support and encouragement

Acknowledgments

Contents

List of Figures

Chapter 1

Introduction

Historic studies related to earthquakes such as in 1985 Mexico City, 1994 Northridge, 1995 Kobe, 1999 Kocaeli, 2001 Bhuj, 2008 Sichuan, 2008 Chile, and 2012 Emilia expose that earthquakes have caused severe damage in civil structures all over the world. The process of modification or to control the building structures from severe damages has became a salient topic in structural engineering. The control of building structures from the hazardous earthquake waves is an area of great interest for the researchers that is growing rapidly [40][41]. The challenging part of the job lies on the protection of super structures in the whole of geographic locations from the seismic events thus providing a means of safer environment for the human occupants. The extensive damages due to an earthquake can be noteworthy and so there is utter necessity to develop an effective methods for protection.

The structural control methodology and its applications during earthquakes was first suggested by the researches more than a century ago. Although, Yao in 1972 [146] had proposed the first idea of structural control that played a major role in the advancement of the field of structural engineering, but major developments have been noticed during the last 25 years where the structures with preventive systems have been developed. In the area of structural design and its control, the following points should be taken care of:

- The pattern in which the ground and earthquake vibrates during earthquake.

- The design techniques of buildings to withstand earthquakes.

- Innovative strategies for the response control of building structures.

Passive and active control systems plays an important role in the response reduction of civil engineering structures subjected to strong seismic vibrations. Passive, active and

semi-active control systems are the most important class of structural engineering. The two techniques that can be utilized for the control of structural vibrations are:

- Implementation of smart materials in the construction of buildings [59].

- The use of control devices like actuators, dampers and isolators in the building structures [94].

A worldwide popularity and high demand of structural control and its application had given rise to various researches leading to the publication of many textbooks for example [36]. [59] had suggested different types of passive, active, semi-active, and hybrid control systems in his review paper that opens up the importance of control theory in the vibration control of structures. [40] had focused on in depth studies about active, semi-active and hybrid control devices along with some control strategies. The main factors affecting the performance of structural control can be categorized as

- Excitation criteria (e.g., unidirectional or bidirectional earthquake and winds).

- Structural characteristics (e.g., natural frequency, degree of freedom and nonlinearity in structures).

- Design of the control system (e.g., devices types and quantity, device placements, system models and control algorithm) [147].

Although the most of research has been vested on the seismic analysis considering unidirectional seismic waves, very less researches has been conducted on bidirectional seismic waves. The fact cannot be denied that the earthquake has indeed an arbitrary direction, represented by a bidirectional ground movement [30][54]. The bidirectional seismic inputs in buildings will induce translation-torsion coupled vibrations in buildings which is more severe with severe structural damage and should be taken into consideration [154]. The intensive research in the field of earthquake engineering revealed the fact that one of the prime factor of building collapse in recent times is asymmetric building structures under the grip of bidirectional seismic ground motions [90].

The active devices are capable of adding forces onto the structures. If the control forces for these active devices are generated by unstable controller then it may cause unusual vibrations to the building structure thus effecting the performance. So it is utter necessary to analyze the stability of the controller. Also it is very important to study the controllers

performance and effectivity under the effect of bidirectional forces. The bidirectional forces acting on the building will result in torsion in the building which is an important area of research and should be taken into consideration. Apart from that, the experimental verification of these controllers in mitigation of bidirectional seismic waves were not given due consideration. Hence, the implementation of a controller will be a challenging if these issues are not handled in an efficient manner. The motivation of this work is to validate the performance and abilities of the structural vibration control system by analyzing and handling the above issues in an effective manner.

1.1 Objectives

It is an important aspect of structural control system to sense response of the structure continuously and give efficient response in order to mitigate the vibration caused by seismic waves. Several types of controllers were implemented to attenuate the structural vibrations due to unidirectional earthquake. So more focus should be vested in control action involving bidirectional forces. Torsion is an important aspect in buildings under the effect of earthquake and needs to be dealt in efficient manner. The designed controller should possess the capability of measuring the response and act on the controller mechanism of the damper and actuator in order to minimize the vibrations main intention is to perform the regulation of output so as to keep the system states such as position and velocity very close to zero. An innovative and efficient control design will broaden the effectiveness of the bidirectional vibration mitigation. One more important criteria while designing a controller is its stability. The controller instability will result in the unsuitable system operation and consequently may incur significant damages to the building ultimately causing harm to humans. Another important aspect is parameter uncertainty incorporated in the buildings. So it is essential to design an innovative controller that requires minimum system parameters. Stability and robustness are the important criterion that should be taken into consideration while proposing a high-performing controller. Finally, the performance of the proposed controller should be verified under the impact of bidirectional seismic waves.

Based on the above discussions, the objectives of this thesis can be enlisted as follows:

- A need of developing a novel mechanism to control the lateral-torsional vibration due to bidirectional forces on the structure.

- To propose a high performance controller design that involves least information of

structural parameters.

- Validation of the stability of proposed controller from theoretical point of view.

- To verify experimentally the performance of the proposed algorithms and to compare the performance of the controller based on the experimental analysis in order to validate the most superior controller for the mitigation of structural vibration.

1.2   Contributions and Significance

As a result of discussions in the previous section and by giving due importance to the objectives, our first contribution is the design of the PD/PID control algorithm. It is one of the effective control as it shows its efficiency without the knowledge of the model. It is simple in nature and can be incorporated with distinct physical meanings. In the second phase of the contribution, we combine the classic PD/PID (Proportional-Integral-Derivative) and type-2 fuzzy control techniques to handle the uncertainties present in the building. The type-2 fuzzy system has effective ways to deal with knowledge uncertainty compared with classical type-1 fuzzy logic, because the type-2 fuzzy sets can deal uncertainties with more parameters and more design degrees of freedom. The main parts of the controllers are PD and PID, while the nonlinearity are compensated by the type-2 fuzzy system. So the controller possesses the advantages of PD/PID and type-2 fuzzy techniques. A method for tuning the fuzzy weights in order to reduce the regulation error is developed. Also the conditions for choosing PD/PID gains are laid down. The tuning techniques are extracted using Lyapunov stability theorem and is done to validate the stability of the entire system.

The previously mentioned control design requires the knowledge of the parameters of the structure to some extent while tuning the PD/PID gains. So in the final phase, we proposed a Fuzzy discrete sliding mode controller (FDSMC) which does not need the system parameters. In general cases, discrete-time control or sampling control is most suited for the structural control. The sampling period is considered to be the important feature that play significant role in the performance of the control system. The stability of the proposed controller is verified using Lyapunov candidate. The application of these controller to uncertain building structures is widespread.

The most crucial part of our work is the ability to deal structural uncertainty using on-line adaption scheme. Also as an important criteria, the closed-loop stability of our proposed methodology is expressed theoretically. Also we have tested our controllers for bidirectional
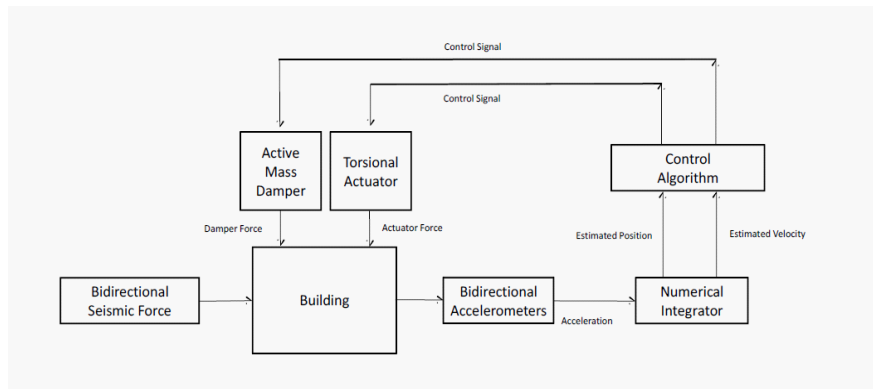
Figure 1.1: Bidirectional vibration control scheme

seismic excitations. The other contribution of this thesis work is the development of a Torsional Actuator (TA) in order to attenuate the torsion vibration which is raised due to the effect of bidirectional forces on the structure. The Torsional Actuator (TA) is a disc and motor arrangements which is placed on the centre of the structure and is controlled with the proposed controller. An additional contribution of this thesis is the state-of-the-art review [104], which presents a detailed review on various passive, semi-active and hybrid control system applied to control the translation-torsion coupled response of structure under bidirectional seismic events are portrayed in sequential manner. A detailed review paper is essential to judge about the criteria of selection of dampers,actuators and controllers. On the basis of review chapter the selection of active devices is achieved. Also PD/PID, combination of PD/PID with fuzzy and Sliding mode controller for this work has been selected on the basis of review chapter. So this chapter delivers a significant contribution on this work. Chapter 2 depicts a version of this mentioned review. The bidirectional structure vibration control system is expressed by Figure 1.1. Chapter 3 discusses the modeling of building structures under the effect of bidirectional seismic loadings. The active control algorithms of horizontal and torsional actuator are also proposed. Chapter 4 elaborates the application of PD/PID controller and its effect on controlling the movement of Active mass damper (AMD) and Torsional actuator (TA) in order to control the movement of the building under the effect of bidirectional excitations. Chapter 5 illustrates the implementation of Type-2 fuzzy to PD/PID control to deal with the uncertainties in an effective manner. Chapter 6 brings demonstrates the application of fuzzy discrete sliding mode controller in mitigating the bidirectional vibration. The final phase concludes with chapter 7 that summarizes the thesis, our contributions in the field of structural lateral-torsional vibration control and investigates

the successes as well as constraints of our methodologies.

1.3   Publications

Most contributions described in this thesis have appeared in various publications. Below are the publications:

International journals

1. S. Paul, W. Yu & X. Li, "Recent Advances in Bidirectional Modeling and Structural Control," Shock and Vibration, vol. 2016, Article ID 6275307, 17 pages, 2016.

2. S. Paul & W. Yu, "A method for bidirectional active control of structures", *Journal of Vibration and Control*, First published date: May-16-2017.

3. S. Paul & W. Yu, "Bidirectional active control of structures with type-2 fuzzy PD and PID", *International Journal of Systems Science*. (Under Review).

4. S. Paul & W. Yu, "Discrete-time sliding mode for building structure bidirectional active vibration control", *Transactions of the Institute of Measurement and Control*. (Under Review)

International conferences

1. S. Paul & W. Yu,, "Advances in Bidirectional Modeling and Structural Control, *8th International Symposium on Resilient Control Systems*, Philadelphia, USA, pp. 23-28, 2015.

2. S. Paul & W. Yu,, " Stable Active Vibration Control of Building Structure Subjected to Bidirectional Earthquake, *13th International Conference on Electrical Engineering, Computing Science and Automatic Control (CCE16)*, Mexico City, Mexico, 2016.

3. S. Paul & W. Yu, Intelligent Techniques for Bidirectional Structural Health Monitoring, *5th International Conference on Mechatronics and Control Engineering (ICMCE16)*, Venice, Italy, 52-56, 2016.

4. S. Paul & W. Yu, Bidirectional Fuzzy PD Control for Active Vibration Control of Building Structure, IEEE International Conference on Industrial Technology (ICIT 2017), Toronto, ON, Canada, 2017.

5. S. Paul & W. Yu,Type-2 fuzzy PID for active control of bidirectional structures, *14th International Conference on Electrical Engineering, Computing Science and Automatic Control (CCE17)*, Mexico City, 2017.

Chapter 2

Vibration Control

This chapter provides an overview of control of structures under bidirectional seismic waves. It focuses on different types of bidirectional control devices, control strategies, and bidirectional sensors used in structural control systems. It also highlights the various issues like system identification techniques, the time-delay in the system, estimation of velocity and position from acceleration signals, and optimal placement of the sensors and control devices. The importance of control devices and its applications to minimize bidirectional vibrations has been illustrated. Finally, the applications of structural control systems in real buildings and their performance have been illustrated.

2.1   Structural control devices

Vibration suppression in appropriate quantity can prevent the structures from fracture or collapse. Some devices play this suppression role to prevent the structure from damages. The control devices, such as actuators, isolators and dampers, are installed to suppress the external vibrations. These structural control devices are getting more popularity and attention along with their applications in building structures. The structural control devices for the seismic hazards can be categorized as passive, active, hybrid, and semi active [123]. In last two decades, the active, semi active and hybrid control are paid more attentions than the passive devices [122]. The conception and characteristic of the structural control devices for bidirectional seismic waves are illustrated below.

2.1.1   Passive devices

A passive control device is incorporated to a structure. It modifies the stiffness or the damping of the structure in an suitable way. The passive control system does not require an external power source for its operation. It generates control force opposite to the motion of controlled structured system [92]. The passive systems can be divided into two basic categories: 1) base isolation systems; 2) energy dissipation systems.

There are many passive control devices, for example viscoelastic dampers, tuned mass dampers, frictional dampers, tuned liquid dampers, and base-isolation systems [121]. The principal function of a passive energy dissipation system is to reduce the inelastic energy dissipation demand on the framing system of a structure [27].

The forces of the passive control devices solely dependent on the structural motion. They can be expressed as [147]

$$f_i(t) = -c_i \dot{x}_{di}(t) \tag{2.1}$$

where $\dot{x}_{di}$ is relative velocity across ith device, c_i is the damping coefficient associated with the ith device.

Additionally we use the next section to describe some famous dampers for the bidirectional control.

The tuned mass damper (TMD) is considered to be an energy dissipation system, although the primitive concept of this system is not to dissipate energy. It transfers the energy from the building structure to the tuned mass dampers (absorbers).

The basic principle of TMD is to obtain optimal damping parameters, in order to control the displacement of an undamped system subjected to a harmonic force [53]. The coupled lateral-torsional motions under seismic excitations are exhibited by the building structures with intended eccentricities between their mass and stiffness centers.

In [35], investigation of tuned mass dampers in arrangements termed as coupled tuned mass dampers (CTMDs) were carried out, where translational springs and viscous dampers are used to connect mass in an eccentric manner. The CTMD works in coupled mode that includes lateral and rotational vibration. This technology is utilized to control coupled lateral and torsional vibrations of asymmetric buildings. The results revealed that CTMDs are more effective and robust in controlling coupled lateral and torsional vibrations of asymmetric buildings.

In [143], Multiple tuned mass dampers(MTMDs) was proposed with distributed natural frequencies. The several researches had been carried out to establish the effectiveness of mul-
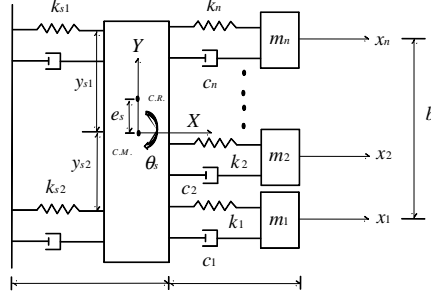
Figure 2.1: The multiple tuned mass damper(MTMD)

tiple tuned mass dampers and it had been verified that MTMDs had advantages over single TMD. A multiple tuned mass damper(MTMD) system is shown in Figure 2.1.It consists of a main system, which has n tuned mass dampers with different dynamic characteristics. The main system is subjected to a lateral force. The main system and each TMD vibrate in the lateral direction. Due to torsional coupling, the main system has torsional vibration. The total degrees-of-freedom of the combined system is $n + 2$.

Two uncoupled frequency parameters of the main system are defined by

$$w_{sxy} = \sqrt{\frac{K_{sxy}}{m_{sxy}}}, w_\theta = \sqrt{\frac{K_\theta}{m_{sxy}r_S^2}}, J_0 = m_{sxy}r_S^2, m_{sxy} = \begin{bmatrix} M_x & 0 & 0 \\ 0 & M_y & 0 \\ 0 & 0 & J_0 \end{bmatrix}, K_{sxy} = \begin{bmatrix} K_{xx} & 0 & -K_{x\theta} \\ 0 & K_{yy} & K_{y\theta} \\ -K_{x\theta} & K_{y\theta} & K_{\theta\theta} \end{bmatrix}$$

(2.2)

where m_{sxy} is the mass of the main system, K_{sxy} is the main system lateral stiffness, K_θ and r_S are the torsional stiffness and radius of gyration respectively related to the main system about the center of mass, J_0 is the polar moment of inertia related to the story. Radius of gyration refers to distribution of the components of an object around an axis. It is the perpendicular distance from the axis of rotation to a point mass that gives an equivalent inertia to the original object.

Tuned liquid column damper(TLCD) have uniform cross-section with U shaped tube attached. The schematic view has been shown in Figure 2.2. The vibrational energy from the structure is transferred to the TLCD liquid via the movement of the rigid TLCD container thus stimulating the TLCD liquid.

In [82], the methodology of vibration control of eccentric structures using TLCD mod-
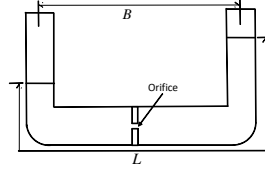
Figure 2.2: The tuned liquid column damper

eled as torsionally coupled multi-story shear structures which is under the grip of multi
dimensional seismic excitations has been investigated. For a multi-story eccentric model
with TLCD arrangements where O, S and M being the geometry, stiffness and mass centers
respectively, with:

    u, v denoting floor translational displacement along x axis and y axis respectively and

    θ denoting the rotational angle about vertical z axis

The equation of motion along $x-$direction and $y-$direction are illustrated by equation
(2.4) and (2.5)

$$m_h\ddot{h} + c_h\dot{h} + k_h h = -\rho A_h B_h \left[\ddot{x}_l + \ddot{u}_g - l_{vh}(\ddot{\theta}_l + \ddot{\theta}_g)\right] \tag{2.3}$$

$$m_s\ddot{s} + c_s\dot{s} + k_s s = -\rho A_s B_s \left[\ddot{y}_l + \ddot{v}_g + l_{us}(\ddot{\theta}_l + \ddot{\theta}_g)\right] \tag{2.4}$$

where, $m_h = \rho A_h L_h, m_s = \rho A_s L_s, c_h = \frac{1}{2}\rho A_h \xi_h \left|\dot{h}\right|, c_s = \frac{1}{2}\rho A_s \xi_s \left|\dot{s}\right|, k_h = 2\rho A_h g, k_s = 2\rho A_s g$, where m_h, c_h and k_h are the mass, damper and stiffness respectively of TLCD in
$x-$direction, m_s, c_s and k_s are the mass, damper and stiffness respectively of TLCD in
$y-$direction.

Natural frequencies are $\omega_h = \sqrt{\dfrac{k_h}{m_h}} = \sqrt{\dfrac{2g}{L_h}}, \omega_s = \sqrt{\dfrac{k_s}{m_s}} = \sqrt{\dfrac{2g}{L_s}},$
and $\rho =$Liquid Density,ξ_h and ξ_s are damping ratios related to TLCD, h and s are the
displacements of liquid in the TLCD of u and v directions.

    L_h and L_s, B_h and B_s, A_h and A_s are the notations for length, width and cross sectional
area respectively of the liquid in two TLCDs.

Coordinate position of the TLCDs in $x-$direction are represented by l_{uh} and l_{vh}. Coordinate position of the TLCDs in y-direction are represented by l_{us} and l_{vs}.
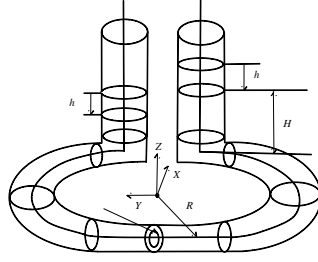
Figure 2.3: The circular tuned mass damper(CTLCD)

$\ddot{u}_g, \ddot{v}_g$ and $\ddot{\theta}_g$ are the ground seismic acceleration along u, v and θ directions. $\ddot{x}_l, \ddot{y}_l$ and $\ddot{\theta}_l$ are the accelerations of the ith floor along x, y and θ directions.

The circular tuned liquid column damper (CTLCD) is shown in Figure 2.3. This advance control device is highly responsive to the torsion. CTLCD can be applied for both torsional vibration and torsionally coupled vibration. The effectiveness of CTLCD for the structural torsional response are studied by [56]. Stochastic vibration theory is applied to identify the optimal parameters of CTLCD in [77].

The motion equation of CTLCD is given by [60]

$$\rho A(2H + 2\pi R)\ddot{h} + \frac{1}{2}\rho A\xi \left|\dot{h}\right| \dot{h} + 2\rho Agh = -2\rho A\pi R^2(\ddot{u}_\theta + \ddot{u}_{g\theta}) \tag{2.5}$$

where R is the radius of the horizontal circular column, $\ddot{u}_\theta$ is the structures torsional acceleration, $\ddot{u}_{g\theta}$ is the torsional acceleration of ground motion.

In [54], a new type of control device termed as tuned liquid mass damper (TLMD) was presented in order to control the torsional response of building structures subjected to bidirectional earthquake waves. The mass of TLMD includes both TLCD tank and the liquid in the tank. The stiffness is compensated by natural rubbers. The main working concept of TLMD is to operate a TLCD in one direction, and run a TMD in the other orthogonal direction, see Figure 2.4.

The stiffness of TMD, and the liquid high are determined as

$$k = m(2\pi f_m)^2, \quad L = \frac{2g}{(2\pi f_L)^2} \tag{2.6}$$
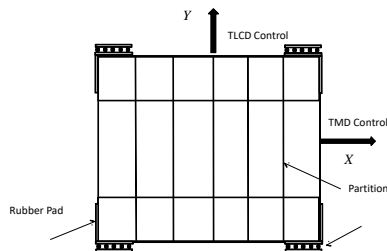
Figure 2.4: The tuned liquid mass damper

where m and f_m are the mass and the tuned frequency in the TMD control direction, g and f_L are the gravity acceleration and the tuned frequency of TLCD.

Tuned Liquid Column Dampers (TLCDs) are a special type of TLDs that depends on the motion of a column of liquid in a U-tube like container to neutralize the forces acting on the structure. The introduction of the damping factor is done in the oscillating liquid column through an orifice in the liquid passage. The damping, however unlike TMDs, is amplitude dependent, and thus the TLCD dynamics are associated with non-linearity. On the other hand, circular Tuned Liquid Column Dampers (CTLCD) is very much active when exposed to torsional response. As the earthquake is practically multi-dimensional, the torsionally coupled vibration factor cannot be ignored and so CTLCD is much favored in this case.

In [43], the control performance of the novel sealed, torsional tuned liquid column gas damper (TTLCGD) in order to minimize the coupled flexural torsional response of plan-asymmetric buildings under the grip of seismic loads has been discussed. The analysis of technique associated, reveals that TTLCGD is an effective control device in suppressing the time-harmonic excitation and the earthquake response.

2.1.2   Active devices

The main drawback of the passive control devices is that they cannot adapt the change of the natural frequency caused by the structural nonlinearity and huge seismic excitations, especially for multiple floor buildings [40], although multiple and tuned dampers can be applied for different frequencies.

Since 1970s, remarkable progress has been made in the field of active control of civil engineering structures subjected to natural forces such as winds and earthquakes [122]. The
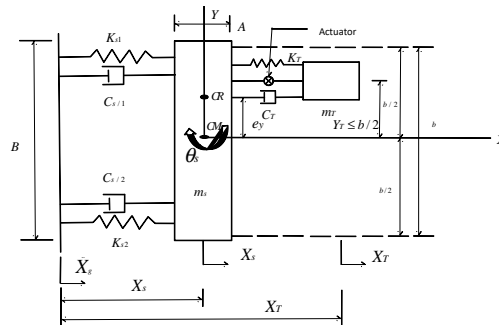
Figure 2.5: The active tuned mass damper for a 2-DoF structure

active structure control modifies the structural motion by some external forces. Topics covered on active structural control can be found in [33]. Compared with the passive devices, the active systems have the following advantages [121]:

1. Motion control can be achieved with greater effectivity.

2. In account of ground motions, it is relatively insensitive.

3. It can be applied to the multi-hazard remission circumstances.

4. Control objectives can be selected flexibly.

In order to control actively, the external excitations and inner structural responses are needed. These measured information are sent to the control algorithm to generate desired control forces. So the active devices usually use displacement sensors.

The active tuned mass damper (ATMD) uses control strategy to improve the tuned mass damper (TMD). It improves the effectiveness in minimizing the structural response [26]. As the proof of [19], the qualities of TMD can be enhanced by introducing an active force between the structure and the TMD. ATMD methodology can be also regarded as a modification version of ATMD, robustness version of TMD.

The active controller should be able to absorb the translation-torsion coupled vibrations. Besides the translational vibrations, the torsional vibrations under the seismic waves also affect the performance of ATMD. An asymmetric structures is under the coupled lateral–torsional responses is discussed in [81]. The lateral displacement of asymmetric structures and the optimum parameters incorporated in ATMD are shown by a two- degree-of-freedom(2-DoF) structure, see Figure 2.5.

The mathematical expression of the ATMD active control force that is generated is

$$U(t) = -m_t\ddot{x}_s - c_t[\dot{x}_T - (\dot{x}_s + y_T\dot{\theta}_s)] - k_t[x_T - (x_s + y_T\theta_s)] \tag{2.7}$$

where, m_t is the feedback gain of acceleration associated with asymmetric structure, c_t is the feedback gain of the velocity of the ATMD, k_t is the feedback gain of the displacement of the ATMD.

In [145], a new performance index for active vibration control of three-dimensional structures was proposed. To analytically proof the existence of the proposed performance index, a six story three-dimensional structure is taken into consideration as an example with a fully active tendon controller system implemented in one direction of the building. The building under analysis is modeled as a structure made up of members joint by a rigid floor diaphragm in a manner so that it has three degrees of freedom at each floor, lateral displacements in two perpendicular directions and a rotation with respect to a vertical axis for the third dimension.

2.1.3   Semi-active devices

Semi-active control devices are regarded as controllable passive devices. The main objective of these devices is saving control resources. The actuators of the semi-active control do not add mechanical energy to the structure directly. The power break down semi-active control system offers some degrees of protection with the help of embedded passive components.

The semi-active devices take the advantages of the passive and the active control. It requires less power than the active control devices. They can even be operated by the battery in the case of power failure during the seismic event [122]. They perform significantly better than passive devices. An exhaustive review on the semi-active devices is proposed in [123].

The magnetorheological (MR) damper is the most popular semi-active damping device. It works on the magnetorheological fluid and is controlled by a magnetic field. Generally, the magnetic field is produced by electromagnet. It requires minimal power for its operation. The suspended minute iron particles in a base fluid are termed as MR fluids. This type of liquids have the capability of changing from free flowing linear viscous state to semi-solid state with controllable yield strength under a magnetic field.

The result of uncovering the liquid to a magnetic field is the particles use the form of chains. These chains obstruct the flow and solidifies the fluid in a span of milliseconds. The stress is directly proportional with the magnitude of the applied magnetic field [69]. The
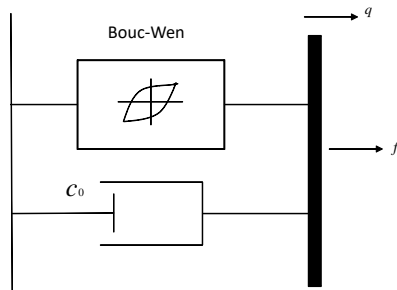
Figure 2.6: Simple mechanical model of MR

behavior of MR fluid can be simulated by the Bingham plastic model, which is an extension of the Newtonian flow. The other way of determining the behavior of MR fluid is to analyze the yield stress of the fluid. The total stress is given by [144]

$$\tau = \tau_y sgn(\dot{\gamma}) + \eta\dot{\gamma} \tag{2.8}$$

where τ_y is the yield stress induced by the magnetic field, $\dot{\gamma}$ is the shear rate, η is the viscosity of the fluid.

The application of MR damper to control the torsional and torsionally coupled responses subjected to bidirectional seismic waves is investigated in [150]. The MR damper contributes significantly in the field of civil engineering. The simple mechanical model of MR is shown in Figure 2.6. In [148], a prototype shear-mode MR damper is proposed.

The governing force f generated by MR device is

$$f = c_o\dot{q} + \alpha z$$
$$\dot{z} = -\gamma\,|\dot{q}|\,|z|\,|z|^{n-1} - \beta\dot{q}\,|z|^n + A\dot{q} \tag{2.9}$$

where q is the device displacement, z is the evolutionary variables that keeps track of the response history dependence, γ, β, n, and A can control the linearity in the unloading and the smoothness of the transition from the pre-yield to the post-yield region.

2.1.4   Hybrid devices

Hybrid base isolation(HBI) had been a matter of interest for a number of researchers due to its effectivity and consists of a passive base isolation system combined with a control actuator to generate the effects of the base isolation system. Several research on base isolation system
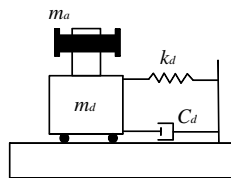
Figure 2.7:   HMD system installed in Nth floor

have been carried out and installed in several structural engineering projects due to its positive attributes like simplicity, reliability, and effectiveness.

In [4], the application of Hybrid mass damper (HMD) system consisting of tuned mass damper and active mass damper to control torsionally coupled building structures under bidirectional seismic force was proposed. In this context, the fuzzy logic controller is used to control the HMD system. Complex structural systems have non-linearities and uncertainties in both the structural properties and the magnitude of the loading. Thus, it is difficult to derive and identify an appropriate and accurate dynamic model for designing the traditional controller. An intelligent controller can be designed without specifying a very precise and accurate dynamic model of the structure. Such an intelligent controller has been introduced, using a fuzzy logic control system. The schematic view is shown in Figure 2.7

The equation of motion for HMD system installed in N-story building is given by equation (2.10)

$$M_h \ddot{u}_h + C_h \dot{u}_h + K_h u_h = -M_h P_h \ddot{u}_{aN} + K_h P_c u_c \qquad (2.10)$$

where, the mass, damping and stiffness matrices of the HMD system are M_h, C_h and K_h respectively. u_h is a vector of displacements of the HMD system relative to the Nth floor. P_h and P_c are position vectors of the absolute acceleration of Nth floor, $\ddot{u}_{aN}$ and control command vector u_c, respectively

Kim and Adeli, 2005 [71] had investigated hybrid damper-TLCD control system to control 3D coupled irregular buildings subjected to bidirectional seismic waves. Simulation results for control of two multi-story moment resisting space steel structures with vertical and plan irregularities show clearly that the hybrid damper-TLCD control system significantly reduces
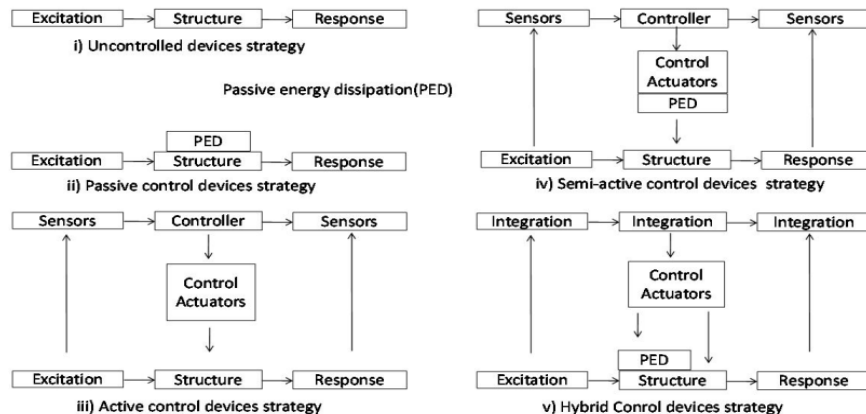
Figure 2.8: Comparision of control devices

responses of irregular buildings subjected to various earthquake ground motions as well as increases reliability and maximum operability during power failure.

The comparison between uncontrolled, passive control, active control, semi-active control and hybrid control devices are demonstrated by Figure 2.8 below[122]:

2.2 Vibration control

The appropriate design of a controller is utter necessary so that it can send essential control signal to the control devices in order to reduce the structural responses. The main strategy involved within the control scheme to prevent the collapse of building structures under bidirectional seismic waves is to control the coupled translation-torsion response of the building structures[11, 47, 87, 155]. In this section, various control strategy on the basis of various techniques is presented. The main object of the bidirectional control is to change the coupled translation-torsion response of the building structure, in order to prevent the collapse of building under bidirectional seismic waves [118]. Robustness, fault tolerance, simplicity and realiziablilty criteria are considered [127].

2.2.1 Time delay problem in vibration control

Time delay from the measurement to the actuator is a limit for vibration control. The control loop includes vibration data measurement, data filtration, control algorithm, data

transmission, and actuation. The control loop has also phase shift by time delay [7]. The time delay may cause instability in the closed-loop [126].

The motion equation of n-DoF structure with time delay t_d is

$$M\ddot{x}(t) + C\dot{x}(t) + Kx(t) = \Gamma u(t - t_d) - M\Lambda\ddot{x}_g(t) \tag{2.11}$$

If t_d is the fixed, the Laplace form transformation is

$$F_d(s) = e^{-st_d}(g_1 s + g2) \tag{2.12}$$

A review on time-delay compensation methods can be found in [3].

2.2.2   Optimal placement

The proper placement of sensing and control devices is an important research field of structural control. It results the measurement and control operation effectively. It also affects the controllability and observerability of the controlled system [8][100].

In [48], the location performance index of the actuator and sensor are presented, which can be computed by the Hankel singular values γ_{wz}^2 and γ_{uy}^2

$$k^2 = \frac{(\gamma_{wz}^2)^T \gamma_{uy}^2}{\left\|\gamma_{wz}^2\right\|_z \left\|\gamma_{uy}^2\right\|_z} \tag{2.13}$$

where k is the non-negative correlation coefficient, γ_{wz}^2 and γ_{uy}^2 denotes the Hankel singular values of the transfer function G_{wz} and G_{uy}, u and w represents the input to the system, y and z represents the output of the system.

In [10], the placing of the sensor at the center of mass is suggested. The proposal validated that the center of mass may not be good for the sensor position. Arbitrary arrangement of sensors is better subjected to bidirectional seismic motion. In [41], a detailed survey on the optimal placement of control devices was presented. In [135], energy dissipation was utilized to analyze the position of the controller, in order to minimize translation-torsion coupling effects. It suggests the locations which are nearby to the geometric centre of the structure can minimize the torsional effect.

2.2.3   Linear controllers

The working principle of PID controller is based on the feedback error e(t) which is otherwise used to calculate the required control force. In case of a structural applications if the desired

state is in the equilibrium position then the reference signal is considered to be taken as zero. The principle of PID control is to use the feedback error $e(t)$, which is the difference between the output signal $y(t)$ and the reference signal $r(t)$.Once the error is calculated, the main aim of the controller is to minimize the error for the next iteration process by carefully manipulating the inputs. It has the following form

$$u(t) = K \left[e(t) + \frac{1}{T_i} \int e(t)dt + T_d \frac{de(t)}{dt} \right]. \tag{2.14}$$

where K is the proportional gain, T_i is the integral time, T_d is the derivative time, $e(t) = r(t) - y(t)$. PID control is a negative feedback algorithm. It can force $e(t)$ to zero. It is the most popular industrial controller.

A comparison between a sliding mode control and PID control for the structural system is investigated by [50]. In [133], the effects of measure seismic waves on a six-story asymmetric structural model compiled with frictional dampers was investigated. The methodology deals with the control of torsional response of asymmetric structures and to obtain a lower level of torsional balance by arranging empirical centre of balance (ECB) of the structure at same distance from the edges of the building plan. The axial displacement of each actuator is controlled using a conventional PID-controller. In this research, frictional dampers proved its effectiveness of controlling lateral-torsional coupling of torsionally flexible as well as stiff structures.

The most important optimal controllers are the linear quadratic regulator (LQR) and linear quadratic Gaussian (LQG) control. The equation of motion can be exhibited in the form mentioned below-

$$\dot{X} = Ax + Bu \tag{2.15}$$

where the state and input system matrices are A and B respectively. The LQR algorithm calculates a control law u in the form of criteria of performance or cost function

$$J = \int_0^\infty (x_{ref} - x(t))^T Q(x_{ref} - x(t)) + u(t)^T Ru(t)dt \tag{2.16}$$

is minimal. The design matrices Q and R takes back the compensation on the deviations of state variables from their set point and the control actions, respectively.

The increase in elements of Q results in the increase of cost function, the compensation associated with any track change from the desired set point of that state variable, and thus

the specific control gain will be larger. The increase in R matrix results in a larger penalty that is applied to the audacity of the control action, and the control gains are uniformly decreased.. The feedback gain of the optimal control is computed by minimizing a cost function $J = J(z, t, u(t))$ [7]

$$J = \lim_{\tau \to \lambda} \frac{1}{\tau} E \left[\int_0^\tau \left\{ y_r^T Q y_r + f^T R f \right\} dt \right] \tag{2.17}$$

In [149], a semi-active control to the coupled translational and torsional vibration of a 2-story asymmetric building subjected to seismic excitations was presented. A LQG controller is involved as a nominal linear controller, considering the ground acceleration with white noise. The LQG controller is given by

$$\hat{z} = (A - LC)\hat{z} + Ly_m + (B - LD)f_m, f_c = -K\hat{z} \tag{2.18}$$

where L is the state estimator gain matrix, K is the LQR gain matrix.

In [20], active isolation was implemented and conducted experiments in order to verify the behavior of seismically excited buildings under multidirectional earthquake force. Active isolation technique works in combination with base isolation system and controllable actuators. The base isolation methodology offers effective approach in reducing interstory drifts and floor accelerations that works in phase with the adaptive nature of the active system in order to generate higher level performance against wide range of earthquakes. In this methodology, LQG control steps are obtained using LQR and Kalman estimator. The optimal control gain is achieved using the following-

$$u(t) = -K\bar{x}(t), \tag{2.19}$$

where K is optimal control gain with respect to the states of the augmented system.

In [71], the control of 3D coupled irregular buildings subjected to bidirectional seismic waves was investigated. To find the optimal control forces, a wavelet based algorithm involving optimal control is utilized. It has been suggested in their work that LQR or LQG algorithm can be use as a control algorithm for the feedback controller as per the investigation mentioned [121, 1, 25]

In [37], a sequential optimal control for serially connected isolated structure subjected to bidirectional earthquake was suggested. Sequential control algorithm has inherent capabilities to construct control objective function under bidirectional earthquake situations. The objective function which is in quadratic form can be illustrated as in equation (2.40)

$$J = \int_{t_0}^{t_f} \left[\frac{1}{2} \{X(t)\}^T [Q] \{X(t)\} + \{f_c(t)\}^T [R] \{f_c(t)\} \right] \tag{2.20}$$

weighted matrices are Q and R represents structure response and control force.

x,y structural response is contained in $X(t)$, t_0 = control starting time, t_f = control conclusion time.

The mathematical expression of sequential optimal control is depicted by the equations (2.21), (2.22) and (2.23)

$$\{f_c(t_A)\} = - [R]^{-1} [B]^T \{\lambda(t_A)\} \tag{2.21}$$

$$\{\dot{\lambda}\} = - [A]^T \{\lambda\} - [Q] \{X\}, \{\lambda(t_f)\} = 0 \tag{2.22}$$

$$\{\dot{X}\} = [A] \{X\} + [B] \{f\}_c + \{E\} \ddot{U}_g^T \tag{2.23}$$

where t_A =current time, The domain is expressed in $[t_A, t_f]$, The value of λ can be computed directly.

The result of the entire analysis was in the favor of the algorithm being not only an effective measure to control the bidirectional horizontal response of earthquake but also reducing the isolation layer movement by large extent.

In [24], the lateral-torsional earthquake response control of two single-story asymmetric plan buildings associated with multiple magnetorheological (MR) dampers was investigated. The desired control forces are generated using LQR technique. The damper forces are extracted using the method of least square minimization.

In [152], the responses related to seismic and harmonic waves for a true free-plan tall building equipped with two tuned pendular inertial masses (TMs) and magnetorheological (MR) dampers was investigated. The technique of LQR strategy is considered as a benchmark in order to compare the performance with the proposed physical controller. A 21 stories reinforced concrete structure building is investigated of typical story height of 3.6 m with total height of 90m. In the transverse y-direction, the building being more flexible, there is existence of lateral torsional coupling. As a result, two pendular TMs, one along the flexible edge and one along the stiff edge of the building were designed and built on the 21st story. The controller used in this investigation is quite similar to the LQR controller which was implemented to control TM-MR damper.
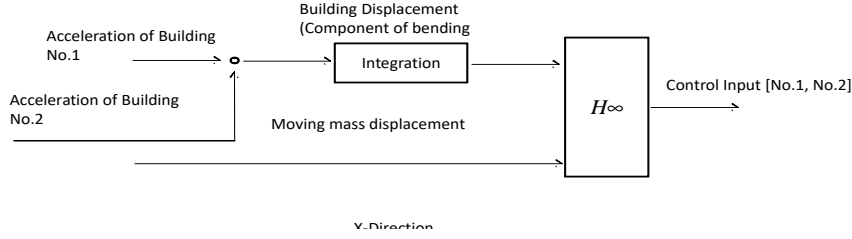
Figure 2.9: X-Direction

H∞ control methodology has been relied as and effective approach in structural vibration control which is classified as linear robust control. This scheme is unresponsive to the disturbances and parametric differences and so it is most preferred for multiple input multiple output(MIMO) type structural control systems [132]. Design method of H∞control system and its effectiveness was presented by [44]. The analysis was carried out on 23-storey building in Tokyo using a pair of hybrid mass dampers. Bidirectional seismic excitations was considered during the investigation. The control technique was established by taking into consideration x-direction and y-direction separately. The bending component of the vibration was controlled along x-direction only while along the y-direction, control of bending and torsion are considered. The scheme of the control system is shown in Figure 2.9 and 2.10

H∞control theory was applied to design the controller on the basis of reduced order model depicted in (2.24) and (2.25)

$$\dot{x}_r = A_r x_r + B_r u + D_r w \tag{2.24}$$

$$y = [\xi_1 + l\xi_3 z]^T = C_r x_r \tag{2.25}$$

The designed controller should follow the following inequality
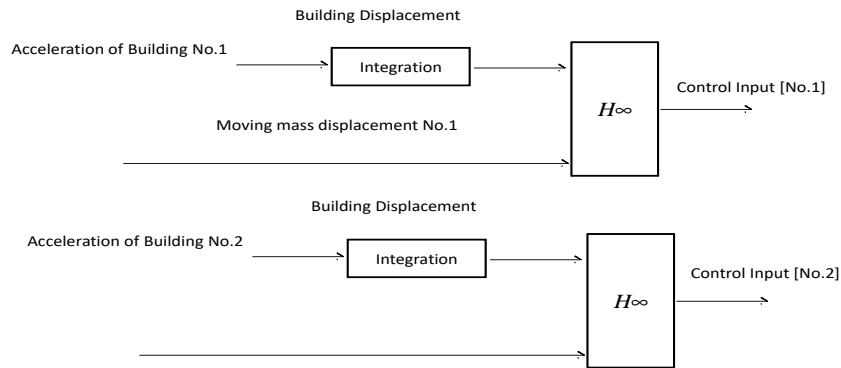
Figure 2.10: Y-Direction

$$\left\| \begin{array}{c} W_1(s)N(s) \\ W_2(s)M(s) \end{array} \right\|_{\infty} < 1 \tag{2.26}$$

where $N(s)$ and $M(s)$ means the transfer function from external input to control input and from external force to output, respectively.

The controller were installed and then the vibration tests are performed. These test results suggested that the control action generated was effective and as per the design.

In [79], the use of a robust optimal H∞control for the two AMD systems was elaborated. The AMD system was placed on the top of the unsymmetrical building for the vibration control. The building was subjected to bidirectional seismic excitations. The H∞control uses the technique of LMI-based solution blended with robustness specifications. In this paper, the efficient and necessary control forces are determined and then optimized using H∞control via LMI as illustrated in (2.27)

For an uncertain structural system-

$$(M + \Delta M)\ddot{v} + (C + \Delta C)\dot{v} + (K + \Delta K)v = (M + \Delta M)Ew(t) + B_s u(t) \tag{2.27}$$

where, $\Delta M, \Delta K, \Delta C$, and ΔBs are corresponding disturbances.

The bound condition satisfied by ΔM, is given by, $\|\Delta M M^{-1}\| \leqslant \|\delta\| \leqslant 1$,

Then using the above criteria, the state space equation can be written as

$$\dot{Z}(t) = (A + \Delta A)Z(t) + (B + \Delta B)u(t) + Hw(t) \tag{2.28}$$

Considering linear time invariant criteria for the above state space equation, the performance index is given by

$$J = \int_0^\infty (Z^T(t)QZ(t) + u^T(t)Ru(t))dt \tag{2.29}$$

where $Q \geqslant 0$ and $R > 0$ are weighted matrix

H∞ direct output feedback control of buildings under bidirectional acceleration considering the effects of soil-structure interaction was investigated by [89]. In the investigation, the tendon displacement vector of feedback control with direct approach was found to be as depicted by

$$U(t) = GY(t) \tag{2.30}$$

Where, G is a time-invariant feedback gain matrix of $4xs$.

H∞ control algorithm was used to find the entries of G matrix.

2.2.4   Nonlinear controllers

Sliding mode control

The sliding mode control (SMC) is designed for uncertain nonlinear systems [132]. It is effective in terms of robustness against the changes in the parameters and external disturbances. It has been successfully applied for structural control [97].

The control action of sliding mode control is

$$u(\hat{v}_c, t) = u_{eq}(\hat{v}_c, t) - \rho sgn(\sigma(\hat{v}_c)) \tag{2.31}$$

where, u_{eq} is the linear part of control force, $\sigma(\hat{v}_c)$ is the sliding surface, ρ is the control gain.

In [64], SMC is used to control bending and torsional vibration of a six-story flexible structure. The controller takes into accounts two conditions:

1) controller design considering only nonlinear control inputs

The dynamic system and the switching function are given by

$$\dot{x}(t) = Ax(t) + Bu(t) \tag{2.32}$$

$$y(t) = Cx(t) \tag{2.33}$$

$$\sigma(t) = Sy(t) \tag{2.34}$$

where $S =$ Switching hyperplane.

The controller has the following nonlinear form

$$u(t) = -K_{nt}(SCB)^{-1}\frac{\sigma(t)}{\|\sigma(t)\|} \tag{2.35}$$

also, $K_{nt} =$ Scalar coefficient and $SCB =$ Multiplication factor of the matrix S, C and B.

2) Controller design considering nonlinear and sub-equivalent control inputs.

The controller has the following nonlinear form

$$u_{nt}(t) = -K_{nt}(SCB)^{-1}\frac{\sigma}{\|\sigma\|} \tag{2.36}$$

Also,

$$u = u_t + u_{nt} \tag{2.37}$$

The inputs of sliding mode control are designed as the combination of linear and nonlinear inputs.

Sub-equivalent control inputs can be generated from the solo measured outputs as given below:

$$u_t = u_{eq} = -k_{eq}y \tag{2.38}$$

Where $k_{eq} =$ Scalar equivalent

The important feature of SMC is robustness under the uncertainties and disturbances. Lyapunov stability theory is implemented to prove the system stability in [97]

Neural network based structure control

A neural network (NN) is characterized by: 1) an area which consists of number of neurons along with their interconnections and layers; 2) its technique of implementing the weights on the connections and is termed as learning algorithm. In [49], a neural network based emulator computes the response of a 2D frame structure involving 3-story building. The feedforward multilayer perceptron with the backpropagation algorithm is used in [127] for structure control. [66] presents a wavelet neural network (WNN) based active non-linear controller for a 3D buildings subjected to seismic excitation in both x and y directions.

The combination of NN with the classical control theory yields better control results than conventional controllers [13, 70]. The hybrid intelligent control algorithm applied to semi-active control of the magnetorheological (MR) damper is presented in [79]. It is subjected to bidirectional seismic wave.

The training data for structure usually need to be normalized into $[0, 1]$

$$\bar{N}_i = \frac{2(N_i - N_{i,\min})}{N_{i,\max} - N_{i,\min}} - 1 \tag{2.39}$$

where N_i is the input component, its domain is $(N_{i,\min}, N_{i,\max})$

In [125], a direct adaptive neural controller subjected to bidirectional earthquake inputs was presented. Both the system parameters and the nonlinear estimation of force have uncertainties, which can be canceled by the adaptive controller.

The control law is

$$F_c^*(k) = \bar{G}(z(k-1), ..., z(k-n_1), A_g(k), ..., A_g(k-n_1)) = \bar{G}(V) \tag{2.40}$$

where $n_1 \geq n$, $\bar{G}$ is the mapping function, $F_c^*(k)$ is the desired control force. NN is used to model $\bar{G}$.

In [73], and [72], NN for the structural reliability analysis was utilized. In [74], a NN based prediction scheme was proposed for the dynamic behavior of structural systems under multiple seismic excitations. The NN prediction includes two different ways: 1) A non-adaptive scheme that uses multiple accelerometers in training NN, and utilizes for the prediction of the structural seismic response ; 2) An adaptive scheme uses multiple accelerometers in the training.

Fuzzy control

Linguistic criteria is an effective feature of fuzzy control rules that can be easily modified and understood clearly [151]. In [4], a fuzzy logic controller with multipurpose optimal design was proposed to drive Hybrid mass damper(HMD) for the response control of the torsionally coupled seismically excited buildings. HMD system consists of four HMDs arranged in such a way that this system can control the torsional mode of vibration effectively in addition to the texture modes of vibration. The design of the fuzzy logic controller(FLC) based on the selection procedure that includes five membership functions for each of input variable and seven membership function for the output variable. The input and output variables includes acceleration and velocity in x-, y- , θ-directions and control command u_c respectively. The input subsets are categorized as - NL=negative large; NE=negative; ZE=zero;

PO=positive and PL=positive large. The output subsets are categorized as-NL=negative large; NE=negative; NS=negative small; ZE=zero; PS=positive small; PO=positive and PL=positive large. In their study, bell shaped membership function have been used and is represented by

$$\mu_x = \frac{1}{1 + |(x - c)/a|^{2b}} \qquad (2.41)$$

where a =half-width of the membership function at 0.5 membership grade,

b = membership function slope, c =central position of the membership function.

The minimization of structural torsion responses using semi-active dampers has been presented by [117]. In their investigation, the MR damper is employed for the real time control of the response of structures under seismic excitations. The methodology of fuzzy modeling of MR dampers have been shown in [116]. In [107], supervisory fuzzy controller was implemented to control two lower level fuzzy controllers. The weighted is determined by

$$Vd = \frac{W_N V_N + W_F V_F}{W_N + W_F} \qquad (2.42)$$

where W_N and W_F are the weighting factors, V_N and V_F are the command voltages.

In [2], it has been illustrated that the dynamic fuzzy wavelet NN can precisely forecast structural displacements.

In [66], the wavelet neural network (WNN) model based active non-linear controller for the response control of 3D buildings subjected to seismic excitation in both x and y directions has been presented. The main aim is to control the torsional and lateral motions of 3D irregular structures. The structural responses are predicted using a dynamic fuzzy WNN which is a fuzzy wavlet neuroemulator. Estimation of future time steps is utter necessary to control the structural responses effectively. This method is essential in determining the magnitude of the required control forces.

Structure control with genetic algorithm

Holland, 1975 was the first to propose the general scheme of Genetic algorithm (GA) uses natural genetic theory to build an optimal search algorithm [57]. A GA can be divided into three parts [18]

1. Code and decode the variables into the strings form.

2. Evaluating the fitness of each solution string.

3. Evaluate strings of the next generation by applying genetic operators.

The aim of the optimization problem is to evaluate the minimum of the performance index,

$$Adaptality = \left\{ \begin{array}{cc} J_{\max} - J & \text{if } J < J_{\max} \\ 0 & \text{otherwise} \end{array} \right\} \tag{2.43}$$

The applications of the GA method to structural control are published by various researchers. In [80], GA is utilized to MR dampers in the reduction of translation-torsion coupled responses of an asymmetric structure. The experiment was carried out at the State Key Lab of Coastal and Offshore Engineering in Dalian University of Technology. The parameters of the multi-state control strategy (MSC) which utilizes the velocity response as the state-switch parameter are optimized by genetic algorithm(GA) method. This MSC is developed in the intention to control torsional seismic response of an asymmetric structure. In their research, also the threshold vector of the MR damper is optimized using genetic algorithm. The parameters from the velocity response and the threshold vector of the MR damper are optimized by the GA method. In [67], a new neuro-genetic algorithm was presented to evaluate the optimal control forces for active control of 3D building structures. It includes geometrical and material nonlinearities, coupling action between lateral and torsional motions, and actuator dynamics. In this case a floating point GA was used. The methodology used can be categorized as follows-

i) Representation of chromosomes ,ii) initial population, iii) function related to fitness, iv) selection function, v) genetic operator, vi) termination scheme.

In the investigation mentioned , a non uniform mutation operator applied as the genetic operator to evaluate better solution for the new generation. It is expressed by

$$F_j^{/} = \left\{ \begin{array}{cc} F_j + (F_{\max} - F_j)h(g), \text{if } r_1 \geq 0.5 \\ F_j & \text{otherwise} \end{array} , j = 1, 2, ..., N_p \right\} \tag{2.44}$$

where, F_j = jth variable value in the chromosomes related to current population,

$F_j^{/}$ = improved value of the same variable related to the new generation,

$h(g)$ = probability function of mutation.

The study results suggest that the new control technique efficiently reduces the response of two irregular 3D building structures under seismic inputs including structures with plan and irregular elevation. The study results suggest that the new control technique efficiently

reduces the response of two irregular 3D building structures under seismic inputs including structures with plan and irregular elevation.

In [66], a new non-linear control model for the active control of a 3D building structure was developed. The optimal control forces is computed with the floating-point GA. GA can help to decide the positions of the control devices [150]. The coupled torsional-lateral response is attenuated by a semi active control under bidirectional seismic input. In [78], technique of reducing the seismic effects of the spatial structures by the installation of magneto-rheological (MR) dampers was proposed. It uses small populations to solve the optimization problem embedded in the semi active control. GA is used to optimize dampers passive parameters and controller gain in [12].

The concept of absorber system with multi-objective optimal design for torsionally coupled earthquake excited structures is presented by [4]. It use a multi-objective version of GA to extract the design parameters of absorber system. The two branch tournament genetic algorithm as mentioned by [29] extends two branch tournament GA to three-branch tournament GA and applies to the multi-objective optimization of the TMD system.

2.3   Summary

In this chapter, the modeling and structural control techniques of building structures subjected to bidirectional earthquake is consider. The main difference with normal structure controllers, is the lateral-torsional coupled response. We discuss recent new techniques, methodology and concepts in this areas. We focus all important results in last two decades in the field of structural engineering with respect to the bidirectional earthquakes. The important observations from this chapter are

1. Most of existing research only consider the structure control under unidirectional seismic wave. This chapter explores the effects of bidirectional seismic waves, which is normal for the real earthquake.

2. Real buildings are generally asymmetric in nature to some extent. This criteria induces lateral and torsional vibrations in combination.

3. The reduction of translational and torsional response of structures often involves the usage of multiple dampers [83].

4. Few research related to sliding mode control are carried out in order to reduce translation-torsion coupled vibration with bidirectional seismic inputs.

5. In case of building structures subjected to multiple excitations, the use of online identification technique is better.

6. The intelligent control like fuzzy logic is favored for the structural control, because it does not require system information.

7. PD/PID controller are robust, fault tolerant and very easy to implement.

Chapter 3

Bidirectional Modeling of Building Structures and Active Control

This chapter provides an overview of modeling of building structures under bidirectional earthquakes. Structural mechanics involves the study of vibrations incorporated in structures. In order to control a structure effectively, it is important to have the knowledge about its dynamics. The control of structures are associated with the safeguard of building structures from unidirectional or bidirectional seismic forces. One of the structural design object is to model dynamic loadings and to produce innovative approach to curb vibration. The vibration control generates the required dynamics in the building structures within a stable range. This control design is decided by the structure of mathematical model [42][153]. In [59], a compact relationship between the controller and the structure model is established.

All engineering structures are composed of intrinsic mass and elastic characteristics. The dynamic modeling has similar characteristics with the static analysis. However, the dynamic analysis is much complex than static analysis. For example, the mass modeling technique for the dynamic model requires an elastic model and a mass model minutely refined by discrete masses [36].

3.1   Bidirectional excitation

Recent earthquakes exhibits that the bidirectional effect is the main damage source of the structural damage. The seismic analysis should consider the bidirectional excitation. The normal method of building structure design regards the seismic response arising from the

ground motion that acts separately in the two orthogonal directions. Generally, the earthquake exhibits arbitrary direction which is represented as bidirectional ground movement, and it could reduce the participation of the traverse frames to the structure torsional and lateral stiffness. A noteworthy change in the elastic torsional behavior of the building is observed considering a non-linear behavior in the transverse frames.

The effect of the magnitude of the axial forces acting in the corner columns in case of bidirectional ground motion subjected to structures is different from that in case of unidirectional ground motion [30]. In [131], it was suggested that for a structure exposed to two simultaneous horizontal earthquake components, the transverse element behavior can be nonlinear and so the contribution to the real torsional stiffness is smaller. In [28] the analysis of one-story models with and without transverse elements subjected to unidirectional and bidirectional earthquakes was presented. Their study concluded that the addition of the transverse elements in the model significantly hampers the response of the border elements when the structure is subjected to the bidirectional seismic waves.

The analysis of real buildings suggests that it is asymmetric in nature to some degree with a formal symmetric plan. The asymmetric nature of building will induce lateral as well as torsional vibrations simultaneously and is termed as torsion coupling (TC) considering the case of pure translational excitations. Soil-structure interaction(SSI) effects are considered and can be significant in case of the building structures constructed on soft medium. The effects of SSI can critically modify the dynamic characteristics of a structure such as natural frequencies, damping ratios and mode shapes [136].

The knowledge of behavior and impact of the excitation forces plays a significant role in the formulation of the building structures dynamic model. The movement of the portion of the earth crust is termed as earthquake which is accompanied with the sudden release of stresses. Usually the epicenters for earthquake exists less then 25 miles below the earth's surface and are followed by series of vibrations. The bidirectional ground forces exerting on the building structure are shown in Figure 3.1. These forces result series of structure vibrations.

The forces acting on the x-axis and y-axis can be illustrated by the following dynamic equations

$$f_x = -m\ddot{x}_g \quad f_y = -m\ddot{y}_g \tag{3.1}$$

where m is the mass, $\ddot{x}_g$ and $\ddot{y}_g$ are the ground accelerations, caused by the seismic waves.

The main factors of the seismic movement for the building are the amplitude (displace-
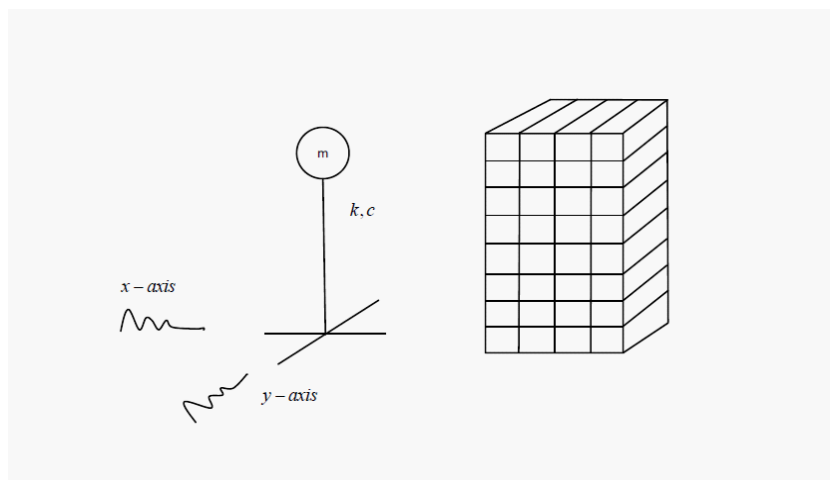
Figure 3.1: Bidirectional ground forces exert on the building structures

ment, velocity, and acceleration), and the frequency of the ground motion. The ground motion is complex, and the vibration frequency is time-varying. The ground motion and the building vibration affect each other, depending on the distance between the natural frequency of the building structure and seismic motion frequency. When the seismic wave frequency is close to the natural frequency of the building, the damages become bigger. Structure analysis shows that the shorter the building, the higher the natural frequency. One of the prime concern is to control the structure vibrating with respect to low frequency, because the major part of the structure elastic energy is stored in low frequency zone [22].

3.2   Structure model under bidirectional excitation

A controllable building structure can be regarded as a planar structure on a fixed base. The asymmetric characteristic of the building induces simultaneous lateral and torsional vibration, known as torsion coupling (TC) [89], which are subjected to bidirectional seismic inputs. The schematic plan view of structure involving torsion coupled(TC) is shown in Figure 3.2. The impacts of seismic forces in x and y directions result in building oscillation as in Figure 3.3. In includes: x oscillation, y oscillation, and the torsional oscillation defined as Φ.

The simplest structure is a one-story under lateral translational motion at the roof level. It is a single degree of freedom system. The motion model is [9]

$$m\ddot{v} + c\dot{v} + kv = p(t) \tag{3.2}$$
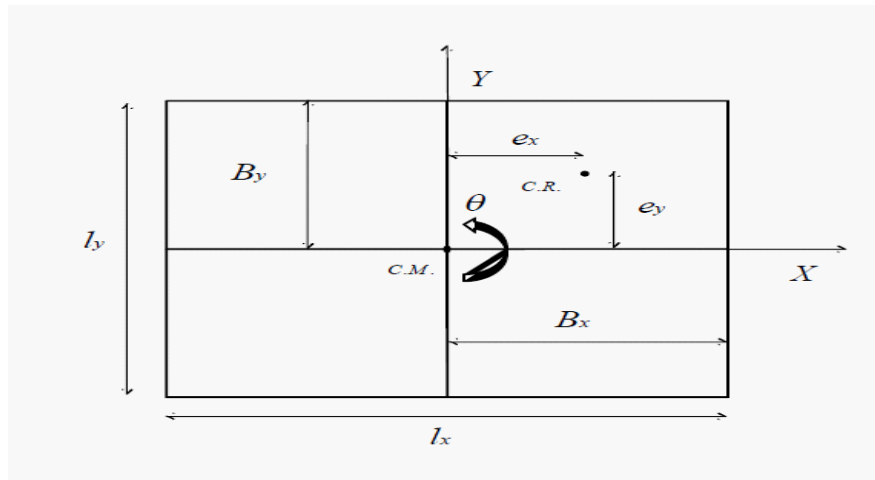
Figure 3.2: The torsion coupled force
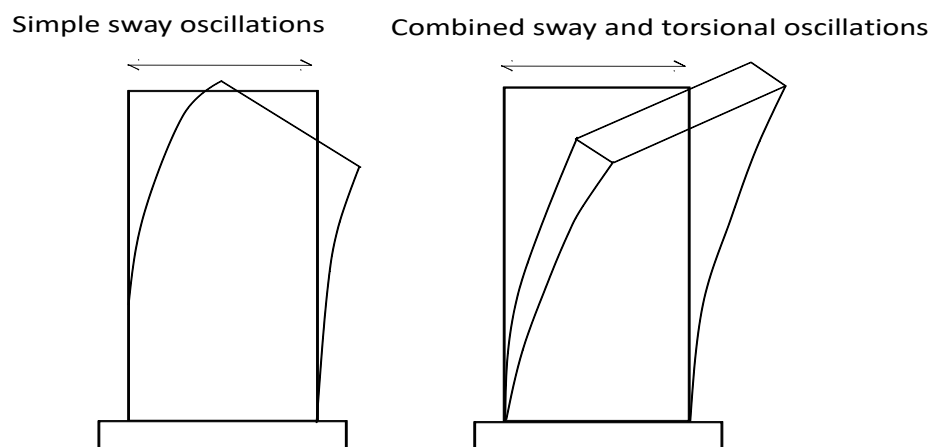
Figure 3.3: The seismic forces result in building oscillation
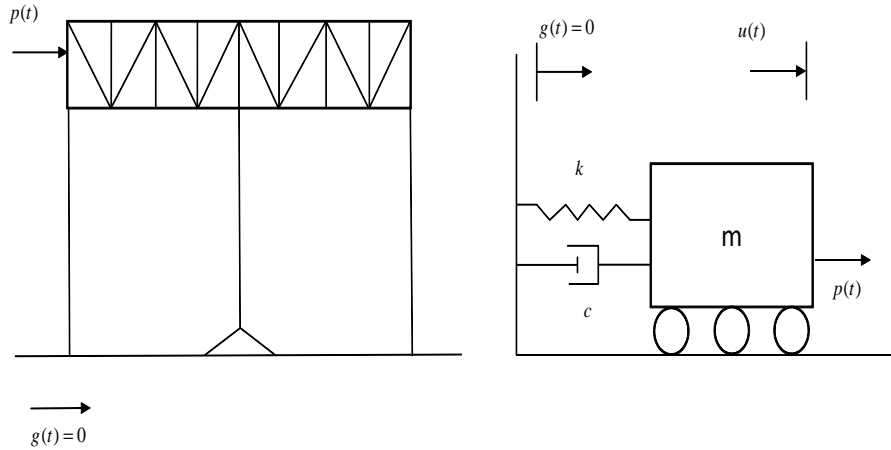
Figure 3.4: A single degree of freedom system for one-story building

where m is the mass, c is the damping, k is the stiffness, $\ddot{v}$ is the acceleration of the mass, $\dot{v}$ is the velocity of the mass relative to the base, v is the displacement, $p(t)$ is the applied force, see Figure 3.4.

Similarly, the equation of motion of a linear structure with n-Degree-of-Freedom (n-DOF) can be expressed as

$$M\ddot{X} + C\dot{X} + KX = P(t) \tag{3.3}$$

where M, C, and $K \in \mathbb{R}^{n \times n}$ are the mass, damping, and stiffness matrices respectively, $\ddot{X}$, $\dot{X}$, and $X \in \mathbb{R}^{n \times 1}$ are the relative acceleration, velocity, and displacement vectors respectively, and $P(t) \in \mathbb{R}^{n \times 1}$ is the external force vector.

The technique of modeling the stiffness parameter K can be on the basis of either a linear (elastic) or a nonlinear (inelastic) component [96]. The linear case means the relationship between the lateral force and the resulting deformation is linear [23].

When both ground translation and rotation are consider, the motion equation is [21]

$$M\ddot{X} + C\dot{X} + KX = F - MI_n\ddot{a}_g \tag{3.4}$$

where $\ddot{a}_g$ represents the earthquake acceleration component, I_n is the system influence co-efficient vector, $X = [x^T, y^T, \theta^T]^T$, $x = [x_1, \cdots x_n]^T$, $y = [y_1, \cdots y_n]^T$, $\theta = [\theta_1, \cdots \theta_n]^T$, $I_n = [I_1\ I_2\ 0]^T$, $\ddot{a}_g = [\ddot{x}_g\ \ddot{y}_g\ 0]$.

The mathematical analysis of the TC structure yields the following mass matrix, damping

matrix and stiffness matrix

$$
M = \begin{bmatrix} M_x & 0_{nxn} & 0_{nxn} \\ 0_{nxn} & M_y & 0_{nxn} \\ 0_{nxn} & 0_{nxn} & J_0 \end{bmatrix}, \quad K = \begin{bmatrix} K_{xx} & 0_{nxn} & -K_{x\theta} \\ 0_{nxn} & K_{yy} & K_{y\theta} \\ -K_{x\theta} & K_{y\theta} & K_{\theta\theta} \end{bmatrix}
$$

where $J_0 = diag\,[m_1 r_1^2, \cdots m_n r_n^2]$, J_0 is the polar moment of inertia of the story, r is the radius of gyration of the floor, n is the number of stories of the building, C is the damping matrix which is proportional to mass and stiffness matrix by the Rayleigh method [52].

For a simple case, the mass of each floor is concentrated at the floor plate (N-storey shear model). Two seismic waves are in the x direction and the y direction. Here the torsional components are zero, see Figure 3.5. The left figure represents 3-dimensional building structures and the right figure exhibits the parameters of each floor. The motion equations show the relative displacements of the building structures with respect to the ground motions [154]

$$
\begin{aligned}
m_j \ddot{x}_j + p_{j-1} - p_j &= -m_j \ddot{x}_g(t) \\
m_j \ddot{y}_j + q_{j-1} - q_j &= -m_j \ddot{y}_g(t) \\
J_j \ddot{\theta}_j + r_{j-1} - r_j &= 0
\end{aligned}
\tag{3.5}
$$

where x_j and y_j are the jth floor displacement in $x-$direction and $y-$direction respectively, θ_j is the jth floor torsion angle relative to the ground. p_{j-1} and q_{j-1} are the jth floor column shear forces in x-direction and y-direction, p_j and q_j are the $j+1$th floor column shear forces in $x-$direction and $y-$direction respectively, r_{j-1} is the jth floor torque generated by the shear forces, r_j is the $j+1$th floor torque, m_j is the mass of the jth floor, J_j is the rotational inertia. In the above motion equation, the $\ddot{x}_g(t)$ and $\ddot{y}_g(t)$ are the ground accelerations that strikes the building structures due to an earthquake. The total forces exerted on the each floor of the buildings in $x-$direction and $y-$direction are multiplied by the mass of the building at each floor. The torsional component of the ground acceleration are neglected and so the right hand side of the third equation is zero. The movement of the buildings in $x-$direction and $y-$direction that is the acceleration components are $\ddot{x}_j$ and $\ddot{y}_j$ respectively. Due to the bidirectional motion of the building, there will be coupling action on the building which give rises to the torsional motion in the building which is denoted by the component $\ddot{\theta}_j$.

If we only consider x-axis seismic wave, the torsion effect on the building is in $x-$component
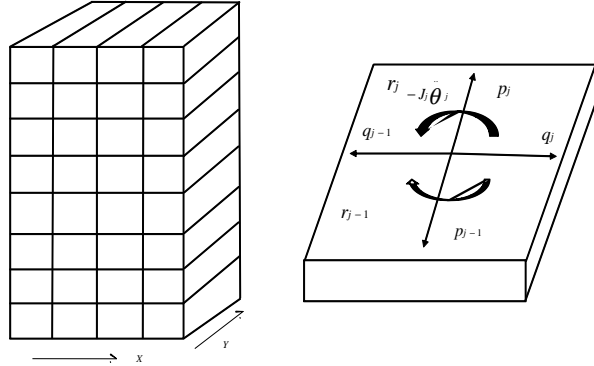
Figure 3.5: 3-dimensional building structures with parameters of each floor

[135], see Figure 3.6. The motion equations are

$$p_{j-1} = K_j(x_j - x_{j-1}) + C_j(\dot{x}_j - \dot{x}_{j-1}) + B_j(\theta_j - \theta_{j-1}) + D_j(\dot{\theta}_j - \dot{\theta}_{j-1})$$

$$r_{j-1} = B_j(x_j - x_{j-1}) + D_j(\dot{x}_j - \dot{x}_{j-1}) + E_j(\theta_j - \theta_{j-1}) + F_j(\dot{\theta}_j - \dot{\theta}_{j-1}) \qquad (3.6)$$

$$r_j = B_{j+1}(x_{j+1} - x_j) + D_{j+1}(\dot{x}_{j+1} - \dot{x}_j) + E_{j+1}(\theta_{j+1} - \theta_j) + F_{j+1}(\dot{\theta}_{j+1} - \dot{\theta}_j)$$

where $K_j = \sum_{i=1}^{I} K_{j,i}$, $C_j = \sum_{i=1}^{I} C_{j,i}$, $B_j = \sum_{i=1}^{I} K_j, il_{j,i}$, $D_j = \sum_{i=1}^{I} C_j, il$, $E_j = \sum_{i=1}^{I} K_j, il_{i,j}^2$, $F_j = \sum_{i=1}^{I} C_{i,j} l_{i,j}^2$, K_j, i and C_j, i are the stiffness and viscous damping coefficient respectively of the ith plane frame at the jth floor, m_j is the mass of the jth floor, J_j is the moment of inertia of the jth floor, $l_{j,i}$ is the distance of mass centre of the jth floor to the ith plane frame, I is total number of plane frames. $l_{j,i}$ is positive if the ith plane frame is located on the left of the mass centre, otherwise it is negative.

3.3   Bidirectional modeling for two-floor building

The normal method of structure design regards the seismic response arising from the ground motion that acts separately in the two orthogonal directions. Generally, the earthquake exhibits arbitrary direction which is represented as bidirectional ground movement, and it could reduce the participation of the traverse frames to the structure torsional and lateral stiffness, see Figure 3.1.
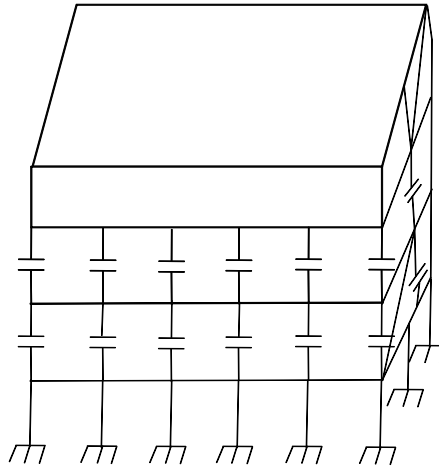
Figure 3.6: The torsion effect on the building is in x-component
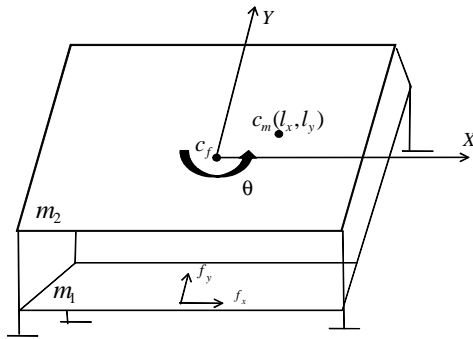
Figure 3.7: A two-floor building

The simplest structure is a one-story building, for one-direction it can be modeled by [5],

$$m\ddot{x} + c\dot{x} + s\, x = f_e \tag{3.7}$$

where m is the mass, c is the damping coefficient, s is the stiffness, f_e is an external force applied to the structure, and x, $\dot{x}$, and $\ddot{x}$ are the displacement, velocity, and acceleration, respectively.

If the external force is in bidirectional, there are not only vibrations in X and Y axes, but also torsion coupling. The torsional oscillation comes from the asymmetric characteristic of the building, i.e., the physical center (c_f) is different with the mass center (c_m), see the two-floor building in Figure 3.7.

The motion of a n-floor structure can be expressed as [23][109],

$$M\ddot{\mathbf{x}} + C\dot{\mathbf{x}} + \mathbf{f}_s = \mathbf{f}_e \tag{3.8}$$

where $\mathbf{x} \in \Re^n$, $M \in \Re^{n \times n}$, $C \in \Re^{n \times n}$, $f_s = [f_{s,1} \cdots f_{s,n}] \in \Re^n$ is the structure stiffness force vector, and $f_e \in \Re^n$ is the external force vector applied to the structure.

Also $M = diag\,(M_x, M_y, J_t) \in \Re^{(3n) \times (3n)}$, $diag\,(\cdot)$ is a diagonal matrix, $M_x = M_y = diag\,(m_1 \cdots m_n)$, m_i is the mass of the i-th floor, $J_t = diag\,(m_1 r_1^2 \cdots m_n r_n^2)$ is the polar moment of inertia. $f_e = [f_x, f_y]^T = \begin{bmatrix} -M_x & 0 \\ 0 & -M_y \\ 0 & 0 \end{bmatrix} \begin{bmatrix} a_x \\ a_y \end{bmatrix}$ where a_x are a_y are the accelerations of the external force in X and Y directions. The displacements of the structure, with respect to the bidirectional force $f_e = [f_x, f_y]^T$, have 3 components $x = [x, y, \theta]^T$, θ is the torsional angle.

The structure stiffness force f_s can be modeled as a linear model or a nonlinear model. In simple linear case

$$\mathbf{f}_s = S\mathbf{x} \tag{3.9}$$

where $x = [x_1 \cdots x_n, y_1 \cdots y_n, \theta_1 \cdots \theta_n]^T \in \Re^{3n}$,

$$S = \begin{bmatrix} S_x & 0 & -S_{x\theta} \\ 0 & S_y & S_{y\theta} \\ -S_{x\theta} & S_{y\theta} & S_\theta \end{bmatrix}, S_\rho = \begin{bmatrix} s_{\rho_1} + s_{\rho_2} & -s_{\rho_2} & \cdots & 0 & 0 \\ \vdots & \vdots & \ddots & \vdots & \vdots \\ 0 & 0 & \cdots & -s_{\rho_n} & s_{\rho_n} \end{bmatrix}, \rho = (x, y, \theta)$$

$s_{\theta i} = s_{\theta_i} + s_{x_i} l_{y_i}^2 + s_{y_i} l_{x_i}^2$, $\quad i = 1 \cdots n$ represents floor, s is the stiffness

$$S_{x\theta} = \begin{bmatrix} s_{x_1} l_{y_1} + s_{x_2} l_{y_2} & -s_{x_2} l_{y_2} & \cdots & 0 & 0 \\ \vdots & \vdots & \ddots & \vdots & \vdots \\ 0 & 0 & \cdots & -s_{x_n} l_{y_n} & s_{x_n} l_{y_n} \end{bmatrix} \in \Re^{3n}$$

$$S_{y\theta} = \begin{bmatrix} s_{y_1} l_{x_1} + s_{y_2} l_{x_2} & -s_{y_2} l_{x_2} & \cdots & 0 & 0 \\ \vdots & \vdots & \ddots & \vdots & \vdots \\ 0 & 0 & \cdots & -s_{y_n} l_{x_n} & s_{y_n} l_{x_n} \end{bmatrix} \in \Re^{3n}$$

The matrix S represents the overall stiffness matrix whereas the matrix S_ρ represents the stiffness matrix in x, y and θ directions respectively by substituting ρ. Also l_{x_i} and l_{y_i} represents the length of the structure in X-direction and Y-direction respectively, $i = 1, 2$. The overall stiffness matrix S can be calculated by substituting S_x, S_y and S_θ using S_ρ and also by substituting $S_{x\theta}$ and $S_{y\theta}$.

The damping matrix C is proportional to mass matrix M and stiffness matrix S

$$C = aM + bS$$

Using Rayleigh method, represented by the equation. Therefore the damping matrix C has the same form as of the stiffness matrix S, $C = \begin{bmatrix} C_x & 0 & -C_{x\theta} \\ 0 & C_y & C_{y\theta} \\ -C_{x\theta} & C_{y\theta} & C_\theta \end{bmatrix}$.

3.3.1   Non-linear stiffness

When the structure is under the grip of very strong force which deforms the structure beyond its limit of linear elastic behavior, the structure stiffness force f_s cannot be modeled as a linear model. The behavior of the structure can be demonstrated using Bouc-Wen model. The advantages incorporated in the Bouc–Wen model is that it can demonstrate inelastic behavior of the structure where the strength/stiffness degradation can be easily incorporated. The relationship between the forces and displacements is [75]

$$f_{\rho,i} = \epsilon_{\rho i} s_{\rho i} x_{\rho i} + (1 - \epsilon_{\rho i}) s_{\rho i} \phi_{\rho i} \tag{3.10}$$

where $\rho = (x, y)$, $i = 1 \cdots n$, $\epsilon_{\rho i}$ are positive numbers.

The first part of (3.10) is the elastic stiffness, the second part is the inelastic stiffness. The nonlinear function $\phi_{\rho i}$ is

$$\phi_{\rho i} = \frac{1}{\eta_{\rho i}} [A \dot{x}_{\rho i} - \beta_{\rho i} |\dot{x}_{\rho i}| \, |a_{\rho i}|^{\eta_{l_i} - 1} a_{\rho i} v_{\rho i} + \gamma_{\rho i} |\dot{x}_{\rho i}| \, |a_{\rho i}|^{\eta_{l_i} - 1} v_{\rho i} a_{\rho i} sign(\dot{x}_{\rho i} a_{\rho i})] \tag{3.11}$$

where $A, \beta_{\rho i}, \gamma_{\rho i}, \alpha_{\rho i}, n$ and η are positive numbers.

$\eta_{\rho i} = 1 + \delta_{\rho i} E_{\rho i}$ controls the stiffness degradation, $v_{\rho i} = 1 + \delta_{\rho i} E_{\rho i}$ controls strength degradation. Normalized dissipated hysteretic energy is

$$E_{\rho i} = (1 - \alpha_{\rho i}) \int_0^t \frac{\dot{x}_{\rho i} a_{\rho i}}{\Delta_{\rho i} \Delta_{\rho i}} dt \quad \Delta_{\rho i} = (\beta_{\rho i} + \gamma_{\rho i})^{-\frac{1}{\eta \rho i}} \tag{3.12}$$

The property of passivity states that the system storage energy is always lesser than the energy supplied. In [61], it was demonstrated that the Bouc-Wen model is considered to be passive with respect to its energy storage. The nonlinear differential equation (3.11) is continuous and also it is dependent on time. The property of local Lipschitz is also maintained. It can be validated that (3.11) has a unique solution on a time interval $[0, t_0]$. In the stability analysis involved in the later part, this property will be utilized.

3.4   Active Control
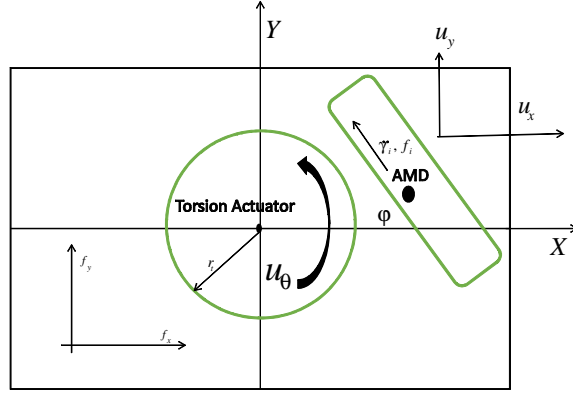
Figure 3.8: Bidirectional active control of structures

3.4.1 Active mass damper (AMD) and torsional actuator (TA)

In order to minimize the vibrations caused by the bidirectional external forces (f_x and f_y), an active mass damper (AMD) and a torsional actuator (TA) are installed on the structure as shown in Figure 3.8. The active mass damper (AMD) is placed near the mass centre of the building. The torsional actuator (TA) is placed on the physical center of the building. The control force are $u = [u_x, u_y, u_\theta]^T$. Considering the building model (3.8) and the control, the closed-loop system is

$$M\ddot{\mathbf{x}} + C\dot{\mathbf{x}} + \mathbf{f}_s - \mathbf{f}_e = \Gamma(\mathbf{u} - \mathbf{d_u}) \tag{3.13}$$

The closed loop system represented by (3.13) is the control equation that is utilized for control and stability analysis. In the forthcoming section, this equation is subdivided in to three components mainly $X-$component, $Y-$component and $\theta-$component and then analysis is carried out.

where $u \in \Re^{3n}$ is the control signals which is fed to the dampers, where dampers signifies active mass damper (AMD) and torsional actuator (TA) in combination, $d_\mathbf{u}$ is the damping and friction force vector of the dampers, Γ is the location matrix of the dampers which is defined as

$$\Gamma_{i,j} = \begin{cases} 1 & \text{if } i = j = f_l \\ 0 & \text{otherwise} \end{cases} \tag{3.14}$$

where $\forall i, j \in \{1, ..., n\}, f_l \subseteq \{1, ..., n\}$, f_l are the floors on which the dampers are installed. For a two-floor building, $\Gamma = \begin{bmatrix} \Gamma_{1,1} & \Gamma_{1,2} \\ \Gamma_{2,1} & \Gamma_{2,2} \end{bmatrix}$. If the damper is placed on the second floor,

$f_l = \{2\}$, $\Gamma = \begin{bmatrix} 0 & 0 \\ 0 & 1 \end{bmatrix}$. If the damper is placed on both first and second floor, $f_l = \{1, 2\}$,

$\Gamma = \begin{bmatrix} 1 & 0 \\ 0 & 1 \end{bmatrix}$.

If we illustrate the closed loop system mentioned by (3.13) along all three directions that is $X-$direction, $Y-$direction and $\theta-$direction then

$$M_x \ddot{x} + C_x \dot{x} + f_{sx} - f_x = \Gamma(u_x - d_{ux})$$
$$M_y \ddot{y} + C_y \dot{y} + f_{sx} - f_y = \Gamma(u_y - d_{uy}) \qquad (3.15)$$
$$J_t \ddot{\theta} + C_\theta \dot{\theta} + f_{s\theta} = \Gamma(u_\theta - d_{u\theta})$$

The AMD force in i-th floor is defined as f_i

$$f_i = m_{di}(\ddot{d}_i + \ddot{\gamma}_i) \qquad (3.16)$$

where m_{di} is the mass of the AMD, $\ddot{d}_i$ is the acceleration of the AMD, $\ddot{\gamma}_i$ is the acceleration of the structure along the AMD, $\ddot{\gamma}_i = \sqrt{a_{i,x}^2 + a_{i,y}^2}$. f_i should be separated into X and Y directions as

$$u_{i,x} = f_i \cos\varphi = m_{di}(\ddot{d}_i \cos\varphi + a_{i,x})$$
$$u_{i,y} = f_i \sin\varphi = m_{di}(\ddot{d}_i \sin\varphi + a_{i,y})$$
$$\ddot{\gamma}_i = \frac{a_{i,x}}{\cos\varphi} = \frac{a_{i,y}}{\sin\varphi}$$
$$\ddot{x}_{i,x} = a_{i,x} + \ddot{d}_i \cos\varphi$$
$$\ddot{x}_{i,y} = a_{i,y} + \ddot{d}_i \sin\varphi$$

where φ is the angle of the AMD along X-axis, $\ddot{x}_{i,x}$ and $\ddot{x}_{i,y}$ are the relative acceleration of the AMD along X and Y directions. So

$$f_i = m_{di}\left(\ddot{d}_i + \frac{a_{i,x}}{\cos\varphi}\right) = m_{di}\left(\ddot{d}_i + \frac{a_{i,y}}{\sin\varphi}\right)$$

We define the control force of the AMD along X and Y directions as $u_d = [u_x, u_y]^T$

$$u_{di} = m_{di}\left[\ddot{x}_{i,x}, \ddot{x}_{i,y}\right]^T$$

Consider the friction of the AMD,

$$fr_{i,x} = c\dot{x}_{i,x} + \epsilon m_{di}g \tanh\left[\beta\dot{x}_{i,x}\right]$$
$$fr_{i,y} = c\dot{x}_{i,y} + \epsilon m_{di}g \tanh\left[\beta\dot{x}_{i,y}\right]$$

where c, β and ϵ are the damping coefficients of the Column friction [108]. The final control of the AMD is

$$u_x = m_{di}\ddot{x}_{i,x} - fr_{i,x}$$
$$u_y = m_{di}\ddot{x}_{i,y} - fr_{i,y} \qquad (3.17)$$

Using (3.15) and (3.17)

$$M_x\ddot{x} + C_x\dot{x} + f_{sx} - f_x = \Gamma(m_{di}\ddot{x}_{i,x} - fr_{i,x} - d_{ux})$$
$$M_y\ddot{y} + C_y\dot{y} + f_{sx} - f_y = \Gamma(m_{di}\ddot{x}_{i,y} - fr_{i,y} - d_{uy})$$

(3.18)

The third element of the control $u = [u_x, u_y, u_\theta]^T$ is the torsion force u_θ. The TA is a rotating disc equipped with DC motor and is placed at the center of physical center, see Figure 3.8. The control object is to decreased the torsional response of the structures due to the bidirectional movements and the mass center and the physical center being different.

The inertia moment of TA is

$$J_t = m_t r_t^2$$

(3.19)

where, m_t is the mass of the disc and r_t is the radius of the disc. The torque τ generated by the disc is

$$u_\theta = J_t(\ddot{\theta}_t + \ddot{\theta})$$

(3.20)

where, $\ddot{\theta}$ is the angular acceleration of the building, $\ddot{\theta}_t$ is the angular acceleration of the torsional actuator. Obviously, to decrease the torsional response, the directions of $\ddot{\theta}_t$ and $\ddot{\theta}$ should be different.

Consider the friction of the TA

$$fr_t = c\dot{\theta}_t + F_c \tanh(\beta\dot{\theta}_t)$$

(3.21)

where c is the torsional viscous friction coefficient, F_c is the coulomb friction torque, tanh is the hyperbolic tangent depending on β and motor speed. The final torsion control is

$$u_\theta = J_t(\ddot{\theta}_t + \ddot{\theta}) - fr_t$$

(3.22)

Using (3.15) and (3.22)

$$J_t\ddot{\theta} + C_\theta\dot{\theta} + f_{s\theta} = \Gamma(J_t(\ddot{\theta}_t + \ddot{\theta}) - fr_t - d_{u\theta})$$

(3.23)

The main role of the AMD is to reduce the response of acceleration of building in X and Y directions whereas the main role of the TA is to minimize the torsional effect on the building. For the closed-loop system (3.13),

$$\mathbf{d_u} = \begin{bmatrix} c\dot{x}_{i,x} + \epsilon m_{di}g \tanh\left[\beta\dot{x}_{i,x}\right] = d_{ux} \\ c\dot{x}_{i,y} + \epsilon m_{di}g \tanh\left[\beta\dot{x}_{i,y}\right] = d_{uy} \\ c\dot{\theta}_t + F_c \tanh(\beta\dot{\theta}_t) = d_{u\theta} \end{bmatrix}$$

(3.24)

The movements of the AMD and TA are sliding in nature. The sliding mechanism of the actuators absorb the energy from the friction. The kinetic energy is converted into heat energy in this phenomena. So the coefficients in the friction models are assumed to be Coulomb.

3.5   Summary

This chapter highlights the importance of modeling of building structures under bidirectional earthquakes. It is important to have the knowledge of the model dynamics for effective implementation of the control law. In this chapter the modeling equation of the two floor building is extracted. Also modeling equation of the AMD and TA are laid down. The equation of active control of both the actuator are proposed. This procedure will facilitate the successful implementation of PD/PID control, Type-2 Fuzzy control and discrete time sliding mode control in the forthcoming chapters.

Chapter 4

Bidirectional PD/PID Control of Building Structures

4.1   Introduction

The role of the structural control is to minimize the vibrations of the buildings under the effect of bidirectional earthquake via an effective external control force. In an active control system it is essential to design an effective control strategy, which is simple, robust, and fault tolerant. Several attempts have been made to implement advanced controllers for the active vibration control of structures as discussed in Chapter 2.

The Chapter 2 clearly justifies that the control device plays a superior role in preventing structure from damages. A good control law gives good performance of the anti-vibration. Researchers have made several attempts to incorporate high level controllers for the active vibration control of structures. The pole-placement H_∞ control with target damping ratio is proposed by [102]. In [38], the genetic algorithm is applied to determine the feedback control. Many optimal control algorithms are applied for the active vibration control of structures, for example filtered linear quadratic control [113], linear quadratic regulator [5] and linear quadratic Gaussian control [55]. The active mass damper is widely implemented, which utilizes the mass without spring and dashpot [19]. Due to the existence of translation-torsion coupled vibrations with respect to the bidirectional seismic waves, in this work a torsional actuator (TA) is utilized. It is a disc-motor device, which is incorporated in the structure to minimize the torsional response of the building.

For real application, an effective controller should be simple, robust, and fault tolerant. The PD/PID control has been widespread applied in industrial processes. It may be the best

control, because it shows its effectivity without the knowledge of the model and also due its simplicity as well as it is incorporated with distinct physical meanings. In [145], MR damper is utilized in the combination with the magneto-rheological damper (MR-MD) scheme to control a three dimensional structure from bidirectional seismic excitations. The controller used the mechanism of PD control. It calculates the essential forces required to control the structural vibrations. In [51], PD and PID controllers are used in the numerical simulations to control structure under unidirectional earthquake. [98] used active tendons to control torsionally irregular and multistory structures under the effect of near fault ground motion excitation. In their work, PID type controllers were used to generate the control signals. In [99], various feedback control strategies in relation to active control of earthquake utilizing PID type controllers was presented. A numerical algorithm was taken into consideration for finding out the parameters of PID.

The problems of existed bidirectional PD/PID control are: 1) they do not consider the lateral-torsional control mechanism that is only horizontal actuator was used to mitigate the lateral-torsional vibration but a combination of horizontal actuator and torsional actuator are not implemented; 2) they do not analyze the stability of closed-loop system.

In this work, standard PD and PID control are utilized as active vibration control of the structure in order to solve the above two problems. Initially the analysis are based on the lateral-torsional vibration, linear and nonlinear structure stiffness, and the hysteresis of the structure model under the bidirectional wave. Then the sufficient conditions for asymptotic stability of the PD/PID control are validated by utilizing Lyapunov stability analysis. These conditions are quite convenient for the designer to choose the controller gains straightaway. An active vibration control system with two floors equipped with a horizontal actuator and a torsional actuator is setup in order to carry out the experimental analysis. The experimental results using the PD and PID controller validate their effectiveness and stability.

4.2   Bidirectional PD/PID control

4.2.1   Closed loop system with PD control

As PD control is very simple and robust to uncertainties, it is the most popular controller for mechanical systems. It is the simplest controller for the structural vibration control system. PD controller is the best choice. PD control has the following form when the horizontal

actuator control is coupled with the torsional actuator control

$$\mathbf{u} = -K_p\mathbf{e} - K_d\dot{\mathbf{e}} \tag{4.1}$$

where $e = x - x^d$, $x = [x, y, \theta]^T$, x^d is desired reference vector, for the vibration control, $x^d = 0$. K_p and K_d are positive-definite constant matrices that correspond to the proportional and derivative gains. The PD control (4.1) for structures becomes

$$\mathbf{u} = -K_p\mathbf{x} - K_d\dot{\mathbf{x}} \tag{4.2}$$

The design of the controller are based on the suitable gain selection K_p and K_d in (4.1), such that the closed-loop system is stable and good performances are achieved. For the bidirectional structure control, the gains of one-floor PD are: $K_P = diag\,(K_{px}, K_{py}, K_{p\theta}) \in \Re^{6x6}$, $K_d = diag\,(K_{dx}, K_{dy}, K_{d\theta})$. The closed-loop system (3.13) with the PD control shown in (4.2) is

$$M\ddot{\mathbf{x}} + C\dot{\mathbf{x}} + S\mathbf{x} + \mathbf{f}_e + \Gamma\mathbf{d_u} = \Gamma(-K_p\mathbf{x} - K_d\dot{\mathbf{x}}) \tag{4.3}$$

Here the terms $(S\mathbf{x} + \mathbf{f}_e + \Gamma\mathbf{d_u})$ can be regarded as uncertainties. In the following section, we assume it satisfies the Lipschitz condition.

It is well known that the regulation error becomes smaller while increasing the derivative gain. The cost of large derivative gain results in slow transient performance. Only when derivative gain tends to infinity, the regulation error converges to zero [76]. However it would seem better to use a smaller derivative gain if the system contains high-frequency noise signals.

4.2.2   Closed loop system with PID control

In the control viewpoint, the regulation error can be removed by introducing an integral component to the PD control. PID controllers use feedback strategy and have three actions. P action is introduced for increasing the speed of response. D action is introduced for damping purposes. I-action is introduced for obtaining a desired steady-state response [34]. The PID control is,

$$\mathbf{u} = -K_p(\mathbf{x} - \mathbf{x}^d) - K_i \int_0^t (\mathbf{x} - \mathbf{x}^d)d\tau - K_d(\dot{\mathbf{x}} - \dot{\mathbf{x}}^d) \tag{4.4}$$

where K_p, K_i and K_d are positive definite, K_i is the integration gain. For the structure control. $x^d = \dot{x}^d = 0$, (4.4) becomes

$$\mathbf{u} = -K_p\mathbf{x} - K_i \int_0^t \mathbf{x}d\tau - K_d\dot{\mathbf{x}} \tag{4.5}$$

In order to analyze PID controller, (4.5) is expressed by

$$\mathbf{u} = -K_p \mathbf{x} - K_d \dot{\mathbf{x}} - \boldsymbol{\xi}$$
$$\boldsymbol{\xi} = K_i \int_0^t \mathbf{x} d\tau, \quad \boldsymbol{\xi}(0) = \mathbf{0}$$

The closed-loop system (3.13) with the PID control (4.4) becomes

$$M\ddot{\mathbf{x}} + C\dot{\mathbf{x}} + S\mathbf{x} + \mathbf{f}_e + \Gamma \mathbf{d_u} = -K_{px}\mathbf{x} - K_{dx}\dot{\mathbf{x}} - \boldsymbol{\xi}$$
$$\dot{\boldsymbol{\xi}} = K_i \mathbf{x} \tag{4.6}$$

In matrix form, the closed-loop system is

$$\frac{d}{dt} \begin{bmatrix} \boldsymbol{\xi} \\ \mathbf{x} \\ \dot{\mathbf{x}} \end{bmatrix} = \begin{bmatrix} K_{ix}x \\ \dot{\mathbf{x}} \\ -M^{-1}\left(C\dot{\mathbf{x}} + S\mathbf{x} + \mathbf{f}_e + \Gamma \mathbf{d_u} + K_{px}\mathbf{x} + K_{dx}\dot{\mathbf{x}} + \boldsymbol{\xi}\right) \end{bmatrix} \tag{4.7}$$

Unlike the H_2 control [110] and optimal control [5], PD control does not need the model of the structure. The model discussed in the above section will be used for stability analysis in this chapter. The theory analysis of bidirectional PD control is still not appeared in publications [51].

4.3 Stability of the bidirectional PD/PID control

4.3.1 PD control

As the combined forces generated by horizontal actuator and torsional actuator is fed to the structure, this forces may stabilize or destabilize the structure. If the control algorithm generates unstable signal, the horizontal actuator and torsional actuator will generate forces that can make the structure unstable. This matter becomes more complicated for nonlinear devices, as a bounded input signal may also make nonlinear devices to generate unstable output.

In general cases, the structures associated with open-loop systems are asymptotically stable. This is true for the case when there is no external force, $f_e = 0$. The criteria is valid in case of inelastic stiffness because of its BIBO stability and passivity properties. In the event of seismic excitation the ideal active control force required for cancelling out the vibration completely is $\Gamma u = f_e$. But practically it is not possible because f_e is not always measurable and is much bigger than any control device force. Therefore the main intention of the active control is to maintain the vibration as minimum as possible by mitigating

the relative movement between the structural floors. Normally the structural parameters are partly known and the structure model might have embedded nonlinearity such as the hysteresis phenomenon.

It is quite favorable to represent the closed-loop system (4.3) with PD control as

$$M\ddot{\mathbf{x}} + C\dot{\mathbf{x}} + \mathbf{f} = -\Gamma\left(K_p\mathbf{x} + K_d\dot{\mathbf{x}}\right) \tag{4.8}$$

where $f = f_s + f_e + d_{\mathbf{u}}$.

The following theorem gives the stability analysis of the PD control (4.2). To simplify the proof, we assume that $\Gamma_{n\times n} = I_{n\times n}$, which means that each floor has an horizontal actuator and a torsional actuator .

Theorem 4.1 *Consider the structural system as (3.13) controlled by the PD controller as (4.2), the closed-loop system as (4.3) is stable, provided that the control gains are positive. The regulation errors converge to the following residual sets*

$$
\begin{aligned}
D_x &= \left\{ \dot{\mathbf{x}}, \dot{\boldsymbol{\theta}} \mid \|\dot{\mathbf{x}}\|_{Q_x}^2 + \left\|\dot{\boldsymbol{\theta}}\right\|_{Q_x}^2 \le \bar{\mu}_{\mathbf{fx}} + \boldsymbol{\alpha}_{\mathbf{f}}^2 \bar{\mu}_{\mathbf{fx}} \right\} \\
D_y &= \left\{ \dot{\mathbf{y}}, \dot{\boldsymbol{\theta}} \mid \|\dot{\mathbf{y}}\|_{Q_y}^2 + \left\|\dot{\boldsymbol{\theta}}\right\|_{Q_y}^2 \le \bar{\mu}_{\mathbf{fy}} + \boldsymbol{\eta}_{\mathbf{f}}^2 \bar{\mu}_{\mathbf{fy}} \right\} \\
D_\theta &= \left\{ \dot{\boldsymbol{\theta}}, \dot{\mathbf{x}}, \dot{\mathbf{y}} \mid \left\|\dot{\boldsymbol{\theta}}\right\|_{Q_\theta}^2 + \|\dot{\mathbf{x}}\|_{Q_\theta}^2 + \|\dot{\mathbf{y}}\|_{Q_\theta}^2 \le \bar{\mu}_{\mathbf{f\theta}} + \boldsymbol{\alpha}_{\mathbf{f}}^{-2} \bar{\mu}_{\mathbf{fx}} + \boldsymbol{\eta}_{\mathbf{f}}^{-2} \bar{\mu}_{\mathbf{fy}} \right\}
\end{aligned} \tag{4.9}
$$

where $\bar{\mu}_{\mathbf{fx}} \ge f_{\mathbf{x}}^T \Lambda_{\mathbf{f}}^{-1} f_{\mathbf{x}}$, $\bar{\mu}_{\mathbf{fy}} \ge f_{\mathbf{y}}^T \Lambda_{\mathbf{f}}^{-1} f_{\mathbf{y}}$, $\bar{\mu}_{\mathbf{f\theta}} \ge f_{\boldsymbol{\theta}}^T \Lambda_{\mathbf{f}}^{-1} f_{\boldsymbol{\theta}}$, $C_x + \alpha_{\mathbf{f}} C_{x\theta} > \Lambda_{\mathbf{fx}} > 0$, $C_y + \eta_{\mathbf{f}} C_{y\theta} > \Lambda_{\mathbf{fy}} > 0$, $C_\theta + \alpha_{\mathbf{f}}^{-1} C_{x\theta} + \eta_{\mathbf{f}}^{-1} C_{y\theta} > \Lambda_{\mathbf{f\theta}} > 0$.

Proof. The closed-loop system (4.8) can also be represented as

$$
\begin{bmatrix} M_x\ddot{x} \\ M_y\ddot{y} \\ J_t\ddot{\theta} \end{bmatrix} + \begin{bmatrix} C_x\dot{x} - C_{x\theta}\dot{\theta} \\ C_y\dot{y} + C_{y\theta}\dot{\theta} \\ C_\theta\dot{\theta} - C_{x\theta}\dot{x} + C_{y\theta}\dot{y} \end{bmatrix} + \begin{bmatrix} \mathbf{f_x} \\ \mathbf{f_y} \\ \mathbf{f_\theta} \end{bmatrix} = -\Gamma \left\{ \begin{bmatrix} K_{px}x \\ K_{py}y \\ K_{p\theta}\theta \end{bmatrix} + \begin{bmatrix} K_{dx}\dot{x} \\ K_{dy}\dot{y} \\ K_{d\theta}\dot{\theta} \end{bmatrix} \right\} \tag{4.10}
$$

Therefore, we have three sets to represent X, Y and θ directions

$$
\begin{aligned}
M_x\ddot{x} + \left(C_x\dot{x} - C_{x\theta}\dot{\theta}\right) + \mathbf{f}_x &= -\Gamma(K_{px}x + K_{dx}\dot{x}) \\
M_y\ddot{y} + \left(C_y\dot{y} + C_{y\theta}\dot{\theta}\right) + \mathbf{f}_y &= -\Gamma(K_{py}y + K_{dy}\dot{y}) \\
J_t\ddot{\theta} + \left(C_\theta\dot{\theta} - C_{x\theta}\dot{x} + C_{y\theta}\dot{y}\right) + \mathbf{f}_{\boldsymbol{\theta}} &= -\Gamma(K_{p\theta}\theta + K_{d\theta}\dot{\theta})
\end{aligned} \tag{4.11}
$$

We will analyze one by one. Since the damper and actuator are placed in the second floor, so $\Gamma = 1$. If all the individual structural equations in (4.11) with PD controller are stable,

the entire structural is stable using PD controller. For that purpose we select Lyapunov candidate as

$$V_x = \frac{1}{2}\dot{x}^T M_x \dot{x} + \frac{1}{2}x^T K_{px} x \tag{4.12}$$

The first term of (4.12) signifies the kinetic energy and the second term denotes elastic potential energy. As M_x and K_{px} are positive definite matrices, so $V_x \geq 0$. The derivative of (4.12) is

$$\begin{aligned} \dot{V}_x &= \dot{x}^T M_x \ddot{x} + \dot{x}^T K_{px} x \\ &= \dot{x}^T \left(-C_x \dot{x} + C_{x\theta}\dot{\theta} - \mathbf{f}_x - K_{px} x - K_{dx}\dot{x} \right) + \dot{x}^T K_{px} x \\ &= -\dot{x}^T \left(C_x + K_{dx} \right) \dot{x} + \dot{x}^T C_{x\theta}\dot{\theta} - \dot{x}^T \mathbf{f}_x \end{aligned} \tag{4.13}$$

Using the matrix inequality

$$X^T Y + Y^T X \leq X^T \Lambda X + Y^T \Lambda^{-1} Y \tag{4.14}$$

It is valid for any $X, Y \in \Re^{n \times m}$ and any $0 < \Lambda = \Lambda^T \in \Re^{n \times n}$, we can write the scalar variable $\dot{x}^T f_{\mathbf{x}}$ as

$$\dot{x}^T \mathbf{f}_x = \frac{1}{2}\dot{x}^T \mathbf{f}_x + \frac{1}{2}\mathbf{f}_x^T \dot{x} \leq \dot{x}^T \Lambda_{\mathbf{f}x} \dot{x} + \mathbf{f}^T \Lambda_{\mathbf{f}x}^{-1} \mathbf{f} \tag{4.15}$$

where $\Lambda_{\mathbf{f}x}$ is any positive definite matrix. Now $\dot{x}$ and $\dot{\theta}$ are related to each other as the vibration along x-direction will create a torsional movement θ and so we suppose

$$\dot{\theta} = -\boldsymbol{\alpha}_{\mathbf{f}}\dot{x} \tag{4.16}$$

where $\alpha_{\mathbf{f}}$ is a positive definite matrix. As the X component of ground acceleration will give a torsion in the structure in anti-clockwise sense, hence we assumed the relation to be negative. Using (4.16) in (4.13),

$$\begin{aligned} \dot{V}_x &= -\dot{x}^T \left(C_x + K_{dx} \right) \dot{x} - \boldsymbol{\alpha}_{\mathbf{f}}^T \dot{x} C_{x\theta} \dot{x} - \dot{x}^T \mathbf{f}_x \\ \dot{V}_x &= -\dot{x}^T \left(C_x + \boldsymbol{\alpha}_{\mathbf{f}} C_{x\theta} + K_{dx} \right) \dot{x} - \dot{x}^T \mathbf{f}_x \end{aligned}$$

We select $\Lambda_{\mathbf{f}x}$ as

$$C_x + \boldsymbol{\alpha}_{\mathbf{f}} C_{x\theta} > \Lambda_{\mathbf{f}x} > 0 \tag{4.17}$$

So

$$\dot{V}_x \leq -\dot{x}^T \left(C_{xx} + \boldsymbol{\alpha}_{\mathbf{f}} C_{x\theta} + K_{dx} - \Lambda_{\mathbf{f}x} \right) \dot{x} + \mathbf{f}_x^T \Lambda_{\mathbf{f}x}^{-1} \mathbf{f}_x \tag{4.18}$$

If we choose the gain $K_{dx} > 0$, and also since $\alpha_{\mathbf{f}}$ is positive definite matrix, $C_{xx} > 0, C_{x\theta} > 0$ we have:

$$\dot{V}_x \leq -\dot{x}^T Q_x \dot{x} + \bar{\mu}_{\mathbf{f}x} \leq -\lambda_m \left(Q_x \right) \|\dot{x}\|^2 + \mathbf{f}_x^T \Lambda_{\mathbf{f}x}^{-1} \mathbf{f}_x \tag{4.19}$$

where $Q_x = C_x + \alpha_{\mathbf{f}} C_{x\theta} + K_{dx} - \Lambda_{\mathbf{f}x} > 0$. $\dot{V}_x$ is therefore an ISS-Lyapunov function. Using Theorem 1 from [120], the boundedness of $f_x^T \Lambda_{\mathbf{f}x}^{-1} f_x \leq \bar{\mu}_{\mathbf{f}x}$ implies that the regulation error $\|\dot{x}\|$ is bounded,

$$\|\dot{x}\|_{Q_x}^2 > \bar{\mu}_{\mathbf{f}\dot{x}}, \quad \forall t \in [0, T] \tag{4.20}$$

then we can conclude that $\dot{V}_x < 0$ when $\|\dot{x}\|_{Q_x}^2 > \bar{\mu}_{\mathbf{f}\dot{x}}$. From (4.16) we have

$$\dot{x} = -\alpha_{\mathbf{f}}^{-1}\dot{\theta}, \quad |\dot{x}| = -\alpha_{\mathbf{f}}^{-1}\left|\dot{\theta}\right|, \quad |\dot{x}|\,|\dot{x}| = -\alpha_{\mathbf{f}}^{-1}\left|\dot{\theta}\right||\dot{x}|, \quad \|\dot{x}\|^2 = \alpha_{\mathbf{f}}^{-2}\left\|\dot{\theta}\right\|^2 \tag{4.21}$$

Implementing (4.21) in (4.20) we have

$$\left\|\dot{\theta}\right\|_{Q_x}^2 > \alpha_{\mathbf{f}}^2 \bar{\mu}_{\mathbf{f}x}, \forall t \in [0, \Upsilon] \tag{4.22}$$

Above condition also satisfy $\dot{V}_x < 0$ when $\left\|\dot{\theta}\right\|_{Q_x}^2 > \alpha_{\mathbf{f}}^2 \bar{\mu}_{\mathbf{f}x}$. Adding (4.20) and (4.22) we have

$$\|\dot{x}\|_{Q_x}^2 + \left\|\dot{\theta}\right\|_{Q_x}^2 > \bar{\mu}_{\mathbf{f}x} + \alpha_{\mathbf{f}}^2 \bar{\mu}_{\mathbf{f}x}, \forall t \in [0, T + \Upsilon] \tag{4.23}$$

Now we show that the total time during which $\|\dot{x}\|_{Q_x}^2 + \left\|\dot{\theta}\right\|_{Q_x}^2 > \bar{\mu}_{\mathbf{f}x} + \alpha_{\mathbf{f}}^2 \bar{\mu}_{\mathbf{f}x}$ is finite. Let T_k denotes the time interval during which $\|\dot{x}\|_{Q_x}^2 + \left\|\dot{\theta}\right\|_{Q_x}^2 > \bar{\mu}_{\mathbf{f}x} + \alpha_{\mathbf{f}}^2 \bar{\mu}_{\mathbf{f}x}$. $\|\dot{x}\|_{Q_x}^2 + \left\|\dot{\theta}\right\|_{Q_x}^2 > \bar{\mu}_{\mathbf{f}x} + \alpha_{\mathbf{f}}^2 \bar{\mu}_{\mathbf{f}x}$ will stay inside the circle in case $\|\dot{x}\|_{Q_x}^2 + \left\|\dot{\theta}\right\|_{Q_x}^2 > \bar{\mu}_{\mathbf{f}x} + \alpha_{\mathbf{f}}^2 \bar{\mu}_{\mathbf{f}x}$ stay outside the circle of radius $\bar{\mu}_{\mathbf{f}x} + \alpha_{\mathbf{f}}^2 \bar{\mu}_{\mathbf{f}x}$ for finite times and then reenter the circle. Also, $\sum_{k=1}^{\infty} T_k < \infty$, since the total time $\|\dot{x}\|_{Q_x}^2 + \left\|\dot{\theta}\right\|_{Q_x}^2 > \bar{\mu}_{\mathbf{f}x} + \alpha_{\mathbf{f}}^2 \bar{\mu}_{\mathbf{f}x}$ is finite and

$$\lim_{k \to \infty} T_k = 0 \tag{4.24}$$

So $\|\dot{x}\|_{Q_x}^2 + \left\|\dot{\theta}\right\|_{Q_x}^2$ is bounded via an invariant set argument. Also using (4.19) it can be shown that $\|\dot{\mathbf{x}}\|$ and $\left\|\dot{\boldsymbol{\theta}}\right\|$ are also bounded. Let $\|\dot{x}\|_{Q_x}^2 + \left\|\dot{\theta}\right\|_{Q_x}^2$ denotes the largest tracking error during the T_k interval. Then using (4.24) and bounded $\|\dot{x}\|_{Q_x}^2 + \left\|\dot{\theta}\right\|_{Q_x}^2$ imply that

$$\lim_{k \to \infty} \left[\|\dot{x}\|_{Q_x}^2 + \left\|\dot{\theta}\right\|_{Q_x}^2 - (\bar{\mu}_{\mathbf{f}x} + \alpha_{\mathbf{f}}^2 \bar{\mu}_{\mathbf{f}x}) \right] = 0$$

So $\|\dot{x}\|_{Q_x}^2 + \left\|\dot{\theta}\right\|_{Q_x}^2$ will converge to $\bar{\mu}_{\mathbf{f}x} + \alpha_{\mathbf{f}}^2 \bar{\mu}_{\mathbf{f}x}$. Therefore, the derivative of regulation error x and θ converges to the residual set

$$\dot{D}_x = \left\{ \dot{x}, \dot{\theta} \mid \|\dot{x}\|_{Q_x}^2 + \left\|\dot{\theta}\right\|_{Q_x}^2 \leq \bar{\mu}_{\mathbf{f}x} + \alpha_{\mathbf{f}}^2 \bar{\mu}_{\mathbf{f}x} \right\} \tag{4.25}$$

Also for $\|\dot{x}\|^2_{Q_x} > \bar{\mu}_{\mathbf{f}x}$, the total time is finite and hence $V_x = \frac{1}{2}\dot{x}^T M_x \dot{x} + \frac{1}{2}x^T K_{px}x$ is bounded, hence the regulation error $\dot{x}$ is bounded. Also for $\left\|\dot{\theta}\right\|^2_{Q_x} > \alpha^2_{\mathbf{f}}\bar{\mu}_{\mathbf{f}x}$, the total time is finite and hence assuming $V_\theta = \frac{1}{2}\dot{\theta}^T J_t \dot{\theta} + \frac{1}{2}\theta^T K_{p\theta}\theta$ it can be shown to be bounded and so regulation error $\dot{\theta}$ is also bounded, $\dot{\theta} = -\alpha_{\mathbf{f}}\dot{x}$ and $J_t = M_x r^2$. Again using the Lyapunov candidate $V_y = \frac{1}{2}\dot{y}^T M_y \dot{y} + \frac{1}{2}y^T K_{py}y$, and using the similar sort of stability analysis we can infer that the derivative of regulation error y and θ converges to the residual set

$$\dot{D}_y = \left\{\dot{y}, \dot{\theta} \mid \|\dot{y}\|^2_{Q_y} + \left\|\dot{\theta}\right\|^2_{Q_y} \leq \bar{\mu}_{\mathbf{f}y} + \boldsymbol{\eta}^2_{\mathbf{f}}\bar{\mu}_{\mathbf{f}y}\right\} \tag{4.26}$$

where

$$\dot{\theta} = \boldsymbol{\eta}_{\mathbf{f}}\dot{y} \tag{4.27}$$

is positive due to clockwise sense

$$Q_y = C_y + \boldsymbol{\eta}_{\mathbf{f}}C_{y\theta} + K_{dy} - \Lambda_{\mathbf{f}y} > 0.$$

For $\|\dot{y}\|^2_{Q_y} > \bar{\mu}_{\mathbf{f}y}$, the total time is finite and hence $V_y = \frac{1}{2}\dot{y}^T M_y \dot{y} + \frac{1}{2}y^T K_{py}y$ is bounded, hence the regulation error $\dot{y}$ is bounded. Also for $\left\|\dot{\theta}\right\|^2_{Qy} > \alpha^2_{\mathbf{f}}\bar{\mu}_{\mathbf{f}y}$, the total time is finite and hence assuming $V_\theta = \frac{1}{2}\dot{\theta}^T J_0 \dot{\theta} + \frac{1}{2}\theta^T K_{p\theta}\theta$ it can be shown to be bounded and so regulation error $\dot{\theta}$ is also bounded, $\dot{\theta} = \eta_{\mathbf{f}}\dot{y}$ and $J_t = M_y r^2$. Using the Lyapunov candidate $V_\theta = \frac{1}{2}\dot{\theta}^T J_0 \dot{\theta} + \frac{1}{2}\theta^T K_{p\theta}\theta$, and using the similar sort of stability analysis, we can infer that the derivative of regulation error x, y and θ converges to the residual set

$$\dot{D}_\theta = \left\{\dot{\theta}, \dot{x}, \dot{y} \mid \left\|\dot{\theta}\right\|^2_{Q_\theta} + \|\dot{x}\|^2_{Q_\theta} + \|\dot{y}\|^2_{Q_\theta} \leq \bar{\mu}_{\mathbf{f}\theta} + \boldsymbol{\alpha}^{-2}_{\mathbf{f}}\bar{\mu}_{\mathbf{f}x} + \boldsymbol{\eta}^{-2}_{\mathbf{f}}\bar{\mu}_{\mathbf{f}y}\right\} \tag{4.28}$$

where, $\dot{x} = -\alpha^{-1}_{\mathbf{f}}\dot{\theta}, \dot{y} = \eta^{-1}_{\mathbf{f}}\dot{\theta}, Q_\theta = C_\theta + \alpha^{-1}_{\mathbf{f}}C_{x\theta} + \eta^{-1}_{\mathbf{f}}C_{y\theta} + K_{d\theta} - \Lambda_{\mathbf{f}\theta} > 0$. For $\left\|\dot{\theta}\right\|^2_{Q\theta} > \bar{\mu}_{\mathbf{f}_\theta}$, the total time is finite and hence assuming $V_\theta = \frac{1}{2}\dot{\theta}^T J_0 \dot{\theta} + \frac{1}{2}\theta^T K_{p\theta}\theta$ it can be shown to be bounded and so regulation error $\dot{\theta}$ is also bounded. For $\|\dot{x}\|^2_{Q_\theta} > \alpha^{-2}_{\mathbf{f}}\bar{\mu}_{\mathbf{f}x}$, the total time is finite and hence $V_x = \frac{1}{2}\dot{x}^T M_x \dot{x} + \frac{1}{2}x^T K_{px}x$ is bounded, hence the regulation error $\dot{x}$ is bounded. For $\|\dot{y}\|^2_{Q_\theta} > \eta^{-2}_{\mathbf{f}}\bar{\mu}_{\mathbf{f}y}$, the total time is finite and hence $V_y = \frac{1}{2}\dot{y}^T M_y \dot{y} + \frac{1}{2}y^T K_{py}y$ is bounded, hence the regulation error $\dot{y}$ is bounded ∎

4.3.2   PID control

From the above section it is clear that in order to decrease the regulation errors caused by these uncertainties, the derivative gain K_d has to be increased, but will result in slow response. Now we analyze the stability of the bidirectional PID control (4.5). The equilibrium

of (4.7) is $[\boldsymbol{\xi}_x, x, \dot{x}] = [\boldsymbol{\xi}_x^*, \mathbf{0}, \mathbf{0}]$. Since at equilibrium point $x = 0$ and $\dot{x} = 0$, the equilibrium is $[\mathbf{f}(0), \mathbf{0}, \mathbf{0}]$. In order to move the equilibrium to origin, we define

$$\boldsymbol{\xi}_x = \boldsymbol{\xi}_x - \mathbf{f}(0) \tag{4.29}$$

The final closed-loop equation becomes

$$
\begin{aligned}
M_x \ddot{x} + (C_x + \boldsymbol{\alpha}_f C_{x\theta}) \dot{x} + \mathbf{f}_x &= -K_{px} x - K_{dx} \dot{x} - \boldsymbol{\xi}_x + \mathbf{f}(0) \\
\boldsymbol{\xi}_x &= K_{ix} x
\end{aligned} \tag{4.30}
$$

In a similar manner,

$$
\begin{aligned}
M_y \ddot{y} + (C_y + \boldsymbol{\eta_f} C_{y\theta}) \dot{y} + \mathbf{f}_y &= -K_{py} y - K_{dy} \dot{y} - \boldsymbol{\xi}_y + \mathbf{f}(0) \\
\boldsymbol{\xi}_y &= K_{iy} y \\
J_0 \ddot{\theta} + \left(C_\theta + \boldsymbol{\alpha}_f^{-1} C_{x\theta} + \boldsymbol{\eta_f}^{-1} C_{y\theta}\right) \dot{\theta} + \mathbf{f}_{\boldsymbol{\theta}} &= -K_{p\theta} \theta - K_{d\theta} \dot{\theta} - \boldsymbol{\xi}_\theta + \mathbf{f}(0) \\
\boldsymbol{\xi}_\theta &= K_{i\theta} \theta
\end{aligned} \tag{4.31}
$$

In order to analyze the stability of (4.30) and (4.31) we need the following properties.

P1. The positive definite matrix $M = M_x = M_y$ satisfies the following condition

$$
\begin{aligned}
0 &< \lambda_m(M) \leq \|M\| \leq \lambda_M(M) \leq \bar{m} \\
0 &< \lambda_{j_t}(J_t) \leq \|J_t\| \leq \lambda_{J_t}(J_t) \leq \bar{j}_t
\end{aligned}
$$

where $\lambda_m(M)$ and $\lambda_M(M)$ are the minimum and maximum eigenvalues of the matrix M, respectively and $\bar{m} > 0$ is the upper bound, $\lambda_{j_t}(J_t)$ and $\lambda_{J_t}(J_t)$ are the minimum and maximum eigenvalues of the matrix J_t, respectively and $\bar{j}_t > 0$ is the upper bound.

P2. The term f is Lipschitz over $\tilde{x}$ and $\tilde{y}$

$$\|\mathbf{f}(\tilde{x}) - \mathbf{f}(\tilde{y})\| \leq k_{\mathbf{f}} \|\tilde{x} - \tilde{y}\| \tag{4.32}$$

Most of the uncertainties are first-order continuous functions. Since f_s, f_e and $d_{\mathbf{u}}$ are first-order continuous functions and satisfy Lipschitz condition, P2 can be established.

We calculate the lower bound of $\int f \, dx$ as

$$\int_0^t \mathbf{f} \, dx = \int_0^t \mathbf{f}_s dx + \int_0^t \mathbf{f}_e dx + \int_0^t \mathbf{d_u} \, dx \tag{4.33}$$

Here we define the lower bound of $\int_0^t f_s dx$ as $-\bar{f}_s$, and $\int_0^t d_{\mathbf{u}} \, dx$ as $-\bar{d}_u$.

Compared with f_s and $d_{\mathbf{u}}$, f_e is much bigger in the case of earthquake. We define the lower bound of $\int_0^t f_e dx$ as $-\bar{f}_e$. Finally, the lower bound $k_{\mathbf{fx}}$ is

$$k_{\mathbf{fx}} = -\bar{f}_s - \bar{f}_e - \bar{d}_u \tag{4.34}$$

The following theorem gives the stability analysis of PID controller.

Theorem 4.2 *Consider the structural system as (3.13) controlled by the PID controller as (4.5), the closed-loop system (4.30) and (4.31) are asymptotically stable at the equilibriums* $[\boldsymbol{\xi}_x - \mathbf{f}(0), x, \dot{x}]^T = 0$, $[\boldsymbol{\xi}_y - \mathbf{f}(0), y, \dot{y}]^T = 0$ *and* $[\boldsymbol{\xi}_\theta - \mathbf{f}(0), \theta, \dot{\theta}]^T = 0$, *provided that the PID gains satisfy*

$$\lambda_m(K_{dx}) \geq \tfrac{1}{4}\sqrt{\tfrac{1}{3}\lambda_m(M_x)\lambda_m(K_{px})}\left[1 + \tfrac{k_{cx} + \alpha_f k_{cx\theta}}{\lambda_M(M_x)}\right]$$
$$-\lambda_m(C_x) - \lambda_m(\alpha_f C_{x\theta})$$
$$\lambda_M(K_{ix}) \leq \tfrac{1}{6}\sqrt{\tfrac{1}{3}\lambda_m(M_x)\lambda_m(K_{px})}\tfrac{\lambda_m(K_{px})}{\lambda_M(M_x)}$$
$$\lambda_m(K_{px}) \geq \tfrac{3}{2}[k_f + k_{cx} + \alpha_f k_{cx\theta}]$$

$$\lambda_m(K_{dy}) \geq \tfrac{1}{4}\sqrt{\tfrac{1}{3}\lambda_m(M_y)\lambda_m(K_{py})}\left[1 + \tfrac{k_{cy} + \boldsymbol{\eta_f} k_{cy\theta}}{\lambda_M(M_y)}\right]$$
$$-\lambda_m(C_y) - \lambda_m(\boldsymbol{\eta_f} C_{y\theta})$$
$$\lambda_M(K_{iy}) \leq \tfrac{1}{6}\sqrt{\tfrac{1}{3}\lambda_m(M_y)\lambda_m(K_{py})}\tfrac{\lambda_m(K_{py})}{\lambda_M(M_y)}$$
$$\lambda_m(K_{py}) \geq \tfrac{3}{2}[k_f + k_{cy} + \boldsymbol{\eta_f} k_{cy\theta}]$$

$$\lambda_{j_t}(K_{d\theta}) \geq \tfrac{1}{4}\sqrt{\tfrac{1}{3}\lambda_{j_t}(J_t)\lambda_{j_t}(K_{p\theta})}\left[1 + \tfrac{k_{c\theta} + \alpha_f^{-1} k_{cx\theta} + \boldsymbol{\eta_f}^{-1} k_{cy\theta}}{\lambda_{J_t}(J_t)}\right]$$
$$-\lambda_{j_t}(C_\theta) - \lambda_{j_0}(\alpha_f^{-1} C_{x\theta}) - \lambda_{j_0}(\boldsymbol{\eta_f}^{-1} C_{y\theta})$$
$$\lambda_{J_t}(K_{i\theta}) \leq \tfrac{1}{6}\sqrt{\tfrac{1}{3}\lambda_{j_t}(J_t)\lambda_{j_t}(K_{p\theta})}\tfrac{\lambda_{j_t}(K_{p\theta})}{\lambda_{J_t}(J_t)}$$
$$\lambda_{j_t}(K_{p\theta}) \geq \tfrac{3}{2}[k_f + k_{c\theta} + \alpha_f^{-1} k_{cx\theta} + \boldsymbol{\eta_f}^{-1} k_{cy\theta}]$$

Proof. Here the Lyapunov function is defined as

$$V_x = \frac{1}{2}\dot{x}^T M_x \dot{x} + \frac{1}{2}x^T K_{px} x + \frac{\sigma}{4}\boldsymbol{\xi}_x^T K_{ix}^{-1}\boldsymbol{\xi}_x + x^T \boldsymbol{\xi}_x + \frac{\sigma}{2}x^T M_x \dot{x} + \frac{\sigma}{4}x^T K_{dx} x + \int_0^t \mathbf{f}dx - k_{\mathbf{f}x} \quad (4.35)$$

where $V(0) = 0$. In order to show that $V_x \geq 0$, it is separated into three parts, such that $V_x = V_{x1} + V_{x2} + V_{x3}$

$$V_{x1} = \frac{1}{6}x^T K_{px} x + \frac{\sigma}{4}x^T K_{dx} x + \int_0^t \mathbf{f}dx - k_{\mathbf{f}x} \geq 0, K_{px} > 0, K_{dx} > 0 \qquad (4.36)$$

$$V_{x2} = \tfrac{1}{6}x^T K_{px} x + \tfrac{\sigma}{4}\boldsymbol{\xi}_x^T K_{ix}^{-1}\boldsymbol{\xi}_x + x^T \boldsymbol{\xi}_x$$
$$\geq \tfrac{1}{2}\tfrac{1}{3}\lambda_m(K_{px})\|x\|^2 + \tfrac{\sigma\lambda_m(K_{ix}^{-1})}{4}\|\boldsymbol{\xi}_x\|^2 - \|x\|\|\boldsymbol{\xi}_x\| \qquad (4.37)$$

When $\sigma \geq \frac{3}{(\lambda_m(K_{ix}^{-1})\lambda_m(K_{px}))}$,

$$V_{x2} \geq \frac{1}{2}\left(\sqrt{\frac{\lambda_m(K_{px})}{3}}\|x\| - \sqrt{\frac{3}{4(\lambda_m(K_{px}))}}\|\boldsymbol{\xi}_x\|\right)^2 \geq 0 \qquad (4.38)$$

and

$$V_{3x} = \frac{1}{6}x^T K_{px} x + \frac{1}{2}\dot{x}^T M \dot{x} + \frac{\sigma}{2}x^T M \dot{x} \tag{4.39}$$

Because

$$X^T A X \geq \|X\| \|A X\| \geq \|X\| \|A\| \|X\| \geq \lambda_M(A) \|X\|^2 \tag{4.40}$$

when

$$\sigma \leq \frac{1}{2}\frac{\sqrt{\frac{1}{3}\lambda_m(M_x)\lambda_m(K_{px})}}{\lambda_M(M_x)}$$

$$V_{x3} \geq \frac{1}{2}\left(\frac{1}{3}\lambda_m(K_{px})\|x\|^2 + \lambda_m(M_x)\|\dot{x}\|^2 + \sigma\lambda_M(M_x)\|x\|\|\dot{x}\|\right)$$
$$= \frac{1}{2}\left(\sqrt{\frac{\lambda_m(K_{px})}{3}}\|x\| + \sqrt{\lambda_m(M_x)}\|\dot{x}\|\right)^2 \geq 0 \tag{4.41}$$

Now we have,

$$\frac{1}{2}\frac{\sqrt{\frac{1}{3}\lambda_m(M_x)\lambda_m(K_{px})}}{\lambda_M(M_x)} \geq \sigma \geq \frac{3}{(\lambda_m(K_{ix}^{-1})\lambda_m(K_{px}))} \tag{4.42}$$

The derivative of (4.35) is

$$\dot{V}_x = \dot{x}^T M_x \ddot{x} + \dot{x}^T K_{px} x + \frac{\sigma}{2}\boldsymbol{\xi}_x^T K_{ix}^{-1} \boldsymbol{\xi}_x + \dot{x}^T \boldsymbol{\xi_x}$$
$$+ x^T \boldsymbol{\xi}_x + \frac{\sigma}{2}\dot{x}^T M_x \dot{x} + \frac{\sigma}{2}x^T M_x \ddot{x} + \sigma \dot{x}^T K_{dx} x + \dot{x}^T \mathbf{f} \tag{4.43}$$

Using (4.14) we can write

$$-\frac{\sigma}{2}x^T C_{xx}\dot{x} \leq \frac{\sigma}{2}k_{c_x}\left(x^T x + \dot{x}^T \dot{x}\right) \tag{4.44}$$
$$-\frac{\sigma\alpha_f}{2}x^T C_{x\theta}\dot{x} \leq \frac{\sigma\alpha_f}{2}k_{c_{x\theta}}\left(x^T x + \dot{x}^T \dot{x}\right)$$

where $\|C_x\| \leq k_{c_x}$.and $\|C_{x\theta}\| \leq k_{c_{x\theta}}$. So $\xi_x = K_{ix}$, $\xi^T K_{ix}^{-1}\xi$ becomes $x^T\xi$, and $x^T\xi$ becomes $x^T K_{ix}$. Using (4.44) we have

$$\dot{V}_x = -\dot{x}^T\left[C_x + \alpha_f C_{x\theta} + K_{dx} - \frac{\sigma}{2}M_x - \frac{\sigma}{2}k_{c_x} - \frac{\sigma\alpha_f}{2}k_{c_{x\theta}}\right]\dot{x}$$
$$-x^T\left[\frac{\sigma}{2}K_{px} - K_{ix} - \frac{\sigma}{2}k_{c_x} - \frac{\sigma\alpha_f}{2}k_{c_{x\theta}}\right]x - \frac{\sigma}{2}x^T\left[\mathbf{f}_x - \mathbf{f}(0)\right] + \dot{x}^T f(0) \tag{4.45}$$

Now using the Lipschitz condition (4.32)

$$\frac{\sigma}{2}x^T\left[\mathbf{f}(0) - \mathbf{f_x}\right] \leq \frac{\sigma}{2}k_{\mathbf{f}}\|x\|^2 \tag{4.46}$$
$$-\frac{\sigma}{2}x^T\left[\mathbf{f}_x - \mathbf{f}(0)\right] \leq x^T\frac{\sigma}{2}k_{\mathbf{f}}x$$

From (4.14),

$$\dot{x}^T f(0) \geq -f^T(0)\Lambda^{-1T}f(0) \tag{4.47}$$

Using (4.46)

$$
\begin{aligned}
\dot{V}_x = &-\dot{x}^T \left[C_x + \alpha_f C_{x\theta} + K_{dx} - \tfrac{\sigma}{2} M_x - \tfrac{\sigma}{2} k_{c_x} - \tfrac{\sigma\alpha_f}{2} k_{c_{x\theta}} \right] \dot{x} \\
&-x^T \left[\tfrac{\sigma}{2} K_{px} - K_{ix} - \tfrac{\sigma}{2} k_{c_{xx}} - \tfrac{\sigma\alpha_f}{2} k_{c_{x\theta}} - \tfrac{\sigma}{2} k_f \right] x + \dot{x}^T f(0)
\end{aligned}
\tag{4.48}
$$

(4.48) becomes

$$
\begin{aligned}
\dot{V}_x \le &-\dot{x}^T \left[\lambda_m(C_x) + \lambda_m(\alpha_f C_{x\theta}) + \lambda_m(K_{dx}) - \tfrac{\sigma}{2} \lambda_M(M_x) - \tfrac{\sigma}{2} k_{c_x} - \tfrac{\sigma\alpha_f}{2} k_{c_{x\theta}} \right] \dot{x} \\
&-x^T \left[\tfrac{\sigma}{2} \lambda_m(K_{px}) - \lambda_M(K_{ix}) - \tfrac{\sigma}{2} k_{c_{xx}} - \tfrac{\sigma\alpha_f}{2} k_{c_{x\theta}} - \tfrac{\sigma}{2} k_f \right] x
\end{aligned}
\tag{4.49}
$$

So $\dot{V}_x \le 0$, $\|x\|$ minimizes if two conditions are met: 1) $\lambda_m(C_x) + \lambda_m(\alpha_f C_{x\theta}) + \lambda_m(K_{dx}) \ge \tfrac{\sigma}{2}[\lambda_M(M_x) + k_{c_x} + \alpha_f k_{c_{x\theta}}]$; 2) $\lambda_m(K_{px}) \ge \tfrac{2}{\sigma}\lambda_M(K_{ix}) + k_{c_x} + \tfrac{\sigma\alpha_f}{2} k_{c_{x\theta}} + k_f$. Now using (4.42) and $\lambda_m\left(K_{ix}^{-1}\right) = \tfrac{1}{\lambda_M(K_{ix})}$, we have

$$
\lambda_m\left(K_{dx}\right) \ge \frac{1}{4}\sqrt{\frac{1}{3}\lambda_m\left(M_x\right)\lambda_m\left(K_{px}\right)} \left[1 + \frac{k_{c_x} + \alpha_f k_{c_{x\theta}}}{\lambda_M\left(M_x\right)} \right] - \lambda_m(C_x) - \lambda_m(\alpha_f C_{x\theta})
\tag{4.50}
$$

again $\tfrac{2}{\sigma}\lambda_M(K_{ix}) = \tfrac{2}{3}\lambda_m(K_{px})$. Hence,

$$
\lambda_M(K_{ix}) \le \frac{1}{6}\sqrt{\frac{1}{3}\lambda_m\left(M_x\right)\lambda_m\left(K_{px}\right)}\frac{\lambda_m(K_{px})}{\lambda_M\left(M_x\right)}
\tag{4.51}
$$

Also

$$
\lambda_m(K_{px}) \ge \frac{3}{2}[k_f + k_{c_x} + \alpha_f k_{c_{x\theta}}]
\tag{4.52}
$$

By the Lyapunov function

$$
V_y = \frac{1}{2}\dot{y}^T M_y \dot{y} + \frac{1}{2}y^T K_{py} y + \frac{\sigma}{4}\boldsymbol{\xi}_y^T K_{iy}^{-1}\boldsymbol{\xi}_y + y^T \boldsymbol{\xi}_y + \frac{\sigma}{2}y^T M_y \dot{y} + \frac{\sigma}{4}y^T K_{dy} y + \int_0^t \mathbf{f}\,dy - k_{\mathbf{f}y}
\tag{4.53}
$$

Similarly we can prove, $V_y \ge 0$ and thus using stability analysis criteria we can prove $\dot{V}_y \le 0$ if

$$
\begin{aligned}
\lambda_m\left(K_{dy}\right) &\ge \tfrac{1}{4}\sqrt{\tfrac{1}{3}\lambda_m\left(M_y\right)\lambda_m\left(K_{py}\right)} \left[1 + \tfrac{k_{cy} + \boldsymbol{\eta_f} k_{c_{y\theta}}}{\lambda_M(M_y)} \right] - \lambda_m(C_y) - \lambda_m(\boldsymbol{\eta_f} C_{y\theta}) \\
\lambda_M(K_{iy}) &\le \tfrac{1}{6}\sqrt{\tfrac{1}{3}\lambda_m\left(M_y\right)\lambda_m\left(K_{py}\right)}\tfrac{\lambda_m(K_{py})}{\lambda_M(M_y)} \\
\lambda_m(K_{py}) &\ge \tfrac{3}{2}[k_f + k_{c_y} + \boldsymbol{\eta_f} k_{c_{y\theta}}]
\end{aligned}
\tag{4.54}
$$

From Lyapunov function

$$
V_\theta = \frac{1}{2}\dot{\theta}^T J_0 \dot{\theta} + \frac{1}{2}\theta^T K_{p\theta}\theta + \frac{\sigma}{4}\boldsymbol{\xi}\theta K_{i\theta}^{-1}\boldsymbol{\xi}_\theta + \theta^T \boldsymbol{\xi}_\theta + \frac{\sigma}{2}\theta^T J_0 \dot{\theta} + \frac{\sigma}{4}\theta^T K_{dy}\theta + \int_0^t \mathbf{f}\,d\boldsymbol{\theta} - k_{\mathbf{f}\theta}
\tag{4.55}
$$

Similarly we can prove, $V_{\boldsymbol{\theta}} \geq 0$. Thus we can prove $\dot{V}_{\boldsymbol{\theta}} \leq 0, \|\boldsymbol{\theta}\|$ decreases if

$$\lambda_{j_t}(K_{d\theta}) \geq \tfrac{1}{4}\sqrt{\tfrac{1}{3}\lambda_{j_t}(J_t)\lambda_{j_t}(K_{p\theta})}\left[1 + \tfrac{k_{c_\theta}+\alpha_f^{-1}k_{c_{x\theta}}+\boldsymbol{\eta_f}^{-1}k_{c_{y\theta}}}{\lambda_{J_t}(J_t)} - \lambda_{j_t}(C_\theta) - \lambda_{j_t}(\alpha_f^{-1}C_{x\theta}) - \lambda_{j_t}(\boldsymbol{\eta_f}^{-1}C_{y\theta})\right]$$
$$\lambda_{J_t}(K_{i\theta}) \leq \tfrac{1}{6}\sqrt{\tfrac{1}{3}\lambda_{j_t}(J_t)\lambda_{jt}(K_{p\theta})}\tfrac{\lambda_{j_t}(K_{p\theta})}{\lambda_{J_t}(J_t)}$$
$$\lambda_{j_0}(K_{p\theta}) \geq \tfrac{3}{2}[k_f + k_{c_{\theta\theta}} + \alpha_f^{-1}k_{c_{x\theta}} + \boldsymbol{\eta_f}^{-1}k_{c_{y\theta}}]$$

$$(4.56)$$

■

The above theorems suggest that the closed loop system is asymptotically stable. But we cannot decide on the global stability of the closed loop system. This is due to the fact that the hysteresis property is associated with the stiffness of the structure. The hysteresis output depends on the deformation factor all time. This deformation behaves according to the application or removal of forces. So the deformation are not same before and after the application of forces and hence the equilibrium position is also not static. Therefore the equilibrium position before and after the earthquake are not same. The stable point get shifted after an earthquake event.

Let us consider a ball of radius ς in the three dimensional space. This three dimensional space is represented by X-component, Y-component and $\theta-$component. The ball center is at origin of the state space system where: $\dot{V}_x \leq 0, \dot{V}_y \leq 0, \dot{V}_\theta \leq 0$. The origin of the closed loop systems represented by (4.39), (4.40) and (4.41) are stable equilibrium. Now we will prove for the asymptotic stability of the origin. For that we use La Salle´s theorem by defining the term Π_x, Π_y and Π_θ as follows:

$$\Pi_x = \left\{\bar{z}_x(t) = \left[x^T, \dot{x}^T, \xi_x^T\right]^T \in \Re^{3n} : \dot{V}_x = 0\right\}, \xi_x \in \Re^n, x = 0 \in \Re^n, \dot{x} = 0 \in \Re^n$$
$$\Pi_y = \left\{\bar{z}_y(t) = \left[y^T, \dot{y}^T, \xi_y^T\right]^T \in \Re^{3n} : \dot{V}_y = 0\right\}, \xi_y \in \Re^n, y = 0 \in \Re^n, \dot{y} = 0 \in \Re^n \qquad (4.57)$$
$$\Pi_\theta = \left\{\bar{z}_\theta(t) = \left[\theta^T, \dot{\theta}^T, \xi_\theta^T\right]^T \in \Re^{3n} : \dot{V}_\theta = 0\right\}, \xi_\theta \in \Re^n, \theta = 0 \in \Re^n, \dot{\theta} = 0 \in \Re^n$$

Using (4.54) and substituting $x = 0$ and $\dot{x} = 0$, we have $\dot{V}_x = 0$. Similar analysis with $y = 0$ and $\dot{y} = 0$ and also $\theta = 0$ and $\dot{\theta} = 0$ will yield $\dot{V}_y = 0$ and $\dot{V}_\theta = 0$. Similarly these conditions hold good for $\dot{x} = 0, \dot{y} = 0$ and $\dot{\theta} = 0$ for all $t \geq 0$. Therefore $\bar{z}_x(t), \bar{z}_y(t)$ and $\bar{z}_\theta(t)$ belongs to Π_x, Π_y and Π_θ respectively. Also, imparting these conditions to (4.39), (4.40) and (4.41) we have: $\dot{\xi}_x = 0, \dot{\xi}_y = 0$ and $\dot{\xi}_\theta = 0$. Also, $\xi_x = 0, \xi_y = 0$ and $\xi_\theta = 0$ for all $t \geq 0$. So $\bar{z}_x(t)$ is the only initial condition in Π_x, $\bar{z}_y(t)$ is the only initial condition in Π_y and $\bar{z}_\theta(t)$ is the only initial condition in Π_θ. Therefore, origin is asymptotically stable according to La Salle´s theorem.
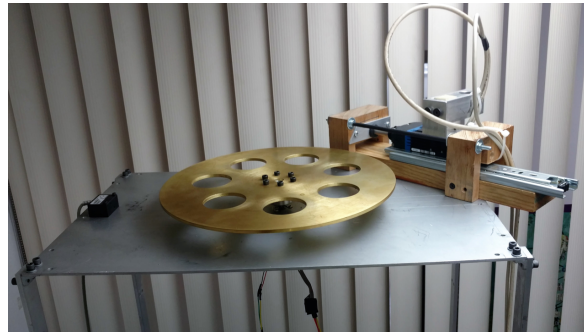
Figure 4.1: Placement of AMD and TA

4.4   Experimental comparison results

In order to analyze and validate the bidirectional PD/PID controllers, a two-floor structure is designed and constructed as mentioned in the section experimental set up.. This structure is then mounted on the shake table to carry out the experimental analysis which is illustrated using Figure 8.7. The bidirectional shake table uses two Quanser one degree of freedom (I-40), which move in X and Y directions.

The AMD and TA are placed on the second floor of the structure. The total moving mass of the horizontal actuator and torsional actuator are taken to be the 5% of the total mass of the structure. The eccentricity of the physical center are 16 cm from X-direction and 27 cm from Y-direction. The eccentricity of the mass center are 15 cm from X-direction and 11 cm from Y-direction. The TA is placed on the physical center whereas the AMD is placed on the mass center. The position of the AMD and the TA can be seen in Figure 4.1

The entire programming is carried out using the Matlab and Simulink version R2011a. The Simulink programs is used to generate the control actions for AMD and TA as well as for the movement of shake table. For creating a synchronization between Matlab and Quanser devices, Quarc accelerate design version 2.3.603 is installed. The control actions between the computer and the dampers are synchronized using RT-DAC/USB data acquisition board. The link between Simulink and RT-DAC/USB is achieved using RT CON toolbox which is provided with the hardware RT-DAC/USB. All the control actions were employed at a sampling frequency of 1 kHz. The biaxial accelerometers (XL403A) are mounted on each floor.

The acceleration of ground floor is subtracted from first floor acceleration and second floor acceleration respectively, to get the relative value of the acceleration. A numerical

integrator is used to compute the velocity and position from the accelerometer signal [129]. The displacement of the floors are calculated using an accelerometer. Since the accelerometer used is a bidirectional one, the acceleration are obtained along X-component and Y-component. These accelerations along X-component and Y- component are integrated to extract velocity in the first instance and again integrated to extract positions in the next instance. Although after each integration, filter is used for the correction of signals. An offset cancellation filter (OCF) is proposed, which completely removes the DC components present in the accelerometer output. In order to avoid the drift caused by low frequency noise signals, a special high-pass filter is used. A frequency-domain method is used to estimate the low frequency noise components present in the accelerometer output. The high-pass filter is designed offline according to these noise components. Since the OCF reduces the number of high-pass filtering stages, there is less phase error. The numerical integrator combines the OCF and a highpass filter.

There is no angular sensor to calculate the angular acceleration of the structure. The angular accelerations are calculated by

$$
\begin{aligned}
\ddot{\theta}_1 = & -\left(\frac{C_{\theta 01}+C_{\theta 02}}{m_1 r_1^2}\right)\dot{\theta}_1 + \left(\frac{C_{\theta 02}}{m_1 r_1^2}\right)\dot{\theta}_2 - \left(\frac{K_{\theta 01}+K_{\theta 02}}{m_1 r_1^2}\right)\theta_1 + \left(\frac{K_{\theta 02}}{m_1 r_1^2}\right)\theta_2 \\
& +\left(\frac{C_{x_1}l_{y_1}+C_{x_2}l_{y_2}}{m_1 r_1^2}\right)\dot{x}_1 - \left(\frac{C_{x_2}l_{y_2}}{m_1 r_1^2}\right)\dot{x}_2 + \left(\frac{K_{x_1}l_{y_1}+K_{x_2}l_{y_2}}{m_1 r_1^2}\right)x_1 - \left(\frac{K_{x_2}l_{y_2}}{m_1 r_1^2}\right)x_2 \\
& -\left(\frac{C_{y_1}l_{x_1}+C_{y_2}l_{x_2}}{m_1 r_1^2}\right)\dot{y}_1 + \left(\frac{C_{y_2}l_{x_2}}{m_1 r_1^2}\right)\dot{y}_2 - \left(\frac{K_{y_1}l_{x_1}+K_{y_2}l_{x_2}}{m_1 r_1^2}\right)y_1 + \left(\frac{K_{y_2}l_{x_2}}{m_1 r_1^2}\right)y_2
\end{aligned}
\tag{4.58}
$$

$$
\begin{aligned}
\ddot{\theta}_2 = & -\left(\frac{C_{\theta 02}}{m_2 r_2^2}\right)\dot{\theta}_1 - \left(\frac{C_{\theta 02}}{m_2 r_2^2}\right)\dot{\theta}_2 + \left(\frac{K_{\theta 02}}{m_2 r_2^2}\right)\theta_1 - \left(\frac{K_{\theta 02}}{m_2 r_2^2}\right)\theta_2 \\
& +\left(\frac{C_{x_2}l_{y_2}}{m_2 r_2^2}\right)\dot{x}_1 + \left(\frac{C_{x_2}l_{y_2}}{m_2 r_2^2}\right)\dot{x}_2 - \left(\frac{K_{x_2}l_{y_2}}{m_2 r_2^2}\right)x_1 + \left(\frac{K_{x_2}l_{y_2}}{m_2 r_2^2}\right)x_2 \\
& +\left(\frac{C_{y_2}l_{x_2}}{m_2 r_2^2}\right)\dot{y}_1 - \left(\frac{C_{y_2}l_{x_2}}{m_2 r_2^2}\right)\dot{y}_2 - \left(\frac{K_{y_2}l_{x_2}}{m_2 r_2^2}\right)y_1 - \left(\frac{K_{y_2}l_{x_2}}{m_2 r_2^2}\right)y_2
\end{aligned}
\tag{4.59}
$$

where $\ddot{\theta}_1$ and $\ddot{\theta}_2$ are the angular accelerations of the first and the second floor, C_i, l_i , m_i, and r_i are structural parameters of the building. They are identified by the least square algorithm [130]. The identification process is achieved by identifying the ratio of the parameters corresponding to the mass, damping and stiffness of a building excited by a seismic activity. The algorithm is based on a parametrization combined with the Recursive Least Square Method with forgetting factor. The algorithm is a real time that identifies the parameters of a building model using acceleration measurements of the floors and the ground.

The structural parameters of the two-floor building are identified and fed into the algorithms along with the values of positions and velocities for the calculation of the angular accelerations. The velocities and positions $\dot{x}_1, \dot{y}_1, \dot{x}_2, \dot{y}_2$ and x_1, y_1, x_2, y_2 extracted from the acceleration signals are substituted in the (4.58) and (4.59) to obtain the angular accelera-

tions of ground and top floor. The angular velocities and angular positions $\dot{\theta}_1, \dot{\theta}_2$ and θ_1, θ_2 are obtained from angular accelerations $\ddot{\theta}_1$ and $\ddot{\theta}_2$ by using the same numerical integrator.

The theorems of this paper provide sufficient conditions for the minimal values of the proportional and derivative gains as well as maximum values of the integral gains. For the sake of carrying out a relevant comparison between the PD and PID controller, it is desirable to use same proportional and derivative gains.

In this paper, the PD/PID gains are chosen so as to ensure satisfactory performance as well as within the range specified by the stability theory analysis. The following PD gains are used for the control design:

$$\begin{aligned} \lambda_m\left(M_x\right) = 10, \lambda_m(k_{c_x}) = 20, \lambda_m(k_{c_{x\theta}}) = 8, \lambda_m\left(M_y\right) = 10, \lambda_m(k_{c_y}) = 22 \\ \lambda_m(k_{c_{y\theta}}) = 6, \lambda_{j_t}\left(J_0\right) = 5, \lambda_m(k_{c_\theta}) = 21, \lambda_m(k_{c_{x\theta}}) = 8, \lambda_m(k_{c_{y\theta}}) = 6, k_f = 700 \end{aligned} \quad (4.60)$$

From Theorem 2, we use the following PID gains

$$\begin{aligned} \lambda_m(K_{px}) \geq 1092, \lambda_m\left(K_{dx}\right) \geq 55, \lambda_M(K_{ix}) \leq 2324, \lambda_m(K_{py}) \geq 1092 \\ \lambda_m\left(K_{dy}\right) \geq 55, \lambda_M(K_{iy}) \leq 2324, \lambda_{j_0}(K_{p\theta}) \geq 1102, \lambda_{j_0}\left(K_{d\theta}\right) \geq 85, \lambda_{J_0}(K_{i\theta}) \leq 3563 \\ K_{px} = 1800, K_{py} = 2000, K_{p\theta} = 2200, K_{dx} = 160 \\ K_{dy} = 220, K_{d\theta} = 300, K_{ix} = 2000, K_{iy} = 2300, K_{i\theta} = 3500 \end{aligned} \quad (4.61)$$

Here the proportional and derivative gains are the same as the PD gains in (4.60).

The performance validation of these controllers are implemented by the vibration control with respect to the seismic execution on the prototype. Northridge earthquake signal is used to vibrate the shake table. The magnitude $6.7M_w$ earthquake that occurred near Northridge, California on 17th January, 1994 produced an extensive set of strong-motion recordings. The epicenter is located about $32km$ nortwest of Los Angeles in the densely populated San Fernando Valley. Analysis by the USGS and Caltech indicates that the earthquake had a thrust mechanism on a fault plane striking $N60^0W$ and dipping $35 - 45^0S$. The estimated location and magnitude of the Northridge earthquake are:

Epicenter: 34.209^0N, 118.541^0W. Focal Depth: $19km$ (Caltech/USGS). Origin Time: $12:30:55.4, 17January1994UTC(4.30AM, PST)$.Magnitude: $6.7M_w$ (Caltech).

The duration of the strong shaking is about $10s$ to $15s$. The peak vertical acceleration is about two-thirds of the peak horizontal. The displacement of the Northridge earthquake is scaled from $16.92cm$ to $1.50cm$, whereas the time is scaled from $39.98s$ to $11.91s$. This is done to suit the experimental conditions as the maximum allowed movement of the shake table from the reference point on the either side is $2\ cm$. So considering the maximum limit
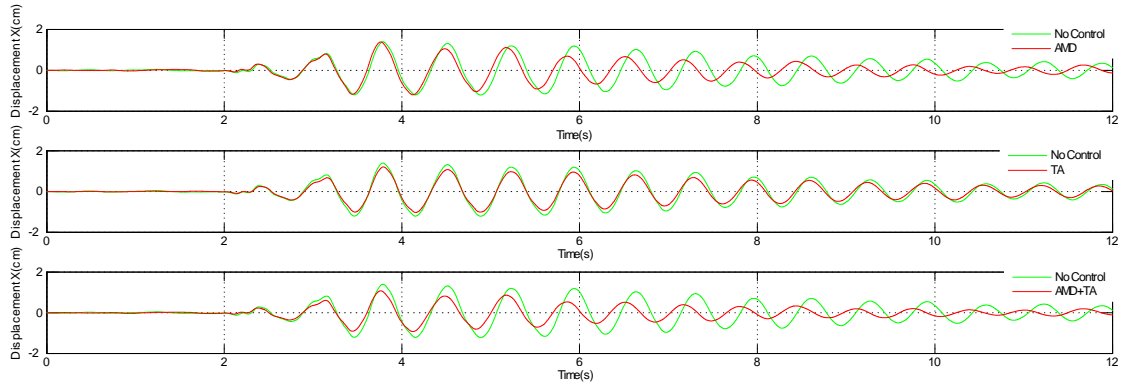
Figure 4.2: PD control of the second floor in X-direction
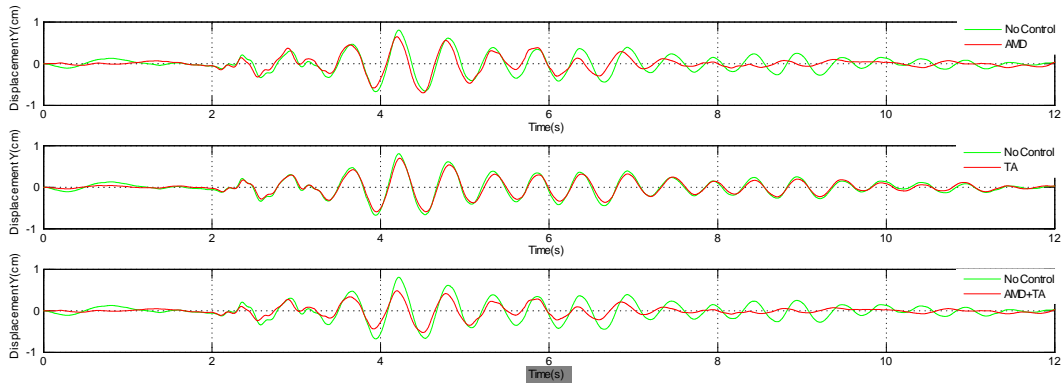
Figure 4.3: PD control of the second floor in Y-direction

of movement, the time is scaled to match the experimental analysis. The control object is to minimize the relative displacement of each floor in bidirection.

The comparisons in the bidirectional PD and PID vibration controllers are carried out considering three cases: 1) without any active control (No Control); 2) with the torsional actuator ; 3) with both the horizontal actuator and the torsional actuator (AMD+TA). The vibration reductions are in three directions: $X-$direction, $Y-$direction and θ-direction.

The average vibration displacement are calculated by the mean squared error as

$$MSE = \frac{1}{N} \sum_{k=1}^{N} x\left(k\right)^2$$

where $x\left(k\right)$ is the displacement of the floor, N is the total data number.
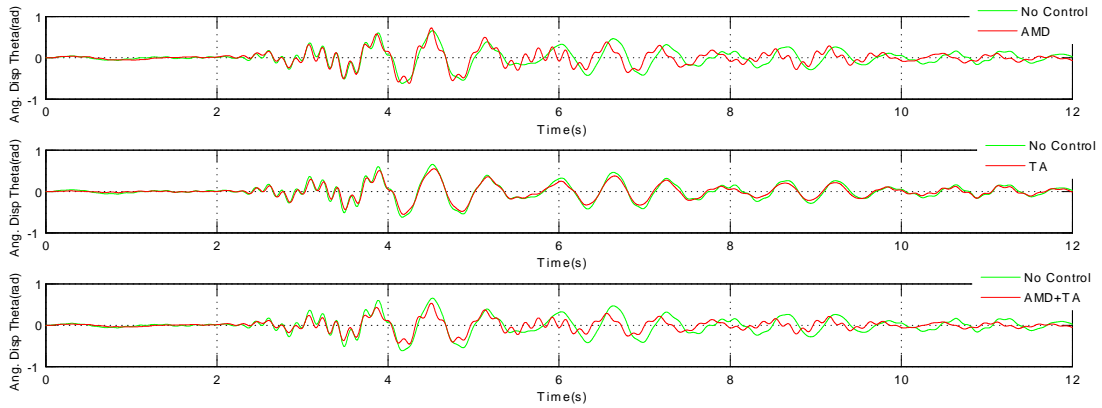
Figure 4.4: PD control of the second floor in θ-direction
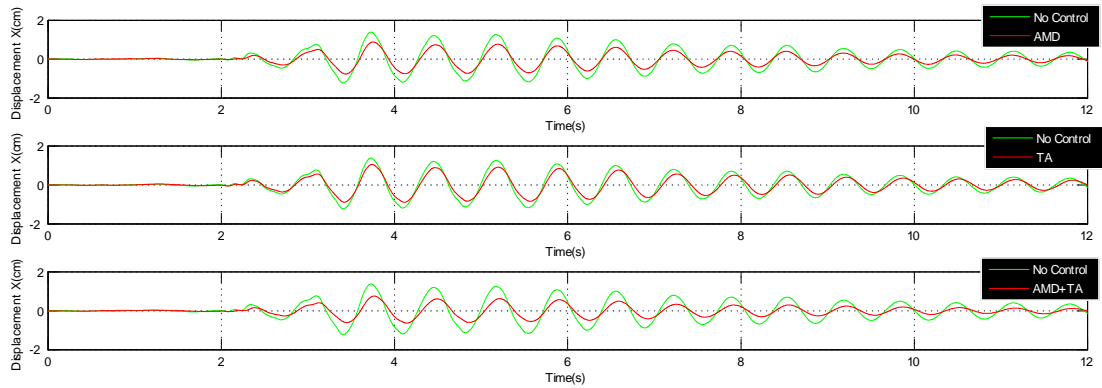
Figure 4.5: PID control of the second floor in X-direction
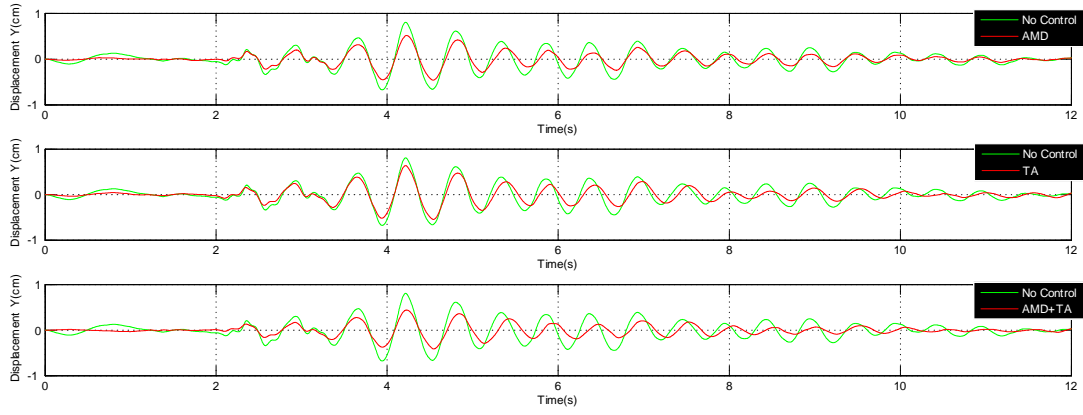
Figure 4.6: PID control of the second floor in Y-direction
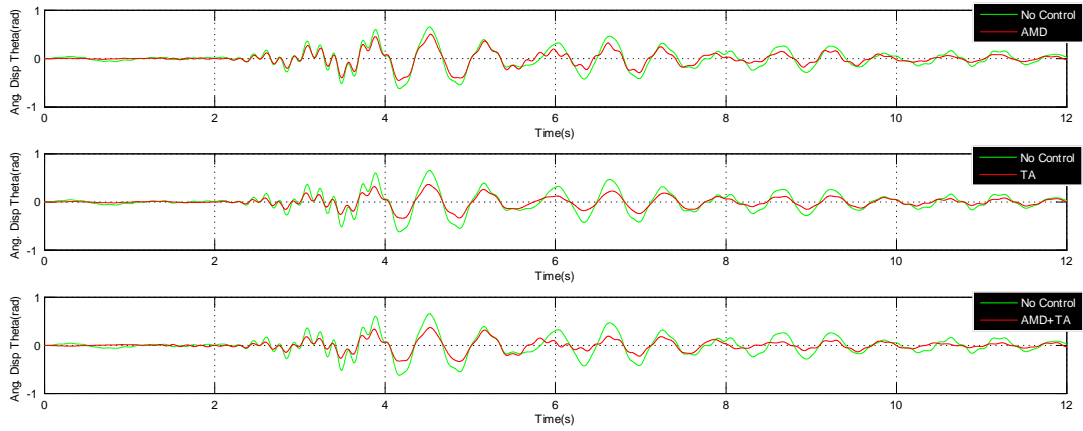
Figure 4.7: PID control of the second floor in θ-direction
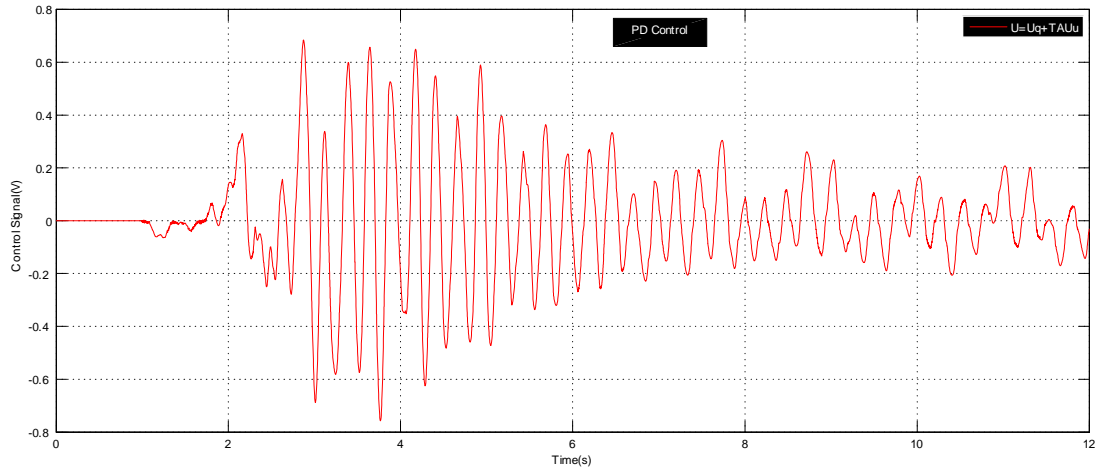
Figure 4.8: The PD control signal
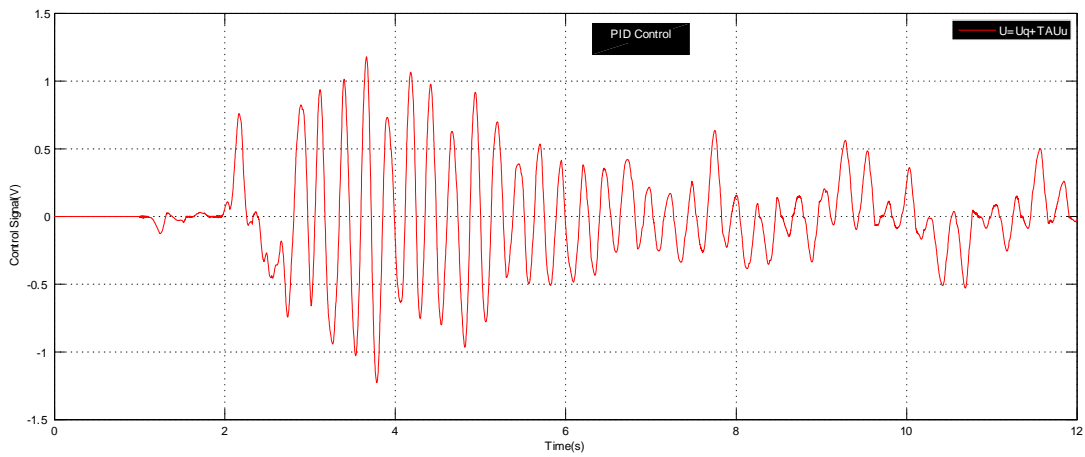
Figure 4.9: PID control signal

The comparison results of the average vibration displacement are shown in Table 1 - Table 3. Here ↓ sign indicate decrease.

Table 1. Average vibration displacement by AMD+TA

	PD control	% ↓ error	PID control	% ↓ error	No control
X-direction	0.2987	60.2	0.2373	68.5	0.7514
Y-direction	0.0719	45.53	0.0783	59.3	0.1320
θ-direction	0.0696	40.8	0.0611	47.6	0.1174

Table 2. Average vibration displacement with PD control

	with AMD	% ↓ error	with TA	% ↓ error	No control
X-direction	0.4832	35.7	0.5802	22.78	0.7514
Y-direction	0.0981	25.68	0.1012	23.3	0.1320
θ-direction	0.0902	23.1	0.0801	31.7	0.1174

Table 3. Average vibration displacement with PID control

	with AMD	% ↓ error	with TA	% ↓ error	No control
X-direction	0.3632	51.6	0.4911	34.6	0.7514
Y-direction	0.0849	35.6	0.0969	26.5	0.1320
θ-direction	0.0811	30.8	0.0713	40.0	0.1174

Figure 4.2 - Figure 4.4 displays the action of the PD control to curb the vibration along $X-$direction, $Y-$direction and θ-direction. Table 1 - Table 3 represents the quantitative analysis of vibration control with both the actuators using PD/PID control along $X-$direction, $Y-$direction and θ-direction. If we analyze Figure 4.2 - Figure 4.4 as well as Table 1 and Table 2, it can be observed that horizontal actuator performs good in the vibration control along $X-$direction and $Y-$direction but fails to mitigate vibration to suitable extent along the θ-direction. But if we analyze the behavior of torsional actuator, it can be observed that torsional actuator performs superiorly in mitigating the vibration along θ-direction but fails to attenuate vibration to acceptable extent along $X-$direction and $Y-$direction. When horizontal actuator and torsional actuator acts simultaneously, it is observed that the results of vibration attenuation is much better along $X-$direction, $Y-$direction and θ-direction. The main reason behind this is that superior vibration control is achieved in combination as respective actuators performs well in their assigned zones. Figure 4.5 - Figure 4.7 displays the action of the PID control to curb the vibration along

X−direction, Y−direction and θ-direction. The analysis of PID control from Table 1 and Table 3 reveals that PID controller performs much better than PD controller in controlling vibration along X−direction, Y−direction and θ-direction. The behavior of horizontal actuator and torsional actuator with PID controller follows the same pattern as with the PD controller and it can be observed from the Figures and quantitative analysis that combined action of the actuators achieves high vibration attenuation. Figure 4.8 and Figure 4.9 represents the control signal of PD control and PID control respectively.

4.5   Summary

In this chapter, a two-floor structure associated with one horizontal actuator and one torsional actuator for active vibration control is proposed. The theoretical contribution is the stability analysis for the bidirectional PD/PID control. The sufficient conditions of stability are extracted in order to tune the PD/PID gains. The two theorems stated in this chapter validates the conditions which are sufficient for selecting the minimum values of the proportional and derivative gains. Also the minimum values of the integral gains are extracted on the basis of the Theorem 2. The range of the proportional, derivative and integral gains are specified using the Lyapunov stability theorem and is assured that on the basis of the selected gains, the controller performs in the superior manner. It is observable that both PD and PID controllers work well with horizontal actuator and torsional actuator. The experimental results shows that the PID controller is better than the PD controller in minimizing the vibration in all three directions. By comparing the quantitative analysis as displayed by Table 1-Table 3, it can be concluded that the PID controller in combination with both horizontal actuator and torsional actuator are considered to be the most efficient in mitigation of vibration along X−direction, Y−direction and θ-direction. The use of Torsional actuator facilities the torsional vibration attenuation but it fails to attenuate vibration along X-direction and Y-direction to considerable extent with PD controller, but when PID controller is used the vibration control using torsional actuator along X-direction and Y-direction is much better. The vibration attenuations along X-direction and Y-direction are effectively achieved by horizontal actuator but it fails to attenuate vibration considerably along θ-direction with PD controller in comparison with PID controller. As we can see from the quantitative analysis that with PID controller, the mitigation of vibration along θ-direction with horizontal actuator is slightly better. Further works on the design of torsional actuator is needed so that it can minimize the vibrations to suitable extent along all three directions.

Chapter 5

Bidirectional Type-2 Fuzzy PD/PID Control of Building Structures

Fuzzy logic has obtained many attentions in control of structure because of its simple nature, robustness and nonlinear mapping capability [22]. [107] presents a numerical study to show the effectiveness of a supervisory fuzzy logic controller for seismic response control of an eight story base isolated structure effected by translation-torsional motion. The combination of fuzzy logic and PD control has more degrees of freedom to tune the mass damper for the structure vibration [50]. In [103], a fuzzy supervisory method is used for the active control of building structures. In [32], the semi-active control of building under the earthquake is implemented with the concept of fuzzification related to MR damper characteristics. The concept of optimal fuzzy control is utilized to the structure under the seismic forces in [39]. An optimal fuzzy control for suppressing vibration of buildings by utilizing magneto-rheological (MR) dampers is proposed in [6]. Fuzzy control with hybrid mass damper for the torsionally couple problem is discussed in [4].

The concept of type-2 fuzzy sets has been presented in [86]. The type-2 fuzzy system has effective ways to deal with knowledge uncertainty compared with classical type-1 fuzzy logic, because the type-2 fuzzy sets can deal uncertainties with more parameters and more design degrees of freedom [112]. A simplified type-2 fuzzy system can be applied in the real-time application [88]. For the vibration control of single degree of freedom, [115] uses active tuned mass damper and type-2 fuzzy control. In [15], a semi-active tuned mass damper combined with adaptive magnetorheological damper are utilized, the type-1 and type-2 fuzzy controllers are implemented.

In this chapter, we will use the type-2 fuzzy control to compensate the regulation errors of

PD and PID controllers. The main parts of the controllers are PD and PID, while the nonlinearity are compensated by the type-2 fuzzy system. We use a disc with motor arrangement as the torsional actuator to minimize the torsional response of the building. The sufficient conditions for asymptotic stability of PD/PID with type-2 fuzzy system are validated. The conditions are quite convenient for the design of the controller gains. An active vibration control system is designed with two floor building structure equipped with AMD and TA . The experimental results are obtained by using the type-2 fuzzy PD/PID controllers. Compared to the other active vibration controllers, our type-2 Fuzzy PD/PID controllers do not have big derivative and integral gains. So the results of our active controllers are much better than the others.

5.1   PD control with type-2 fuzzy compensation

The horizontal actuator (AMD) and torsional actuator (TA) are placed on the structure in the similar manner as mentioned in chapter 3. All the dynamic equations related to AMD and TA are also mentioned in chapter 3. The closed-loop system (3.13) with the control $\mathbf{u}$ is

$$M\ddot{\mathbf{x}} + C\dot{\mathbf{x}} + S\mathbf{x} + \mathbf{f}_e + \Gamma\mathbf{d_u} = \Gamma(-K_p\mathbf{x} - K_d\dot{\mathbf{x}}) \tag{5.1}$$

The active vibration control of the building structure can be regarded as the regulation problem with zero reference,

$$\mathbf{u} = -K_p\mathbf{x} - K_d\dot{\mathbf{x}} \tag{5.2}$$

where $\mathbf{x} = [x, y, \theta]^T$ defined as in (3.8). Here the reference $\mathbf{x}^d = \dot{\mathbf{x}}^d = 0$, the regulation error $\mathbf{e} = \mathbf{x} - \mathbf{x}^d = \mathbf{x}$, K_p and K_d are positive-definite constant matrices that correspond to the proportional and derivative gains. The closed-loop system with the PD control is

$$M\ddot{\mathbf{x}}(t) + C\dot{\mathbf{x}}(t) + \mathbf{F} = -\Gamma\left(K_p\mathbf{x} + K_d\dot{\mathbf{x}}\right) \tag{5.3}$$

where $\mathbf{F}$ is the uncertainty,

$$\mathbf{F} = \mathbf{Sx} + \mathbf{f_e} + \mathbf{\Gamma d_u} = [f_x, f_y, f_\theta]^T \tag{5.4}$$

Since $\mathbf{F}$ is unknown, we use a fuzzy system to approximate it. Compared with normal fuzzy sets, type-2 fuzzy sets can model easily for big magnitude uncertainties with less fuzzy rules. The membership functions of type-2 fuzzy systems are not longer the crisp values , they are in the interval of $[0, 1]$ [86][112].

A generic fuzzy model for the uncertainty $\mathbf{F}$ in i-th floor is provided by a collection of p fuzzy rules for x, y, and θ

R^i: IF $(x_i$ is $A_{1i})$ and $(y_i$ is $A_{2i})$ and $(\theta_i$ is $A_{3i})$ and $(\dot{x}_i$ is $A_{4i})$ and $(\dot{y}_i$ is $A_{5i})$ and $\left(\dot{\theta}_i$ is $A_{6i}\right)$ THEN $(f_x$ is $B_{1i})$ and $(f_y$ is $B_{2i})$ and $(f_\theta$ is $B_{3i})$ (5.5)

where $A_{1i}\cdots$, A_{6i}, B_{1i}, B_{3i}, B_{3i} are type-2 fuzzy sets. The type-2 fuzzy set A with the membership function G_A is defined as

$$A = \{(x, \varsigma), G_A(x, \varsigma) \mid \forall x \epsilon R, \forall \varsigma \epsilon M_x \subseteq [0, 1]\} \tag{5.6}$$

where ς is an auxiliary variable, $0 \leqslant G_A(x, \varsigma) \leqslant 1$, M_x is the primary membership function. For the type-2 fuzzy set A,

$$A = \int_{x\epsilon X} \int_{\varsigma\epsilon M_x} G_A(x, \varsigma)/(x, \varsigma)$$

The integral $\int$ of the classical fuzzy set becomes the sum $\sum$.

The upper and lower membership functions are defined as $G_A^u(x_1, \varsigma)$ and $G_A^l(x, \varsigma)$. They describe the upper and lower bounds of the uncertainties. For i-th rule and the point x_1, the crisp input is fuzzified in the interval of $[f_i^l(x_1), f_i^u(x_1)]$,

$$f_i^u(x_1) = G_{A_{1i}}^u(x_1, \varsigma) * G_{A_{2i}}^u(x_1, \varsigma) * G_{A_{3i}}^u(x_1, \varsigma)$$
$$f_i^l(x_1) = G_{A_{1i}}^l(x_1, \varsigma) * G_{A_{2i}}^l(x_1, \varsigma) * G_{A_{3i}}^l(x_1, \varsigma) \tag{5.7}$$

where $*$ denote t-norm operator, it can be the minimization.

For all l rules, type-2 fuzzy inference engine aggregates with the fuzzified inputs and infers another type-2 fuzzy set,

$$G_O(y) = \sqcup_{x\epsilon X}[G_A(x) \sqcap G_B(x, y)] \tag{5.8}$$

We use the type-reduction method to convert $G_O(y)$ into type-1 fuzzy set. This technique

captures more information about rule uncertainties than does the defuzzified value (a crisp number), and seems to be as fundamental to the design of fuzzy logic systems that include linguistic uncertainties (that translate into rule uncertainties) as variance is to the mean in case of probabilistic uncertainties. The centroids associated with type-2 fuzzy sets are calculated. For i-th rule, the centroid of j-the output fuzzy rule (5.5) is $y_j^i = [y_{lj}^i, y_{rj}^i]$, y_{lj}^i and y_{rj}^i are the most left and right points. The type-2 fuzzy sets are reduced to the type-1 fuzzy set with the interval $[y_{lj}^i, y_{rj}^i]$. The most popular technique for type-reducing an interval

type-2 fuzzy set is the Karnik–Mendel (KM) iterative procedure [68]. The outcome of type-reduction of an interval type-2 fuzzy set is an interval type-1 set considering the criteria that the centroid is placed between the two endpoints. The iterative methodology is a superior technique in order to find these endpoints. The centroid of the type-1 set is considered to be the centre of this interval. Mendel [95] laid down the main design criteria in consideration to type-2 uncertainty measurement as when all sources of uncertainty disappear, a type-2 fuzzy logic system must reduce to a comparable type-1 fuzzy logic system. This proposed statement is valid throughout. So it is valid from the proposed statement that is no uncertainty associated with a type-1 fuzzy set, and therefore the mentioned measures of uncertainty for type-1 fuzzy sets [138] cannot be measuring uncertainty instead they are measuring separate aspect of the type-1 set to be mentioned as vagueness.

For all p rules

$$y_{lj} = \frac{\sum_{i=1}^{p} f_l^i y_{lj}^i}{\sum_{i=1}^{p} f_l^i}, \quad y_{rj} = \frac{\sum_{i=1}^{p} f_r^i y_{rj}^i}{\sum_{i=1}^{p} f_r^i} \tag{5.9}$$

where f_l^i and f_r^i are the firing strengths associated with y_{lj}^i and y_{rj}^i of i-th rule. By the minimization and maximization operation, y_{lj} and y_{rj} can be expressed as

$$y_{lj} = \frac{\sum_{i=1}^{p} f_{lj}^i y_{lj} + \sum_{i=1}^{p} f_{rj}^i y_{lk}}{\sum_{i=1}^{q} f_r^i + \sum_{i=1}^{q} f_l^i}, \quad y_{rj} = \frac{\sum_{i=1}^{p} f_{lj}^i y_{rj} + \sum_{i=1}^{p} f_{rj}^i y_{rk}}{\sum_{i=1}^{q} f_r^i + \sum_{i=1}^{q} f_l^i} \tag{5.10}$$

where $q_{lj}^i = \frac{f_l^i}{\sum_{i=1}^{q} f_r^i + \sum_{i=1}^{q} f_l^i}$, $q_{rj}^i = \frac{f_r^i}{\sum_{i=1}^{q} f_r^i + \sum_{i=1}^{q} f_l^i}$. By singleton fuzzifier, the jth output of the fuzzy logic system can be expressed as

$$\hat{f}_j = \frac{y_{rj} + y_{lj}}{2} = \frac{1}{2} \left[(\phi_{rj}^T(z) w_{rj}(z) + \phi_l^T(z) w_{lj}(z) \right] \tag{5.11}$$

where $j = 1, 2, 3$. w_{rj} is the point at which $\mu_{B_{rj}} = 1$, w_{lj} is the point at which $\mu_{B_{lj}} = 1$, $z = \left[x, y, \theta, \dot{x}, \dot{y}, \dot{\theta} \right]^T$. In matrix form, the estimation of the uncertainty $\mathbf{F}$ is

$$\hat{\mathbf{F}} = \frac{1}{2} \left[\Phi_r^T(z) W_r(z) + \Phi_l^T(z) W_l(z) \right] \tag{5.12}$$

where $\hat{\mathbf{F}} = \left[\hat{f}_1, \hat{f}_2, \hat{f}_3 \right] = [\hat{f}_x, \hat{f}_y, \hat{f}_\theta]^T$.

PD control with type-2 fuzzy compensation is

$$\mathbf{u} = -K_p \mathbf{x} - K_d \dot{\mathbf{x}} - \frac{1}{2} \Phi_r^T(z) W_r(z) - \frac{1}{2} \Phi_l^T(z) W_l(z) \tag{5.13}$$

The new closed-loop system is

$$
\begin{bmatrix} M_x\ddot{x} \\ M_y\ddot{y} \\ J_t\ddot{\theta} \end{bmatrix} + \begin{bmatrix} C_x\dot{x} - C_{x\theta}\dot{\theta} \\ C_y\dot{y} + C_{y\theta}\dot{\theta} \\ C_\theta\dot{\theta} - C_{x\theta}\dot{x} + C_{y\theta}\dot{y} \end{bmatrix} + \begin{bmatrix} f_x \\ f_y \\ f_\theta \end{bmatrix}
$$
$$
= -\Gamma \begin{bmatrix} K_{px}x \\ K_{py}y \\ K_{p\theta}\theta \end{bmatrix} - \Gamma \begin{bmatrix} K_{dx}\dot{x} \\ K_{dy}\dot{y} \\ K_{d\theta}\dot{\theta} \end{bmatrix} - \frac{1}{2}\Gamma \begin{bmatrix} \phi_r^T(z_x)w_r(z_x) + \phi_l^T(z_x)w_l(z_x) \\ \phi_r^T(z_y)w_r(z_y) + \phi_l^T(z_y)w_l(z_y) \\ \phi_r^T(z_\theta)w_r(z_\theta) + \phi_l^T(z_\theta)w_l(z_\theta) \end{bmatrix}
$$

(5.14)

where $K_{px}, K_{dx}, K_{py}, K_{dy}, K_{p\theta}, K_{d\theta}$ are the gains considering $X-$component, $Y-$component and $\theta-$component respectively.

Because the three components, x, y and θ, has the same form, in the following stability analysis, we only discuss $X-$component. $Y-$component and $\theta-$component have similar results. In order to simplify the controller, we let $\Gamma = I$.

Because $K_{px}x + K_{dx}\dot{x} = K_x(\Lambda x + \dot{x})$, Λ is the positive definite matrix, $K_x\Lambda = K_{px}$, $K_x = K_{dx}$, we define an auxiliary variable r_x as

$$r_x = \dot{x} + \Lambda x \tag{5.15}$$

So

$$u_x = -K_x r_x - \frac{1}{2}\phi_r^T(z_x)w_r(z_x) - \frac{1}{2}\phi_l^T(z_x)w_l(z_x) \tag{5.16}$$

where $z_x = (x, \dot{x})$. The closed-loop system of $X-$component becomes

$$M_x\ddot{x} + C_x\dot{x} - C_{x\theta}\dot{\theta} + f_x = u_x \tag{5.17}$$

The X-component also gives the torsion in the structure,

$$\dot{\theta} = -\alpha_f \dot{x} \tag{5.18}$$

(5.17) becomes

$$M_x\ddot{x} + C_x\dot{x} + \alpha_f C_{x\theta}\dot{x} + f_{\mathbf{x}} = u_x \tag{5.19}$$

Because $M_x\dot{r}_x = M_x(\ddot{x} + \Lambda\dot{x})$, using (5.19) we have

$$M_x\dot{r}_x + C_x r_x + \alpha_f C_{x\theta}r_x = u_x + \Delta f_x \tag{5.20}$$

where $\Delta f_x = M_x\Lambda\dot{x} + C_x\Lambda x + \alpha_f C_{x\theta}\Lambda x - f_{\mathbf{x}}$.

With Stone-Weierstrass theorem [16], Δf_x can be estimated by the type-2 fuzzy system (5.12) as

$$\Delta f_x = \frac{1}{2}\phi_r^T(z_x)w_r^*(z_x) + \frac{1}{2}\phi_l^T(z_x)w_l^*(z_x) + \sigma_x \tag{5.21}$$

where σ_x is the modeling error, w_r^* and w_l^* are unknown optimal weights. We assumed it is bounded as

$$\sigma_x^T \Lambda_\sigma^{-1} \sigma_x \leq \bar{\sigma}_x \tag{5.22}$$

where Λ_σ is a known positive definite matrix.

With the type-2 fuzzy PD control (5.16), the closed-loop system (5.20) becomes

$$M_x \dot{r}_x + C_x r_x + \alpha_f C_{x\theta} r_x = -K_x r_x - \frac{1}{2}\phi_r^T(z_x)\tilde{w}_r(z_x) - \frac{1}{2}\phi_l^T(z_x)\tilde{w}_l(z_x) + \sigma_x \tag{5.23}$$

where $\tilde{w}_r = w_r - w_r^*$, $\tilde{w}_l = w_l - w_l^*$.

The following theorem gives the stability analysis of type-2 fuzzy PD control (5.13) with a gradient descent algorithms for $w_r(z_x)$ and $w_l(z_x)$. The major advantage of this method is that fuzzy rules or membership functions can be learned without changing the form of the fuzzy rule table used in usual fuzzy controls, so that the case of weak-firing can be avoided well, which is different from the conventional learning algorithm.

Theorem 5.1 *Consider the structural system (5.1) controlled by the type-2 fuzzy PD controller as (5.16), if the gain satisfies*

$$K_x > \Lambda_\sigma \tag{5.24}$$

Λ_σ is defined in (5.22), the fuzzy system is updated as

$$\begin{aligned}
\frac{d}{dt}w_r(z_x) &= -[k_w r_x^T \phi_r^T(z_x)]^T \\
\frac{d}{dt}w_l(z_x) &= -[k_w r_x^T \phi_l^T(z_x)]^T
\end{aligned} \tag{5.25}$$

$k_w > 0$, then the filter regulation errors r_x and r_θ converges to the residual sets

$$\begin{aligned}
D_x &= \left\{r_x|\, \|r_x\|^2 \leq \bar{\sigma}_x\right\} \\
D_\theta &= \left\{r_\theta|\, \|r_\theta\|^2 \leq \alpha_f^2 \bar{\sigma}_x\right\}
\end{aligned} \tag{5.26}$$

$\bar{\sigma}_x$ is defined in (5.22).

Proof. Since M_x and Λ are positive definite matrices, let us consider Lyapunov candidate V_x for the $X-$component

$$V_x = \frac{1}{2}r_x^T M_x r_x + \frac{1}{4}tr_x[\tilde{w}_r^T(z_x)k_w^{-1}\tilde{w}_r(z_x)] + \frac{1}{4}tr_x[\tilde{w}_l^T(z_x)k_w^{-1}\tilde{w}_l(z_x)] \tag{5.27}$$

Using (5.23) and $r_x^T\left(\dot{M}_x - 2C_x\right)r_x = 0$, the derivative of (5.27) is

$$\begin{aligned}
\dot{V}_x = &-r_x^T K_x r_x - \frac{1}{2}r_x^T \phi_r^T(z_x)\tilde{w}_r(z_x) - \frac{1}{2}r_x^T \phi_l^T(z_x)\tilde{w}_l(z_x) + r_x^T \sigma_x - r_x^T \alpha_f C_{x\theta} r_x \\
&+ \frac{1}{2}tr_x[\tilde{w}_r^T(z_x)k_w^{-1}\frac{d}{dt}\tilde{w}_r(z_x)] + \frac{1}{2}tr_x[\tilde{w}_l^T(z_x)k_w^{-1}\frac{d}{dt}\tilde{w}_l(z_x)]
\end{aligned} \tag{5.28}$$

Using the updating law (5.25), and

$$\frac{1}{2}tr_x[\tilde{w}_r^T(z_x)k_w^{-1}\frac{d}{dt}\tilde{w}_r(z_x)] - \frac{1}{2}r_x^T\phi_l^T(z_x)\tilde{w}_l(z_x) = 0$$
$$\frac{1}{2}tr_x[\tilde{w}_l^T(z_x)k_w^{-1}\frac{d}{dt}\tilde{w}_l(z_x)] - \frac{1}{2}r_x^T\phi_l^T(z_x)\tilde{w}_l(z_x) = 0$$

(5.28) becomes

$$\dot{V}_x = -r_x^T K_x r_x + r_x^T \sigma_x - r_x^T \alpha_f C_{x\theta} r_x \tag{5.29}$$

Now let us consider matrix inequality as follows

$$X^T Y + Y^T X \leq X^T \Lambda X + Y^T \Lambda^{-1} Y \tag{5.30}$$

for all $X, Y \in R^n$, $0 < \Lambda = \Lambda^T$. From (5.22), $r_x^T \sigma_x$ can be estimated as

$$r_x^T \sigma_x \leq r_x^T \Lambda_\sigma r_x + \sigma_x^T \Lambda_\sigma^{-1} \sigma_x \leq r_x^T \Lambda_\sigma r_x + \bar{\sigma}_x \tag{5.31}$$

where $\Lambda_\sigma > 0$. Since $\alpha_f C_{x\theta} > 0$, (5.29) is

$$\dot{V}_x \leq -r_x^T(K_x + \alpha_f C_{x\theta} - \Lambda_\sigma)r_x + \sigma_x^T \Lambda_\sigma^{-1} \sigma_x$$
$$\leq -r_x^T(K_x - \Lambda_\sigma)r_x + \sigma_x^T \Lambda_\sigma^{-1} \sigma_x \tag{5.32}$$

We can choose the gain of the PD control (5.16), such that (5.24) is established, then

$$\dot{V}_x \leq -\|r_x\|_{K_1}^2 + \bar{\sigma}_x \tag{5.33}$$

where $K_1 = K_x - \Lambda_\sigma$. V_x is considered to be ISS-Lyapunov function. In this case, $r_x = \dot{x} + \Lambda x$ is bounded when σ_x is bounded by $\bar{\sigma}_x$ [120]. Because $\int_0^T \dot{V}_x = V_T - V_0 \leq -\int_0^T r_x^T K_x r_x dt + \bar{\sigma}_x T$,

$$\lim_{T\to\infty} \frac{1}{T}\int_0^T \|r_x\|_{K_1}^2 dt \leq \bar{\sigma}_x$$

Since $\dot{x} = -\alpha_f^{-1}\dot{\theta}$ and $|r_x| = -\alpha_f^{-1}|r_\theta|$, the filter regulation error for θ can be

$$r_\theta = \dot{\theta} + \Lambda\theta \tag{5.34}$$

So

$$\dot{V}_x \leq -\|r_\theta\|_{K_2}^2 + \bar{\sigma}_x \tag{5.35}$$

where $K_2 = \alpha_f^{-2}K_1$. So $r_\theta = \dot{\theta} + \Lambda\theta$ is bounded, and

$$\lim_{T\to\infty} \frac{1}{T}\int_0^T \|r_\theta\|_{K_1}^2 dt \leq \alpha_f^2\bar{\sigma}_x \tag{5.36}$$

They are (5.26). ■

Remark 5.1 *Compared with the fuzzy compensation (5.13), the advantage of adaptive fuzzy compensation (5.23) is that we do not need to be concerned about the big compensation error in equation (5.21), which results from a poor membership function selection. The gradient algorithms (5.25) ensures that the membership functions $w_r(z_x)$ and $w_l(z_x)$ are updated such that the regulation errors r_x and r_θ are reduced. The above theorem also guarantees the updating algorithms are stable. It is well known that the regulation error becomes smaller while increasing the derivative gain. The cost of large derivative gain results in slow transient performance. Only when derivative gain tends to infinity, the regulation error converges to zero [76] . However it would seem better to use a smaller derivative gain if the system contains high-frequency noise signals. In order to decrease the steady state errors caused by these uncertainties, the derivative gain K_d has to be increased. The transient performances are worsen, for example the response becomes slow.*

5.2   PID control with type-2 fuzzy compensation

The utilization of fuzzy compensation results in the decrease of regulation error as mentioned in Theorem 1. Considering the control theory, the steady state error can be removed to more extent by introducing an integral component to the PD control. PID controllers use feedback strategy and have three actions: P action is introduced for increasing the speed of response; D action is introduced for damping purposes; I action is introduced for obtaining a desired steady-state response. Considering the effect of all three components of control, the control law is PID control

$$\mathbf{u} = -K_p\mathbf{x} - K_i \int_0^t \mathbf{x}d\tau - K_d\dot{\mathbf{x}} \tag{5.37}$$

where K_p, K_i and K_d are positive definite, K_i is the integration gain, for the structure control considering the reference $x^d = \dot{\mathbf{x}}^d = 0$.

A big integration gain causes unacceptable transient performances and stability problems. Same as of type-2 fuzzy PD control, a type-2 fuzzy compensator for PID control can be applied. PID control with type-2 fuzzy control is

$$\mathbf{u} = -K_p\mathbf{x} - K_i \int_0^t \mathbf{x}d\tau - K_d\dot{\mathbf{x}} - \frac{1}{2}\Phi_r^T(z)\hat{W}_r(z) - \frac{1}{2}\Phi_l^T(z)\hat{W}_l(z) \tag{5.38}$$

Similar with PD control, we only consider the $X-$component (5.19),

$$u_x = -K_{px}x - K_{dx}\dot{x} - K_{ix} \int_0^t xd\tau - \frac{1}{2}\phi_r^T(z_x)w_r(z_x) - \frac{1}{2}\phi_l^T(z_x)w_l(z_x) \tag{5.39}$$

In matrix form, (5.19) is

$$
\frac{d}{dt}\begin{bmatrix} s_x \\ x \\ \dot{x} \end{bmatrix} = \begin{bmatrix} K_{ix}x \\ \dot{x} \\ -M_x(C_x\dot{x} + \alpha_f C_{x\theta}\dot{x} + f_{\mathbf{x}} - u_x) \end{bmatrix} \tag{5.40}
$$

where s_x is auxiliary variable.

By using (5.21), the closed loop systems is

$$
\begin{aligned}
&M_x\ddot{x} + (C_x + \alpha_f C_{x\theta})\dot{x} + \tfrac{1}{2}\phi_r^T(z_x)w_r^*(z_x) + \tfrac{1}{2}\phi_l^T(z_x)w_l^*(z_x) + \sigma_x \\
&= -K_{px}x - K_{dx}\dot{x} - s_x - \tfrac{1}{2}\phi_r^T(z_x)\tilde{w}_r(z_x) - \tfrac{1}{2}\phi_l^T(z_x)\tilde{w}_l(z_x)
\end{aligned} \tag{5.41}
$$

The equilibrium of (5.40) is $[s_x, x, \dot{x}] = [s_x^*, 0, 0]$. Since at equilibrium point $x = 0$ and $\dot{x} = 0$, the equilibrium is $[\sigma_x(0), 0, 0]$. In order to move the equilibrium to origin, we define

$$
\tilde{s}_x = s_x - \sigma_x(0) \tag{5.42}
$$

where σ_x is the unknown modeling error. The closed loop system becomes

$$
\begin{aligned}
&M_x\ddot{x} + (C_x + \alpha_f C_{x\theta})\dot{x} + \tfrac{1}{2}\phi_r^T(z_x)w_r^*(z_x) + \tfrac{1}{2}\phi_l^T(z_x)w_l^*(z_x) + \sigma_x \\
&= -K_{px}x - K_{dx}\dot{x} - \tilde{s}_x - \tfrac{1}{2}\phi_r^T(z_x)\tilde{w}_r(z_x) - \tfrac{1}{2}\phi_l^T(z_x)\tilde{w}_l(z_x) + \sigma_x(0) \\
&\tfrac{d}{dt}\tilde{s}_x = K_{ix}x
\end{aligned} \tag{5.43}
$$

where $\tilde{w}_r = w_r - w_r^*$, $\tilde{w}_l = w_l - w_l^*$.

For the dynamics (3.13) in chapter 3, we need the following properties to prove stability of fuzzy PID control.

P1. The positive definite matrix M_x satisfies the following condition

$$
0 < \lambda_m(M_x) \le \|M_x\| \le \lambda_M(M_x) \le \bar{m} \tag{5.44}
$$

where $\lambda_m(M_x)$ and $\lambda_M(M_x)$ are the minimum and maximum eigenvalues of the matrix M_x, respectively and $\bar{m} > 0$ is the upper bound

P2. The modeling error σ_x is Lipschitz over x_1 and x_2

$$
\|\sigma_x(x_1) - \sigma_x(x_2)\| \le k_{\boldsymbol{\sigma}_{\mathbf{x}}} \|x_1 - x_2\| \tag{5.45}
$$

where $k_{\boldsymbol{\sigma}_{\mathbf{x}}}$ is the Lipschitz constant. Most of the uncertainties are first-order continuous functions. Since f_{sx}, f_{xe} and d_{ux} are first-order continuous functions and satisfy Lipschitz condition, **P2** can be established.

Now we calculate the lower bound of the modeling error $\int \sigma_x dx$,

$$\int_0^t \sigma_x dx = \int_0^t f_{sx} dx + \int_0^t f_{xe} dx + \int_0^t d_{ux} dx - \frac{1}{2} \int_0^t \phi_r^T(z_x) w_r(z_x) dx - \frac{1}{2} \int_0^t \phi_l^T(z_x) w_l(z_x)$$
(5.46)

Here we define the lower bound of $\int_0^t f_{sx} dx$ as $\bar{f}_{sx}$, $\int_0^t f_{xe} dx$ as $\bar{f}_{xe}$ and $\int_0^t d_{ux}\, dx$ as $\bar{d}_{ux}$.

Compared with f_{sx} and d_{ux}, f_{xe} is much bigger in the case of earthquake. Since $\phi_r^T(z_x)$ and $\phi_l^T(z_x)$ are Gaussian function, $\frac{1}{2}\int_0^t \phi_r^T(z_x) w_r(z_x) dx = \frac{W_r(z)}{4}\sqrt{\pi}\operatorname{erf}(z)$ and$\frac{1}{2}\int_0^t \phi_l^T(z_x) w_l(z_x) = \frac{W_l(z)}{4}\sqrt{\pi}\operatorname{erf}(z)$

$$k_{\sigma_\mathbf{x}} = -\bar{f}_{sx} - \bar{f}_{xe} - \bar{d}_{ux} - \frac{W_r(z)}{4}\sqrt{\pi} - \frac{W_l(z)}{4}\sqrt{\pi}$$
(5.47)

Here $\sigma_x(0)$ is considered to be zero as it is concerned to building structures.

The following theorem gives the stability analysis of type-2 fuzzy PID controller (5.39).

Theorem 5.2 *Consider the structural system as (5.1) controlled by the type-2 fuzzy PID controller as (5.39), the closed-loop system (5.41) is asymptotically stable at the equilibriums*

$$[s_x - \sigma_x(0), x, \dot{x}]^T = 0$$

if the PID control gains satisfy

$$\lambda_m(K_{px}) \geq \tfrac{3}{2}[k_{\sigma_\mathbf{x}} + \lambda_M(C_x) + \lambda_M(\alpha_f C_{x\theta})]$$
$$\lambda_M(K_{ix}) \leq \tfrac{1}{6}\sqrt{\tfrac{1}{3}\lambda_m(M_x)\lambda_m(K_{px})}\frac{\lambda_m(K_{px})}{\lambda_M(M_x)} \qquad (5.48)$$
$$\lambda_m(K_{dx}) \geq \tfrac{1}{4}\sqrt{\tfrac{1}{3}\lambda_m(M_x)\lambda_m(K_{px})}\left[1 + \frac{\lambda_M(C_x)+\lambda_M(\alpha_f C_{x\theta})}{\lambda_M(M_x)}\right] - \lambda_m(C_x) - \lambda_m(\alpha_f C_{x\theta})$$

where k_w is positive definite matrix, $\mu_x > 0$ is a design parameter, $\lambda_m(M)$ and $\lambda_M(M)$ are the minimum and maximum eigenvalues of the matrix M. The updating law for the type-2 fuzzy compensator is

$$\frac{d}{dt}w_r(z_x) = -[k_w(\dot{x} + \tfrac{\mu_x}{2}x)^T \phi_r^T(z_x)]^T$$
$$\frac{d}{dt}w_l(z_x) = -[k_w(\dot{x} + \tfrac{\mu_x}{2}x)^T \phi_l^T(z_x)]^T \qquad (5.49)$$

Proof. Here the Lyapunov candidate is defined as

$$V = \tfrac{1}{2}\dot{x}^T M_x \dot{x} + \tfrac{1}{2}x^T K_{px} x + \tfrac{\mu_x}{4}\hat{\xi}_x^T K_{ix}^{-1}\hat{\xi}_x + x^T \hat{\xi}_x + \tfrac{\mu_x}{2}x^T M_x \dot{x} + \tfrac{\mu_x}{4}x^T K_{dx} x$$
$$+ \int_0^t \sigma_x dx - k_{\sigma_\mathbf{x}} + \tfrac{1}{4}tr_x[\tilde{w}_r^T(z_x)k_w^{-1}\tilde{w}_r(z_x)] + \tfrac{1}{4}tr_x[\tilde{w}_l^T(z_x)k_w^{-1}\tilde{w}_l(z_x)]$$
(5.50)

where $V(0) = 0$. In order to show that $V \geq 0$, V is separated into three parts, such that $V = V_1 + V_2 + V_3$

$$V_1 = \tfrac{1}{6}x^T K_{px} x + \tfrac{\mu_x}{4}x^T K_{dx} x + \int_0^t \sigma_x dx - k_{\sigma_\mathbf{x}}$$
$$+ \tfrac{1}{4}tr_x[\tilde{w}_r^T(z_x)k_w^{-1}\tilde{w}_r(z_x)] + \tfrac{1}{4}tr_x[\tilde{w}_l^T(z_x)k_w^{-1}\tilde{w}_l(z_x)] \geq 0, \qquad (5.51)$$
$$K_{px} > 0, K_{dx} > 0$$

$$V_2 = \tfrac{1}{6}x^T K_{px}x + \tfrac{\mu_x}{4}\hat{\xi}_x^T K_{ix}^{-1}\hat{\xi}_x + x^T\hat{\xi}_x$$
$$\geq \tfrac{1}{2}\tfrac{1}{3}\lambda_m(K_{px})\,\|x\|^2 + \tfrac{\mu_x\lambda_m(K_{ix}^{-1})}{4}\,\|s_x\|^2 - \|x\|\,\|s_x\| \tag{5.52}$$

When $\mu_x \geq \frac{3}{(\lambda_m(K_{ix}^{-1})\lambda_m(K_{px}))}$,

$$V_2 \geq \frac{1}{2}\left(\sqrt{\frac{\lambda_m(K_{px})}{3}}\,\|x\| - \sqrt{\frac{3}{4(\lambda_m(K_{px}))}}\,\|s_x\|\right)^2 \geq 0 \tag{5.53}$$

and

$$V_{3x} = \frac{1}{6}x^T K_{px}x + \frac{1}{2}\dot{x}^T M\dot{x} + \frac{\mu_x}{2}x^T M\dot{x} \tag{5.54}$$

Because

$$Y^T A X \geq \|Y\|\,\|AX\| \geq \|Y\|\,\|A\|\,\|X\| \geq \lambda_M(A)\,\|Y\|\,\|X\| \tag{5.55}$$

when

$$\mu_x \leq \frac{1}{2}\frac{\sqrt{\tfrac{1}{3}\lambda_m(M_x)\lambda_m(K_{px})}}{\lambda_M(M_x)}$$

$$V_3 \geq \tfrac{1}{2}\left(\tfrac{1}{3}\lambda_m(K_{px})\,\|x\|^2 + \lambda_m(M_x)\,\|\dot{x}\|^2 + 2\mu_x\lambda_M(M_x)\,\|x\|\,\|\dot{x}\|\right)$$
$$= \tfrac{1}{2}\left(\sqrt{\tfrac{\lambda_m(K_{px})}{3}}\,\|x\| + \sqrt{\lambda_m(M_x)}\,\|\dot{x}\|\right)^2 \geq 0 \tag{5.56}$$

Now we have,

$$\frac{1}{2}\frac{\sqrt{\tfrac{1}{3}\lambda_m(M_x)\lambda_m(K_{px})}}{\lambda_M(M_x)} \geq \mu_x \geq \frac{3}{(\lambda_m(K_{ix}^{-1})\lambda_m(K_{px}))} \tag{5.57}$$

The derivative of (5.50) is

$$\dot{V} = \dot{x}^T[-C_x\dot{x} - \alpha_f C_{x\theta}\dot{x} - K_{dx}\dot{x} + \sigma_x(0)] + \tfrac{\mu_x}{2}s_x^T K_{ix}^{-1}s_x + x^T s_x$$
$$+\tfrac{\mu_x}{2}\dot{x}^T M_x\dot{x} + \tfrac{\mu_x}{2}x^T[-C_x\dot{x} - \alpha_f C_{x\theta}\dot{x} - K_{px}x - \sigma_x - s_x + \sigma_x(0)]$$
$$-\tfrac{1}{2}\tilde{w}_r(z_x)[(\dot{x} + \tfrac{\mu_x}{2}x)^T\phi_r^T(z_x)] - \tfrac{1}{2}\tilde{w}_l(z_x)[(\dot{x} + \tfrac{\mu_x}{2}x)^T\phi_l^T(z_x)]$$
$$+\tfrac{1}{2}tr_x[\tfrac{d}{dt}\tilde{w}_r^T(z_x)k_w^{-1}\tilde{w}_r(z_x)] + \tfrac{1}{2}tr_x[\tfrac{d}{dt}\tilde{w}_l^T(z_x)k_w^{-1}\tilde{w}_l(z_x)] \tag{5.58}$$

Using the updating law (5.49),

$$\tfrac{1}{2}tr_x[\tfrac{d}{dt}\tilde{w}_r^T(z_x)k_w^{-1}\tilde{w}_r(z_x)] - \tfrac{1}{2}\tilde{w}_r(z_x)[(\dot{x} + \tfrac{\mu_x}{2}x)^T\phi_r^T(z_x)] = 0$$
$$\tfrac{1}{2}tr_x[\tfrac{d}{dt}\tilde{w}_l^T(z_x)k_w^{-1}\tilde{w}_l(z_x)] - \tfrac{1}{2}\tilde{w}_l(z_x)[(\dot{x} + \tfrac{\mu_x}{2}x)^T\phi_l^T(z_x)] = 0$$

(5.58) becomes

$$\dot{V} = \dot{x}^T[-C_x\dot{x} - \alpha_f C_{x\theta}\dot{x} - K_{dx}\dot{x} + \sigma_x(0)] + \tfrac{\mu_x}{2}\hat{\xi}_x^T K_{ix}^{-1}\hat{\xi}_x + x^T\hat{\xi}_x$$
$$+\tfrac{\mu_x}{2}\dot{x}^T M_x\dot{x} + \tfrac{\mu_x}{2}x^T[-C_x\dot{x} - \alpha_f C_{x\theta}\dot{x} - K_{px}x - \sigma_x - \hat{\xi}_x + \sigma_x(0)] \tag{5.59}$$

Now using the property $X^T Y + Y^T X \le X^T \Lambda X + Y^T \Lambda^{-1} Y$

$$
\begin{aligned}
-\tfrac{\mu_x}{2} x^T C_x \dot{x} &\le \tfrac{\mu_x}{2} \lambda_M(C_x) \left(x^T x + \dot{x}^T \dot{x} \right) \\
-\tfrac{\mu_x \alpha_f}{2} x^T C_{x\theta} \dot{x} &\le \tfrac{\mu_x}{2} \lambda_M(\alpha_f C_{x\theta}) \left(x^T x + \dot{x}^T \dot{x} \right)
\end{aligned}
\tag{5.60}
$$

where $\|C_x\| \le k_{c_x}$.and $\|C_{x\theta}\| \le k_{c_{x\theta}}$. So $s_x = K_{ix}$, $s_x^T K_{ix}^{-1} s_x$ becomes $x^T s_x$, and $x^T s_x$ becomes $x^T K_{ix}$. have Now using the Lipschitz condition (5.45)

$$
\frac{\mu_x}{2} x^T [\sigma_x(0) - \sigma_x] \le \frac{\mu_x}{2} k_{\boldsymbol{\sigma_x}} \|x\|^2
\tag{5.61}
$$

From (5.60) and (5.61)

$$
\begin{aligned}
\dot{V} = &-\dot{x}^T \left[C_x + \alpha_f C_{x\theta} + K_{dx} - \tfrac{\mu_x}{2} M_x - \tfrac{\mu_x}{2} \lambda_M(C_x) - \tfrac{\mu_x}{2} \lambda_M(\alpha_f C_{x\theta}) \right] \dot{x} \\
&-x^T \left[\tfrac{\mu_x}{2} K_{px} - K_{ix} - \tfrac{\mu_x}{2} k_{\boldsymbol{\sigma_x}} - \tfrac{\mu_x}{2} \lambda_M(C_x) - \tfrac{\mu_x}{2} \lambda_M(\alpha_f C_{x\theta}) \right] x
\end{aligned}
\tag{5.62}
$$

Using (5.44), (5.62) becomes

$$
\begin{aligned}
\dot{V} \le &-\dot{x}^T \left[\lambda_m(C_x) + \lambda_m(\alpha_f C_{x\theta}) + \lambda_m(K_{dx}) - \tfrac{\mu_x}{2} \lambda_M(M_x) - \tfrac{\mu_x}{2} \lambda_M(C_x) - \tfrac{\mu_x}{2} \lambda_M(\alpha_f C_{x\theta}) \right] \dot{x} \\
&-x^T \left[\tfrac{\mu_x}{2} \lambda_m(K_{px}) - \lambda_M(K_{ix}) - \tfrac{\mu_x}{2} k_{\boldsymbol{\sigma_x}} - \tfrac{\mu_x}{2} \lambda_M(C_x) - \tfrac{\mu_x}{2} \lambda_M(\alpha_f C_{x\theta}) \right] x
\end{aligned}
\tag{5.63}
$$

So $\dot{V}_x \le 0$, $\|x\|$ minimizes if two conditions are met: 1) $\lambda_m(C_x) + \lambda_m(\alpha_f C_{x\theta}) + \lambda_m(K_{dx}) \ge \frac{\mu_x}{2}[\lambda_M(M_x) + \lambda_M(C_x) + \lambda_M(\alpha_f C_{x\theta})]$; 2) $\lambda_m(K_{px}) \ge \frac{2}{\mu_x} \lambda_M(K_{ix}) + k_{\boldsymbol{\sigma_x}} + \lambda_M(C_x) + \lambda_M(\alpha_f C_{x\theta})$. Now using (5.57) and $\lambda_m\left(K_{ix}^{-1}\right) = \frac{1}{\lambda_M(K_{ix})}$, we have

$$
\lambda_m(K_{dx}) \ge \tfrac{1}{4} \sqrt{\tfrac{1}{3} \lambda_m(M_x) \lambda_m(K_{px})} \left[1 + \frac{\lambda_M(C_x) + \lambda_M(\alpha_f C_{x\theta})}{\lambda_M(M_x)} \right] - \lambda_m(C_x) - \lambda_m(\alpha_f C_{x\theta})
\tag{5.64}
$$

again $\frac{2}{\gamma} \lambda_M(K_{ix}) = \frac{2}{3} \lambda_m(K_{px})$. Hence,

$$
\lambda_M(K_{ix}) \le \frac{1}{6} \sqrt{\frac{1}{3} \lambda_m(M_x) \lambda_m(K_{px})} \frac{\lambda_m(K_{px})}{\lambda_M(M_x)}
\tag{5.65}
$$

Also

$$
\lambda_m(K_{px}) \ge \frac{3}{2}[k_{\boldsymbol{\sigma_x}} + \lambda_M(C_x) + \lambda_M(\alpha_f C_{x\theta})]
\tag{5.66}
$$

Let us assume that there prevails a ball of radius ς in the three dimensional space. This three dimensional space is represented by x-component, y-component and $\theta-$component. The ball center is at origin of the state space system where: $\dot{V}_x \le 0, \dot{V}_y \le 0, \dot{V}_\theta \le 0$. The origin of the closed loop systems represented by (5.43) is stable equilibrium. Similarly the closed loop system along other components will be in stable equilibrium. Now we will prove

for the asymptotic stability of the origin. For that we use La Salle´s theorem by defining the term Π_x, Π_y and Π_θ as follows:

$$
\begin{aligned}
\Pi_x &= \left\{ z_x(t) = \left[x^T, \dot{x}^T, \xi_x^T \right]^T \in \Re^{3n} : \dot{V}_x = 0 \right\}, \xi_x \in \Re^n, x = 0 \in \Re^n, \dot{x} = 0 \in \Re^n \\
\Pi_y &= \left\{ z_y(t) = \left[y^T, \dot{y}^T, \xi_y^T \right]^T \in \Re^{3n} : \dot{V}_y = 0 \right\}, \xi_y \in \Re^n, y = 0 \in \Re^n, \dot{y} = 0 \in \Re^n \\
\Pi_\theta &= \left\{ z_\theta(t) = \left[\theta^T, \dot{\theta}^T, \xi_\theta^T \right]^T \in \Re^{3n} : \dot{V}_\theta = 0 \right\}, \xi_\theta \in \Re^n, \theta = 0 \in \Re^n, \dot{\theta} = 0 \in \Re^n
\end{aligned}
\tag{5.67}
$$

Using (5.58) and substituting $x = 0$ and $\dot{x} = 0$, we have $\dot{V}_x = 0$. Similar analysis with $y = 0$ and $\dot{y} = 0$ and also $\theta = 0$ and $\dot{\theta} = 0$ will yield $\dot{V}_y = 0$ and $\dot{V}_\theta = 0$. Similarly these conditions hold good for $\dot{x} = 0, \dot{y} = 0$ and $\dot{\theta} = 0$ for all $t \geq 0$. Therefore $z_x(t)$, $z_y(t)$ and $z_\theta(t)$ belongs to Π_x, Π_y and Π_θ respectively. Also, imparting these conditions to (5.43) we have: $\dot{\xi}_x = 0$, $\dot{\xi}_y = 0$ and $\dot{\xi}_\theta = 0$. Also, $\xi_x = 0$, $\xi_y = 0$ and $\xi_\theta = 0$ for all $t \geq 0$. So $z_x(t)$ is the only initial condition in Π_x, $z_y(t)$ is the only initial condition in Π_y and $z_\theta(t)$ is the only initial condition in Π_θ. Therefore, origin is asymptotically stable according to La Salle´s theorem. Now for global stability of the closed loop system mentioned by (5.43), the following conditions needs to be met: $\lim_{t \to \infty}^x (t) = 0$, when the initial condition of $[x, \dot{x}, \xi_x]$ is inside of Π_x. $\lim_{t \to \infty}^y (t) = 0$, when the initial condition of $\left[y, \dot{y}, \xi_y \right]$ is inside of Π_y. $\lim_{t \to \infty}^\theta (t) = 0$, when the initial condition of $\left[\theta, \dot{\theta}, \xi_\theta \right]$ is inside of Π_θ ∎

5.3   Experimental results

In order to analyze and validate the bidirectional type-2 fuzzy PD and PID controllers, a two-floor building structure is designed and constructed. The detailed of the structure and the placements of actuators are mentioned in chapter 3.

The relative acceleration in the second floor is subtracted by the ground floor acceleration. Numerical integrators are used to compute the velocity and position from the accelerometer signal. Since there is not angular sensor, the angular accelerations are calculated by (4.58) and (4.59) mentioned in chapter 3, where $\ddot{\theta}_1$ and $\ddot{\theta}_2$ are the angular accelerations of the first and the second floor.

The theorems of this paper give the sufficient conditions of the minimal proportional and derivative gains and maximum integral gain. To compare with the other algorithm in the same condition, all PID gains are the same. The upper bounds and lower bounds of the

structure model are

$$\lambda_M (M_x) = 10, \lambda_M (M_y) = 10$$
$$\lambda_m(k_{c_x}) = 20, \lambda_m(k_{c_{x\theta}}) = 8 \lambda_m(k_{c_y}) = 22, \lambda_m(k_{c_{y\theta}}) = 6 \qquad (5.68)$$
$$\lambda_{j_t} (J_0) = 5, \lambda_m(k_{c_\theta}) = 21, \lambda_m(k_{c_{x\theta}}) = 8, \lambda_m(k_{c_{y\theta}}) = 6$$

$k_{\boldsymbol{\sigma_x}}$ is effected by the external force $\mathbf{F}$. The maximum force to actuate the building structure prototype during experiment is $300N$. Therefore we select $k_{\boldsymbol{\sigma_x}} = 400$. $Y-$component and $\theta-$component are extracted with the similar method. For $X-$component, ranges of the PID gains are

$$\lambda_m(K_{px}) \geq 1247, \lambda_m (K_{dx}) \geq 50, \lambda_M(K_{ix}) \leq 2677, \lambda_m(K_{py}) \geq 1247$$
$$\lambda_m (K_{dy}) \geq 50, \lambda_M(K_{iy}) \leq 2677, \lambda_{j_0}(K_{p\boldsymbol{\theta}}) \geq 1431, \lambda_{j_0} (K_{d\boldsymbol{\theta}}) \geq 75, \lambda_{J_0}(K_{i\theta}) \leq 3789 \qquad (5.69)$$

We first use type-2 fuzzy logic system toolbox [128] to design the type-2 fuzzy system. Due to its iterative nature, the computational cost of the calculation of the type-2 fuzzy system output is big [140]. In order to tackle with this situations, several TR methods have been proposed for reducing the computational cost of the type-2 fuzzy inference mechanism. The Karnik–Mendel (KM) algorithms are iterative procedures widely used in fuzzy logic theory. They are known to converge monotonically and super exponentially fast; however, several (usually two to six) iterations are still needed before convergence occurs [138].Wu categorized the TR methods as Enhancements to the KMs, which improved the computational cost of the KM, and Alternative TR methods, which are closed-form approximations to the KM algorithm [141]. KM method is most popular due its novelty and adaptiveness [137]. The type reduction and the defuzzification methods supported by type-2 fuzzy logic system toolbox are 1) Karnik-Mendel Algorithm (KM). 2) Enhanced KM Algorithm (EKM). 3) Iterative Algorithm with Stop Condition (IASC). 4) Enhanced IASC (EIASC). 5) Enhanced Opposite Direction Searching Algorithm (EODS). 6) Wu-Mendel Uncertainty Bound Method (WM). 7) Nie-Tan Method (NT). 8) Begian-Melek-Mendel Method (BMM). In type-2 fuzzy logic system toolbox, it is possible to state the antecedent MFs with the MF types that already prevail in the Matlab Fuzzy Logic Toolbox. Hence, it is feasible to implement the Matlab functions of LMF and UMF in a same pattern. But there is an additional parameter associated to each type of MFs that illustrates the height of the corresponding MF. For example, a triangle MF is stated having the parameters $l_{t2}, c_{t2}, r_{t2}, h_{t2}$ which defines the left point, the center point, right point and the height of the MF, respectively. The parameter h_{t2} is generally utilized to develop FOU in the type-2 fuzzy systems, most specifically in type-2 fuzzy controller design. In the analysis, Karnik-Mendel method (Liang & Mendel, 2002)
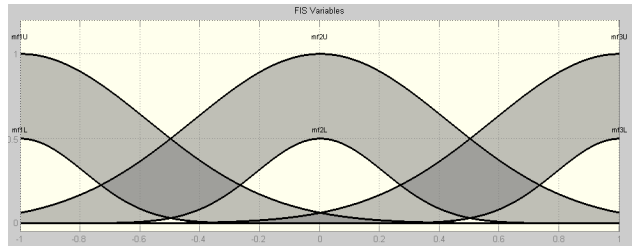
Figure 5.1: Upper and lower limits of Gaussian membership functions

is utilized to defuzzify the type-2 fuzzy system. The control performance is evaluated to minimize the relative displacement of each floor of the building. The membership functions are Gaussian functions and they are designed by the method of [50], see Figure 5.1, where mfU and mfL are the upper and lower membership functions. The advantages of Gaussian membership functions are it is simpler in design because they are easier to represent and optimize, always continuous, and faster for small rule bases . Gaussian type-2 fuzzy logic systems are faster than the corresponding trapezoidal type-2 fuzzy logic systems when the same number of MFs and the same type-reduction and defuzzification method are used. Since small rulebases are usually used in practice, Gaussian type-2 fuzzy logic systems seem more favorable in terms of computational cost [139]. For the floor position and velocity, we use three linguistic variables and three membership functions, they are normalized in $[-1, 1]$. Karnik-Mendel method [86] is utilized to defuzzify the type-2 fuzzy system. For the formulation of type-2 fuzzy rules, the FIS variables selected as input variables (position error and velocity error) and output variable (control force). IF-THEN rules are applied. IF and AND conditions are applied between position error and velocity error, whereas THEN conditions gives the required control force. Considering $X-$component, fifteen fuzzy rules are applied. Also for $Y-$component and $\theta-$component, similar set of fifteen fuzzy rules are applied respectively. We find fifteen fuzzy rules are sufficient to maintain minimum regulation errors. For design purpose, we choose $\mu_x = 6$. We also find that for the type-1 fuzzy, at least nine fuzzy rules are needed to have the similar regulation errors as the type-2 fuzzy system.
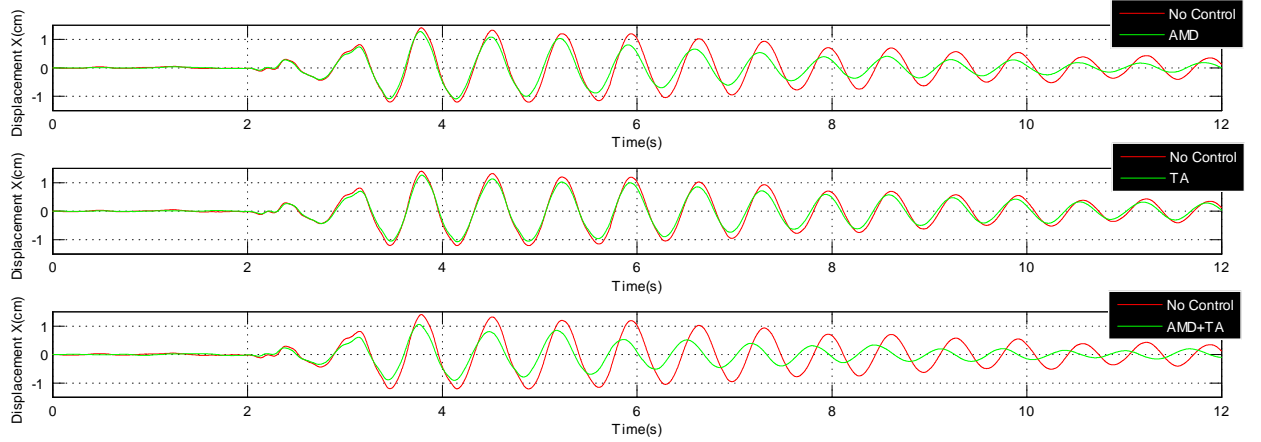
Figure 5.2: PD control in $X-$direction

The signal to the shake table is the Northridge earthquake. The displacement is scaled from $16.92cm$ to $1.50cm$, the time is scaled from 40 seconds to 12 seconds. The control object is to minimize the relative displacement of each floor in bidirection. From (5.69), the PID control gains are

$$K_{px} = 1800, K_{py} = 2000, K_{p\theta} = 2200,$$
$$K_{dx} = 160, K_{dy} = 220, K_{d\theta} = 300, K_{ix} = 2000, K_{iy} = 2300, K_{i\theta} = 3500 \tag{5.70}$$

The PD control gains are $K_{px} = 1800, K_{py} = 2000, K_{p\theta} = 2200, K_{dx} = 160 K_{dy} = 220, K_{d\theta} = 300$

We compare our control with classical PD/PID, type-1 fuzzy PD/PID in three cases: 1) without any active control (No Control); 2) with the torsional actuator (TA); 3) with both the active mass damper and the torsional actuator (AMD+TA). The results of these controllers are shown in Figure 5.2 - Figure 5.7. The control signals of type-2 fuzzy PD and PID are displayed in Figure 5.8 and Figure 5.9. We define the average vibration displacement as $MSE = \frac{1}{N} \sum_{k=1}^{N} x(k)^2$, $x(k)$ is the displacement of the floor, N is the total data number. The comparison results of the average vibration displacement are shown in Table 1-Table 9.
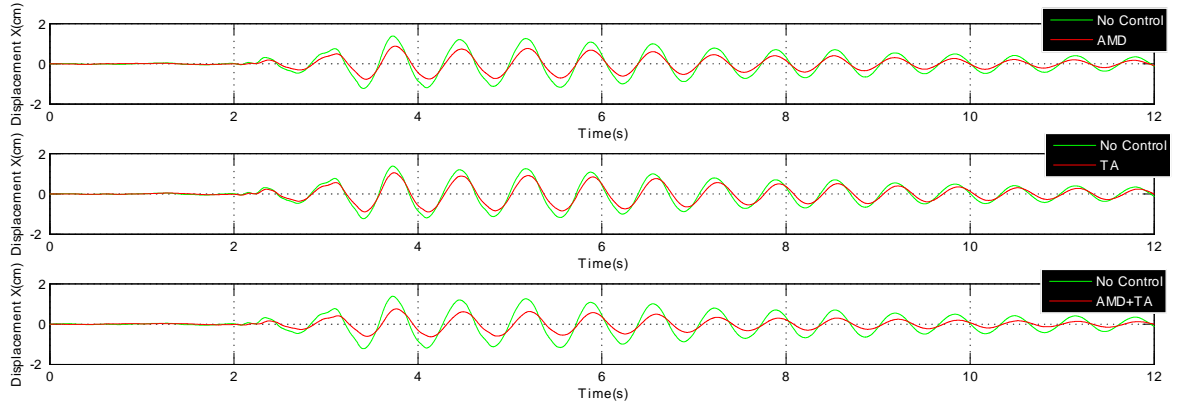
Figure 5.3: PID control in $X-$direction
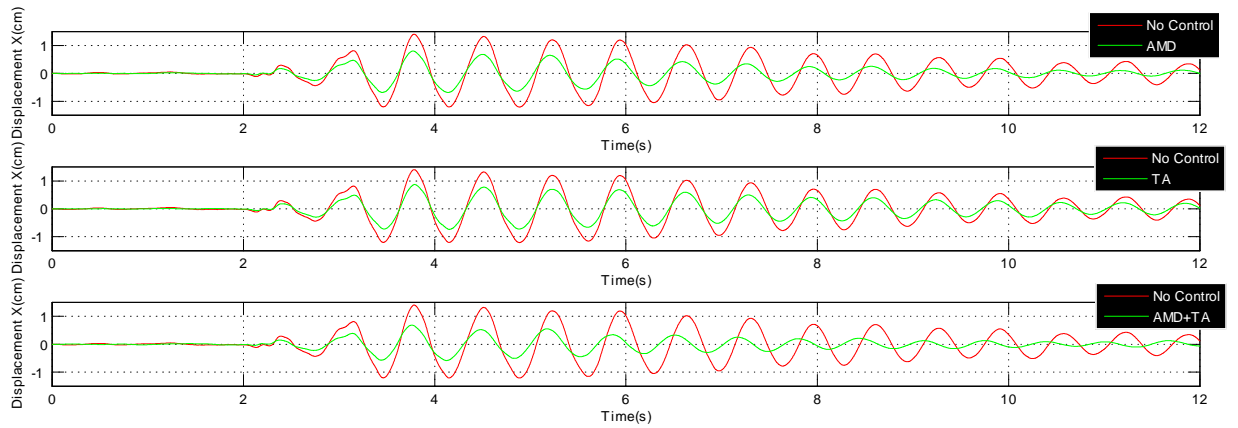
Figure 5.4: Type-1 fuzzy PD control in $X-$direction
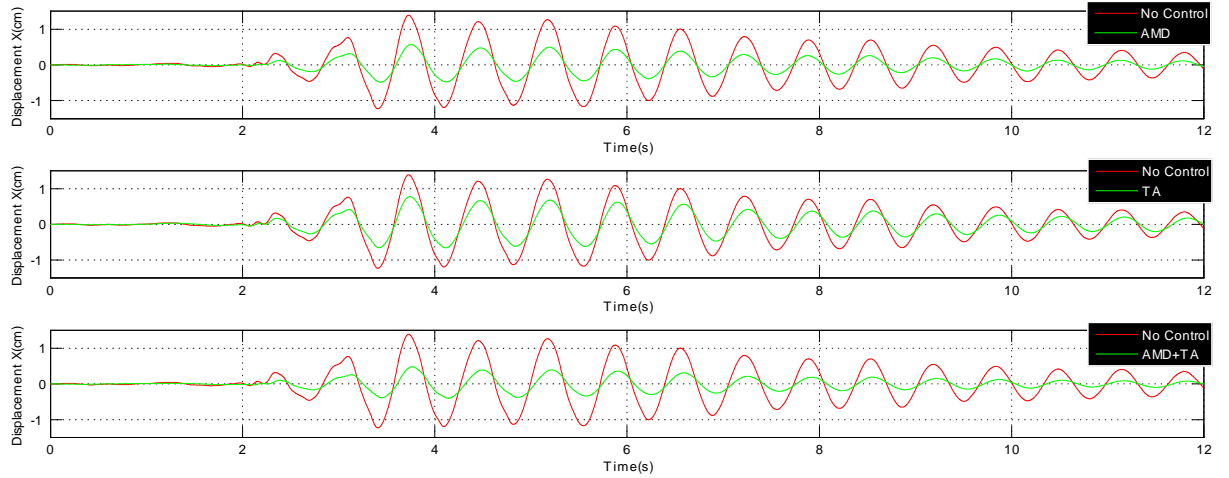
Figure 5.5: Type-1 fuzzy PID control in $X-$direction
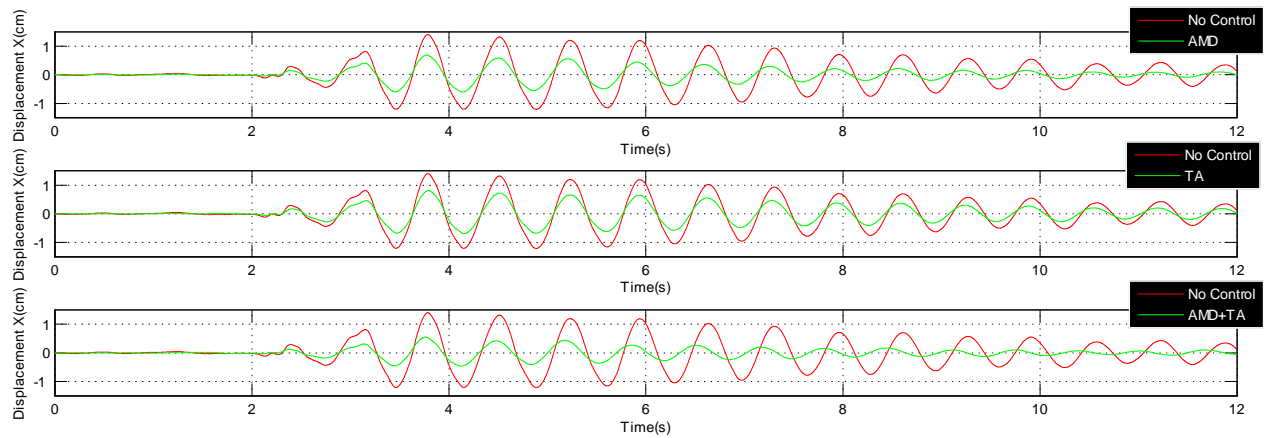
Figure 5.6: Type-2 fuzzy PD control in $X-$direction
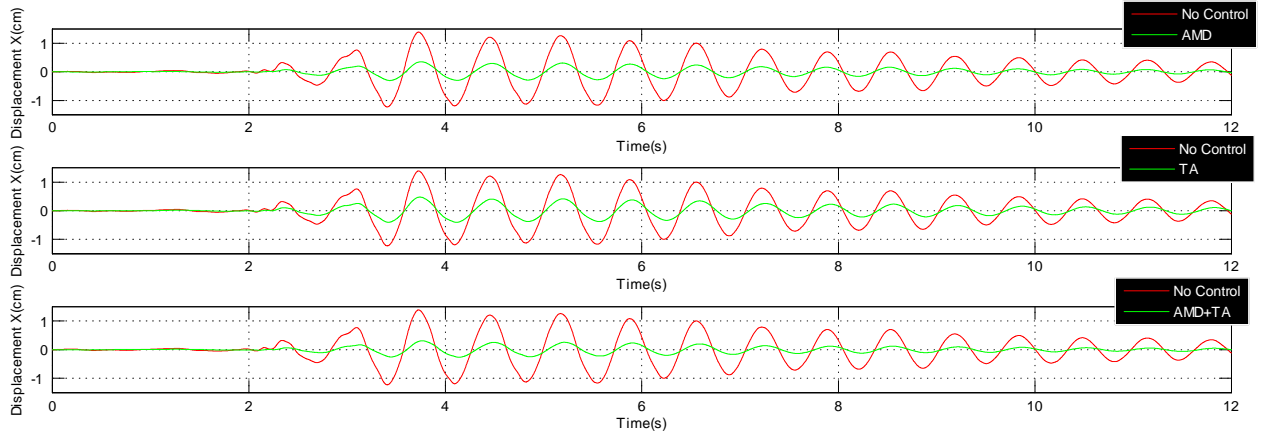
Figure 5.7: Type-2 fuzzy PID control in $X-$direction
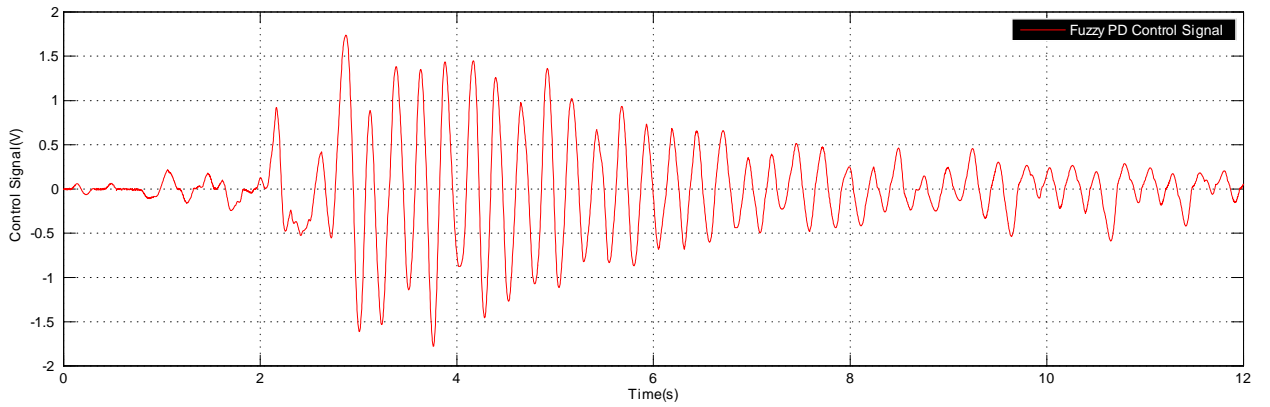
Figure 5.8: Control of type-2 fuzzy PD
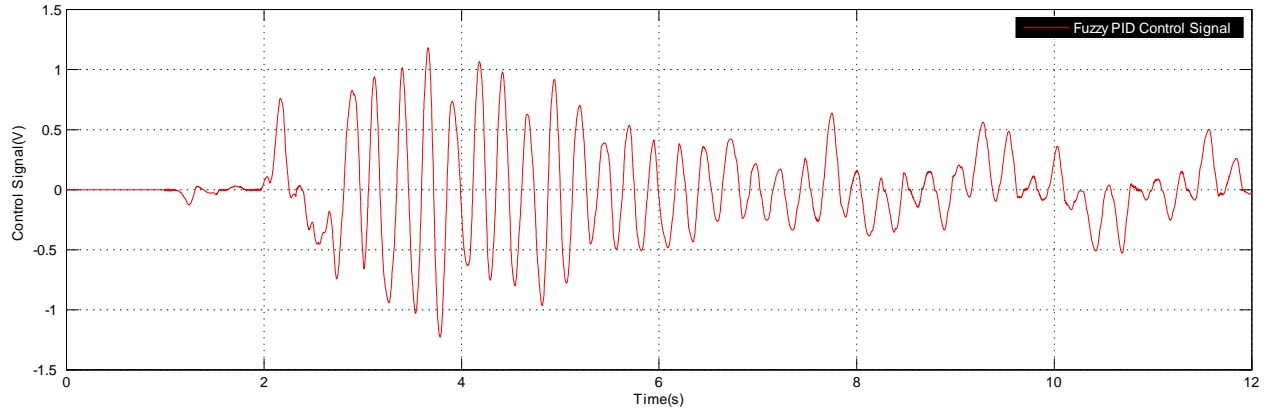
Figure 5.9: Control of type-2 fuzzy PID

Here ↓ sign indicate decrease.

Table 1. Average vibration displacement by AMD+TA

	PD control	% ↓ error	PID control	% ↓ error	No control
X-direction	0.2987	60.2	0.2373	68.5	0.7514
Y-direction	0.0719	45.53	0.0783	59.3	0.1320
θ-direction	0.0696	40.8	0.0611	47.6	0.1174

Table 2. Average vibration displacement with PD control

	with AMD	% ↓ error	with TA	% ↓ error	No control
X-direction	0.4832	35.7	0.5802	22.78	0.7514
Y-direction	0.0981	25.68	0.1012	23.3	0.1320
θ-direction	0.0902	23.1	0.0801	31.7	0.1174

Table 3. Average vibration displacement with PID control

	with AMD	% ↓ error	with TA	% ↓ error	No control
X-direction	0.3632	51.6	0.4911	34.6	0.7514
Y-direction	0.0849	35.6	0.0969	26.5	0.1320
θ-direction	0.0811	30.8	0.0713	40.0	0.1174

Table 4. Average vibration displacement by AMD+TA

	Type-1 Fuzzy PD	% ↓ error	Type-1 Fuzzy PID	% ↓ error	No control
X-direction	0.1843	75.4	0.1590	78.8	0.7514
Y-direction	0.0531	60.0	0.0488	63.3	0.1320
θ-direction	0.0578	50.7	0.0423	63.9	0.1174

Table 5. Average vibration displacement with Type-1 Fuzzy PD control

	with AMD	% ↓ error	with TA	% ↓ error	No control
X-direction	0.2121	71.7	0.3398	54.7	0.7514
Y-direction	0.0633	52.4	0.0733	44.5	0.1320
θ-direction	0.0820	30.1	0.0674	42.6	0.1174

Table 6. Average vibration displacement with Type-1 Fuzzy PID control

	with AMD	% ↓ error	with TA	% ↓ error	No control
X-direction	0.1944	74.1	0.2416	67.8	0.7514
Y-direction	0.0581	55.9	0.0634	51.96	0.1320
θ-direction	0.0711	40.0	0.0481	59.1	0.1174

Table 7. Average vibration displacement by AMD+TA

	Type-2 Fuzzy PD	% ↓ error	Type-2 Fuzzy PID	% ↓ error	No control
X-direction	0.1348	82.1	0.1121	85.1	0.7514
Y-direction	0.0320	75.7	0.0299	77.3	0.1320
θ-direction	0.0395	66.35	0.0278	76.3	0.1174

Table 8. Average vibration displacement with Type-2 Fuzzy PD control

	with AMD	% ↓ error	with TA	% ↓ error	No control
X-direction	0.1693	77.4	0.2339	68.8	0.7514
Y-direction	0.0433	67.1	0.0670	49.2	0.1320
θ-direction	0.0489	58.3	0.0396	66.2	0.1174

Table 9. Average vibration displacement with Type-2 Fuzzy PID control

	with AMD	% ↓ error	with TA	% ↓ error	No control
X-direction	0.1575	79.1	0.2080	72.3	0.7514
Y-direction	0.0389	70.5	0.0584	55.7	0.1320
θ-direction	0.0431	63.2	0.0371	68.3	0.1174

We can see that all PD/PID, type-1 fuzzy PD/PID and type-2 fuzzy PD/PID controllers works well with AMD and TA, because both horizontal actuator and torsional actuator act simultaneously. The vibration attenuations along X-direction and Y-direction are much better than θ-direction, because the active vibration control is achieved by the position of the actuator and the torque direction of the actuator. PID controller is better than PD to minimize the vibration in all three directions. The active control of structures can be improved by adding the fuzzy compensation. The type-2 fuzzy controller is capable of providing more vibration attenuation than the type-1 fuzzy controller. The best results are the type-2 fuzzy PID control.

5.4   Summary

In this chapter, type-2 Fuzzy PD and PID control for building structures with AMD and torsional actuator are proposed. By utilizing Lyapunov theory, sufficient conditions of stability are extracted to tune PD/PID gains. The mentioned methodology is successfully implemented to a two-story building prototype. The experimental results show that the type-2 fuzzy PD/PID controllers work better than type-1 fuzzy PD/PID for the horizontal actuator and torsional actuator.

Chapter 6

Discrete Time Sliding Mode Control of Building Structures

6.1 Introduction

Active vibration control of building structures under earthquake loadings is a popular field among civil and mechanical engineers. Different control devices and algorithms were proposed and implemented in the last few decades [59][105]. One of the main challenges in the structural control design is the presence of uncertainties in the building structures, especially in parametric level. Robust control is a well-established technique, which can deal with these uncertainties and disturbances present in the real systems like the building structures.

Research reveals that sliding mode control (SMC) is considered to be an effective robust control strategy for uncertain systems. The sliding mode control (SMC) is designed for uncertain nonlinear systems [132]. It is very much effective in terms of robustness against the changes in the parameters and external disturbances. It has been successfully applied for structural control [97]. In [64], SMC is used to control bending and torsional vibration of a six-story flexible structure. Soleymani et.al in his work demonstrated new robust control system for an active tuned mass damper (AMD) implemented in a high-rise building. The controller is a blended innovation of two-loop sliding model controller with a dynamic state predictor [119]. In [93], an active vibration control for a two storeyed flexible structure was proposed where the sliding mode controller is designed utilizing LQR approach in order to validate stable motion while undergoing sliding. An approach related to adaptive fuzzy sliding mode in order to eliminate the damage of the nonlinear structure was suggested by [31]

The implementation of digital computers and samplers in the field of control systems has popularized the research of discrete time systems. A necessary and sufficient condition for discrete time sliding motion is suggested by Sarpturk et al. (1987) as follows [111]

$$\mid S(k+1) \mid < \mid S(k) \mid$$

One more important condition for discrete-time sliding mode with the consideration that sliding hyperplane $S(k) = 0$,should satisfy [14]

$$\mid S(k) \mid < g$$

where the parameters $g > 0$ is termed as quasi-sliding mode band width. However, owing to a finite sampling frequency characteristic in discrete-time systems, the system states can only be expected to approach the selected sliding surface and remain around it, instead of remaining on the surface when the system undergoes external disturbances. Therefore, the so-called quasi-sliding-mode (QSM) concept was introduced and discussed in discrete-time systems [14] [65]. A brief summary is given here. The system states are required to monotonically approach the sliding surface until they enter the vicinity of the surface, and they then remain inside. The vicinity of the sliding surface is called a quasi-sliding-mode band (QSMB). Under this QSM definition, it is noted that the system states are not required to cross the sliding surface, as in the definition given by Gao et al. [46]. The undesirable chattering and high-frequency switching between different values of the control signal are avoided. Since its state does not have to cross the sliding hyperplane in each control step, the control strategy can be linear and, consequently, the undesirable chattering is avoided. The strategies guarantee improved robustness, faster transient response, and better steady-state accuracy of the controlled system [14].

In general cases, discrete-time control or sampling control is most suited for the structural control. The sampling period is considered to be the important feature that play significant role in the performance of the control system. In [91], a discrete-time variable structure control strategies on the basis of discrete reaching law method in order to minimizing the dynamic responses of seismically excited structures was suggested. A time delayed discrete-time variable structure control method in order to mitigate vibration in the linear structures was proposed by [17]. A novel discrete-time variable structure control method in combination with fuzzy adaptive regulation for seismically excited linear structure with the intention of subsiding heavy chattering effect was presented by [84]. In [85], a new discrete-time variable structure control method incorporated with discrete-time composite reaching law was proposed for vibration attenuation in seismically-excited linear structure.

In this chapter, we present a fuzzy discrete sliding mode control (FDSMC) for the mini-mization of structural vibration along all three components under the effect of bidirectional earthquake forces. The analysis is based on the lateral-torsional vibration under the bidirec-tional waves. Also in order to reduce chattering, the suggested discrete-time sliding mode control with time-varying gain is effective. We prove that the closed-loop system with slid-ing mode control and fuzzy identifier are uniformly stable by utilizing Lyapunov stability theorem. The experimental results and analysis using the FDSMC validate its effective-ness and stability. Finally the results are compared with standard discrete sliding mode controller(DSMC) and PID controller to verify the superior performance of FDSMC in mitigating the earthquake vibrations.

6.2 Discrete time model of building structure

The continuous time model of $n-$floor building structure under bidirectional external forces is

$$M\ddot{\mathbf{x}}(t) + C\dot{\mathbf{x}}(t) + F_s(\mathbf{x}) + f_e(t) = \Gamma u(t) \tag{6.1}$$

where $\mathbf{x} \in \Re^{3n}$, $\mathbf{x} = [x_1 \cdots x_n, y_1 \cdots y_n, \theta_1 \cdots \theta_n]^T$, $\mathbf{x}$ is the displacement, $M \in \Re^{3n \times 3n}$ is the mass, $C \in \Re^{3n \times 3n}$ the damping coefficient, $F_s = [f_{s,1} \cdots f_{s,n}] \in \Re^{3n}$ is the structure stiffness force vector, and $f_e \in \Re^{3n}$ is the bidirectional external force applied to the structure, $f_e = [f_x, f_y, 0 \cdots 0]^T$, $u \in \Re^{3n}$ is the control signals which is fed to the dampers.

The structure stiffness can be model as

$$F_s(\mathbf{x}) = f_s(\mathbf{x}) + \Gamma d_u \tag{6.2}$$

where $f_s(\mathbf{x})$ is the structure stiffness force, it can an be modeled as a linear model $f_s = K\mathbf{x}$, or a nonlinear model, d_u is the damping and friction force vector of the dampers.

We define $z_{\mathbf{1}}(t) = \mathbf{x}$ and $z_{\mathbf{2}}(t) = \dot{\mathbf{x}}$, the model (6.1) can be transformed into the following state space model

$$\dot{Z}(t) = Az(t) + Bu(t) + F_s(z) + f_e(t) \tag{6.3}$$

where $z(t) = \begin{bmatrix} z_{\mathbf{1}}(t) \\ z_{\mathbf{2}}(t) \end{bmatrix}$, $A = \begin{bmatrix} 0 & 0 \\ 0 & -M^{-1}C \end{bmatrix}$, $B = \begin{bmatrix} 0 \\ M^{-1}\Gamma \end{bmatrix}$, $F_s(z) = M^{-1}F_s(z)$, $f_e(t) = M^{-1}f_e(t)$.

$F_s(\mathbf{x})$ and $f_e(t)$ can be regarded as the uncertainty parts of the linear system $\dot{Z} = Az + Bu$. Clearly, in absence of the external forces, the building structure is stable. So it is reasonable

to assume that $F_s(z)$ is bounded, $\|F_s(z)\| \leqslant d_s$. The external forces are bounded, $\|f_e(t)\| \leqslant d_e$.

In order to discreteize the continuos time model, we assume that the control force and the external forces are constant during the sampling period T, i.e.,

$$u(t) = u(kT), \quad f_e(t) = f_e(kT), \quad kT \leqslant t \leqslant (k+1)T$$

The discrete time model of (6.1) is [91],

$$z(k+1) = A_d + B_d u(k) + F_{ds}[z(k)] + f_{de}(k) \tag{6.4}$$

where $z(k)$ is a state vector, A_d is a state matrix, $A_d = e^{AT}$, B_d is the input vector, $B_d = \left(\int e^{A\tau}d\tau\right)B$, $u(k)$ is a scalar input, $F_{ds}(k)$ is the model uncertainty matrix and $f_{de}(k)$ is the excitation. Since A_d and B_d are unknown, (6.4) is written as the following general nonlinear model

$$z(k+1) = f[z(k)] + g[z(k)]u(k) + d[z(k)] \tag{6.5}$$

where $f[z(k)] = A_d z(k)$, $g[z(k)] = \Gamma_{i,j} B_d$, $d[z(k)] = F_{ds}[z(k)] + f_{de}(k)$, Γ is defined as the location matrix of the dampers,

$$\Gamma_{i,j} = \begin{cases} 1 & \text{if} \quad i = j = s \\ 0 & \text{otherwise} \end{cases} \tag{6.6}$$

where $\forall i, j \in \{1, ..., n\}, s \subseteq \{1, ..., n\}$, s are the floors on which the dampers are installed. For a two-floor building, $\Gamma = \begin{bmatrix} \Gamma_{1,1} & \Gamma_{1,2} \\ \Gamma_{2,1} & \Gamma_{2,2} \end{bmatrix}$. If the damper is placed on the second floor, $\Gamma = \begin{bmatrix} 0 & 0 \\ 0 & 1 \end{bmatrix}$.

6.3   Fuzzy modeling of structure

We use the following fuzzy system to modeling the unknown nonlinear functions $f[z(k)]$, $g[z(k)]$ and $d[z(k)]$ in (6.5). The unknown nonlinear functions f and g are approximated as

$$\begin{aligned} f[z(k)] + d[z(k)] &= \hat{f} + \epsilon_f \\ g[z(k)] &= \hat{g} + \epsilon_g \end{aligned} \tag{6.7}$$

where ϵ_f and ϵ_g are the modeling errors, $\hat{f}$ and $\hat{g}$ are the estimations of $f[z(k)] + d[z(k)]$ and $g[z(k)]$,

We use the following fuzzy system to model $f[z(k)]$, $g[z(k)]$ and $d[z(k)]$. For $p-th$ fuzzy rules for $f[z(k)]$, $g[z(k)]$ and $d[z(k)]$

$$R^i: \text{IF } (x_i \text{ is } A_{1i}) \text{ and } (y_i \text{ is } A_{2i}) \text{ and } (\theta_i \text{ is } A_{3i}) \text{ and } (\dot{x}_i \text{ is } A_{4i}) \text{ and } (\dot{y}_i \text{ is } A_{5i})$$
$$\text{and } \left(\dot{\theta}_i \text{ is } A_{6i} \right) \text{ THEN } f[z(k)] + d[z(k)] \text{ is } B_{1i} \tag{6.8}$$

$$R^i: \text{IF } (x_i \text{ is } A_{1i}) \text{ and } (y_i \text{ is } A_{2i}) \text{ and } (\theta_i \text{ is } A_{3i}) \text{ and } (\dot{x}_i \text{ is } A_{4i}) \text{ and } (\dot{y}_i \text{ is } A_{5i})$$
$$\text{and } \left(\dot{\theta}_i \text{ is } A_{6i} \right) \text{ THEN } g[z(k)] \text{ is } B_{2i} \tag{6.9}$$

where $A_{1i} \cdots, A_{6i}, B_{1i}, B_{3i}, B_{3i}$ are the fuzzy sets.

Now by product inference, center-average defuzzification, and a singleton fuzzifier, the output of the fuzzy logic system can be expressed as [134]

$$\hat{F}p = \frac{(\sum_{i=1}^{l} w_{pi}[\Pi_{j=1}^{n} \mu_{A_{ji}}])}{(\sum_{i=1}^{l}[\Pi_{j=1}^{n} \mu_{A_{ji}}])} = \sum_{i=1}^{l} w_{pi} \sigma_i \tag{6.10}$$

where $\mu_{A_{ji}}$ is the membership functions of the fuzzy sets A_{ji}, w_{pi} is the point at which $\mu_{\beta_{ji}} = 1$, if we define

$$\sigma_i = \frac{\Pi_{j=1}^{n} \mu_{A_{ji}}}{\sum_{i=1}^{l} \Pi_{j=1}^{n} \mu_{A_{ji}}} \tag{6.11}$$

The Gaussian functions are chosen as the membership functions as follows

$$\mu_{A_{ji}} = \exp\left(-\frac{(x_j - c_{ji})^2}{\rho_{ji}^2} \right) \tag{6.12}$$

where c_{ji} and ρ_{ji} are the mean and variance of the Gaussian function, respectively. In the matrix form, (6.10) can be expressed as

$$\hat{F}p = w(k)\sigma[z(k)] \tag{6.13}$$

where

$$w(k) = \begin{bmatrix} w_{11}(k) & & w_{1l}(k) \\ & \ddots & \\ & & \ddots \\ w_{m1}(k) & & w_{ml}(k) \end{bmatrix} \epsilon R^{m \times l}$$

also $\sigma[z(k)] = [\sigma_1 ....\sigma_l] \epsilon R^{l \times 1}$. Now using (6.13) and since $\hat{f}$ and $\hat{g}$ are the estimations of $f[z(k)] + d[z(k)]$ and $g[z(k)]$ then

$$\hat{f} = w_f(k)\sigma_f[z(k)]$$
$$\hat{g} = w_g(k)\sigma_g[z(k)] \tag{6.14}$$

According to the Stone-Weierstrass Theorem [16] the unknown nonlinear functions f and g are approximated as

$$f = w_f^*(k)\sigma_f[z(k)] + \epsilon_f$$
$$g = w_g^*(k)\sigma_g[z(k)] + \epsilon_g$$

(6.15)

The nonlinear system (6.5) can be modeled with fuzzy system as

$$\beta\hat{z}(k+1) = \hat{f}[z(k)] + \hat{g}[z(k)]u(k)$$

(6.16)

where β is a positive constant and $\beta > 1$ which is a design parameter.

We define the modeling error as

$$e_i(k+1) = \hat{z}(k+1) - z(k+1)$$

(6.17)

and

$$\tilde{f} = \hat{f} - f[z(k)] - d[z(k)]$$
$$\tilde{g} = \hat{g} - g[z(k)]$$

(6.18)

Now from (6.5), the nonlinear model can be represented in the fuzzy form as follows

$$\beta z(k+1) = \left[w_f^*(k)\sigma_f[z(k)] + \epsilon_f\right] + \left[w_g^*(k)\sigma_g[z(k)] + \epsilon_g\right]u(k)$$
$$\beta z(k+1) = w_f^*(k)\sigma_f[z(k)] + w_g^*(k)\sigma_g[z(k)]u(k) + \epsilon_f + \epsilon_g u(k)$$

(6.19)

Now from the Taylor series formula we have for n variables

$$f(x_1, ..., x_n) = \sum_{j=0}^{\infty}\left[\frac{1}{j!}\left(\sum_{k=1}^{n}(x_k - a_k)\frac{\partial}{\partial \acute{x}_k}\right)^j f(\acute{x}_1, ..., \acute{x}_n)\right] \acute{x}_1 = x_1.....\acute{x}_n = x_n$$

(6.20)

Now applying the Taylor series to the smooth functions $\hat{f}$ and $\hat{g}$ we have

$$\hat{f} = w_f^*(k)\sigma_f[z(k)] + [w_f(k) - w_f^*(k)]\frac{\partial\hat{f}}{\partial[w_f(k)]} + R_f$$
$$\hat{f} = w_f(k)\sigma_f[z(k)] + R_f$$

(6.21)

$$\hat{g} = w_g^*(k)\sigma_g[z(k)] + [w_g(k) - w_g^*(k)]\frac{\partial\hat{g}}{\partial[w_g(k)]} + R_g$$
$$\hat{g} = w_g(k)\sigma_g[z(k)] + R_g$$

(6.22)

where $\frac{\partial\hat{f}}{\partial[w_f(k)]} = \sigma_f[z(k)]$ and $\frac{\partial\hat{g}}{\partial[w_g(k)]} = \sigma_g[z(k)]$. Also R_f and R_g are the remainders of the Taylor formula. Now using (6.18) we can demonstrate

$$\tilde{f} = (w_f(k) - w_f^*(k))\sigma_f[z(k)] + (R_f - \epsilon_f)$$
$$\tilde{f} = \tilde{w}_f(k)\sigma_f[z(k)] + \xi_f$$

(6.23)

$$\tilde{g} = (w_g(k) - w_g^*(k))\sigma_g[z(k)] + (R_g - \epsilon_g)$$
$$\tilde{g} = \tilde{w}_g(k)\sigma_g[z(k)] + \xi_g \tag{6.24}$$

where $\tilde{w}_f(k) = w_f(k) - w_f^*(k), \tilde{w}_g(k) = w_g(k) - w_g^*(k), \xi_f = R_f - \epsilon_f$ and $\xi_g = R_g - \epsilon_g$. The error dynamics can be expressed using (6.16) and (6.19) as

$$\beta e_i(k+1) = \tilde{w}_f(k)\sigma_f[z(k)] + \tilde{w}_g(k)\sigma_g[z(k)]u(k) + \xi_f + \xi_g u(k) \tag{6.25}$$

In sake of assuring stability of identification and non-singularity in the controller, the following updating laws are implemented

$$\Delta w_f(k) = -\eta(k)\sigma_f[z(k)]e_i^T(k)$$
$$\Delta w_g(k) = -\eta(k)u(k)\sigma_g[z(k)]e_i^T(k) \tag{6.26}$$

Theorem 6.1 *If we use fuzzy model (6.16) to identify nonlinear system (6.5) having the updating law given by (6.26), then the identification error $e_i(k)$ is bounded and it satisfy the following relation*

$$\lim_{k\to\infty} \| e_i(k) \|^2 = \frac{\| \bar{\xi}(k) \|^2 [1 + \pi(k)]}{1 + (1 - \eta(k))\pi(k)} \tag{6.27}$$

provided the dead zone guarantees $\beta \| e_i(k+1) \| > \| e_i(k) \|$ and $0 < \eta(k) < 1, \pi(k) \geq 0$.

Proof. We select the following Lyapunov candidate function $V(k)$ as

$$V(k) = tr[\tilde{w}_f^T(k)\tilde{w}_f(k)] + tr[\tilde{w}_g^T(k)\tilde{w}_g(k]$$
$$= \sum_{i=1}^n \tilde{w}_f(k)^2 + \sum_{i=1}^n \tilde{w}_g(k)^2 \tag{6.28}$$
$$= \| \tilde{w}_f(k) \|^2 + \| \tilde{w}_g(k) \|^2$$

Now we know $\Delta V(k) = V(k+1) - V(k)$. Using this and (6.28)

$$\Delta V(k) = [\| \tilde{w}_f(k+1) \|^2 - \| \tilde{w}_f(k) \|^2] + [\| \tilde{w}_g(k+1) \|^2 - \| \tilde{w}_g(k) \|^2] \tag{6.29}$$

Now from the updating law (6.28) $\tilde{w}_f(k+1) - \tilde{w}_f(k) = -\eta(k)\sigma_f[z(k)]e_i^T(k)$ and $\tilde{w}_g(k+1) - \tilde{w}_g(k) = -\eta(k)u(k)\sigma_g[z(k)]e_i^T(k)$, also from (6.29)

$$\Delta V(k) = [\| \tilde{w}_f(k) - \eta(k)\sigma_f[z(k)]e_i^T(k) \|^2 - \| \tilde{w}_f(k) \|^2]$$
$$+ [\| \tilde{w}_g(k) - \eta(k)u(k)\sigma_g[z(k)]e_i^T(k) \|^2 - \| \tilde{w}_g(k) \|^2]$$
$$= \eta^2(k) \| e_i(k) \|^2 [\| \sigma_f[z(k)] \|^2 + \| \sigma_g[z(k)]u(k) \|^2]$$
$$- 2\eta(k) \| e_i^T(k) \| [\| \tilde{w}_f(k)\sigma_f[z(k)] \| + \| \tilde{w}_g(k)\sigma_g[z(k)]u(k) \|] \tag{6.30}$$

Now using (6.25)

$$
\begin{aligned}
\Delta V(k) &= \eta^2(k) \parallel e_i(k) \parallel^2 [\parallel \sigma_f[z(k)] \parallel^2 + \parallel \sigma_g[z(k)]u(k) \parallel^2] \\
&\quad -2\eta(k) \parallel e_i^T(k) \parallel [\beta e_i(k+1) - \xi_f - \xi_g u(k)] \\
&= \eta^2(k) \parallel e_i(k) \parallel^2 [\parallel \sigma_f[z(k)] \parallel^2 + \parallel \sigma_g[z(k)]u(k) \parallel^2] \\
&\quad -2\eta(k) \parallel e_i^T(k) \parallel \beta \parallel e_i(k+1) \parallel +2\eta(k) \parallel e_i^T(k) \parallel [\xi_f + \xi_g u(k)]
\end{aligned}
\tag{6.31}
$$

Now let $\pi(k) = \parallel \sigma_f[z(k)] \parallel^2 + \parallel \sigma_g[z(k)]u(k) \parallel^2, \xi(k) = \xi_f + \xi_g u(k)$ where $\pi(k) \geq 0, 0 < \eta(k) < 1$ and if $\beta \parallel e_i(k+1) \parallel > \parallel e_i(k) \parallel$ then

$$
\begin{aligned}
\Delta V(k) &\leq -2\eta(k) \parallel e_i(k) \parallel^2 + \eta^2(k) \parallel e_i(k) \parallel^2 \pi(k) \\
&\quad +2\eta(k) \parallel e_i^T(k)\xi(k) \parallel \\
\Delta V(k) &\leq -2\eta(k) \parallel e_i(k) \parallel^2 + \eta^2(k) \parallel e_i(k) \parallel^2 \pi(k) \\
&\quad +\eta(k) \parallel e_i^T(k) \parallel^2 + \eta(k) \parallel \xi(k) \parallel^2 \\
\Delta V(k) &\leq -\eta(k)[\parallel e_i(k) \parallel^2 \{1 - \eta(k)\pi(k)\} + \parallel \xi(k) \parallel^2]
\end{aligned}
\tag{6.32}
$$

Now Let us consider

$$
\eta(k) = \frac{\eta(k)}{1 + \pi(k)}, \eta(k) > 0, \pi(k) > 0
\tag{6.33}
$$

Also the modeling error $\xi(k)$ has the term input in it. This modeling error is considered to be bounded as follows

$$
\parallel \xi(k) \parallel^2 \leq \parallel \bar{\xi}(k) \parallel^2
\tag{6.34}
$$

Now using the conditions (6.33) and (6.34) we can express (6.32) as

$$
\Delta V(k) \leq -\frac{\eta(k)}{1 + \pi(k)} \left[\parallel e_i(k) \parallel^2 \left(\frac{1 + (1 - \eta(k))\pi(k)}{1 + \pi(k)} \right) - \parallel \bar{\xi}(k) \parallel^2 \right]
\tag{6.35}
$$

Now if $\parallel e_i(k) \parallel^2 \geq \frac{\parallel \bar{\xi}(k) \parallel^2 [1 + \pi(k)]}{1 + (1 - \eta(k))\pi(k)}$ then $\Delta V(k) \leq 0$ with the condition that the dead zone satisfy $\beta \parallel e_i(k+1) \parallel > \parallel e_i(k) \parallel, 0 < \eta(k) < 1$. If β is selected too much big then the dead zone becomes small. Hence we can conclude that $V(k)$ is bounded. Also if $\eta(k) = 0$, then from (6.26) it is evident that the weights are not changed and hence they are bounded. Therefore $V(k)$ is bounded. ∎

6.4   Sliding mode control

We define the control error as

$$
e(k) = z^d(k) - z(k) = -z(k)
$$

where $z^d(k)$ is the desired reference vector, for the vibration control, $z^d(k) = 0$.

We propose a novel quasi-sliding mode controller in (6.5) as

$$u(k) = \frac{1}{\hat{g}}\{-\hat{f} + K^T \mathbf{e}(k) + \sigma \, sign\,[s(k)]\} \tag{6.36}$$

where $\mathbf{e}(k) = [e(k+1-n) \cdots e(k)]^T$, $K = [k_n \cdots k_1]^T \in R^{nx1}$ which is selected such that the polynomial $\lambda^n + \sqrt{2}k_1\lambda^{n-1} + \cdots + 2^{\frac{n}{2}}k_n$ is stable, $s(k)$ is switching function which is defined as

$$s(k) = e(k) + K^T \mathbf{e}(k-1) \tag{6.37}$$

Theorem 6.2 *If the gain σ of the discrete-time sliding mode controller (6.36) satisfies*

$$\sigma \geq \frac{\beta H}{\|K\|} \tag{6.38}$$

where H is the upper bound of the modeling error, β is the design parameter of the fuzzy model (6.16), K satisfies the polynomial

$$\lambda^n + \sqrt{2}k_1\lambda^{n-1} + \cdots + 2^{\frac{n}{2}}k_n$$

is stable, then the closed-loop system with sliding mode control and fuzzy identifier is uniformly stable and the upper bound of the tracking error satisfies

$$\lim_{k \to \infty} \frac{1}{T}\sum_{k=1}^{T}\|\mathbf{e}(k)\| \leq \frac{\|P\|}{\lambda_{\min}(Q)}\left(1 + \frac{\beta H}{\sigma}\right) \tag{6.39}$$

where P and Q are given in (6.45).

Proof. We first prove that the switching function $s(k)$ is bounded. From (6.5), (6.16) and (6.19), the modeling error satisfies

$$\beta e_i(k+1) = \widetilde{f} + \widetilde{g}u(k) \tag{6.40}$$

Substitute the control (6.36) into the plant (6.5), the closed-loop system is

$$z(k+1) = \widehat{f} - \widetilde{f} + \frac{\widehat{g}-\widetilde{g}}{\widehat{g}}[-\widehat{f} + K^T \mathbf{e}(k) + \sigma \, sign\,[s(k)]]$$
$$= -\widetilde{f}(k) + K^T e(k) + \sigma \, sign\,[s(k)] - \widetilde{g}(k)u(k)$$

The switching function (6.37) is

$$\begin{aligned} s(k+1) &= e(k+1) + K^T\mathbf{e}(k) \\ &= -z(k+1) + K^T\mathbf{e}(k) \end{aligned} \tag{6.41}$$

Using (6.36)

$$e(k+1) + K^T \mathbf{e}(k) = -\sigma sign\,[s(k)] + \widetilde{f}(k) + \widetilde{g}(k)u(k)$$

Use (6.40),

$$s(k+1) = -\sigma sign\,[s(k)] + \beta e_i(k+1) \tag{6.42}$$

Since $|sign\,[s(k)]| \le 1$ and $|e_i(k+1)| \le H$

$$|s(k+1)| \le \sigma + \beta H \tag{6.43}$$

Because $\mathbf{e}(k) = [e(k-n+1) \cdots e(k)]^T$, and $e(k+1) = -K^T\mathbf{e}(k) + s(k+1)$,

$$\mathbf{e}(k+1) = A\mathbf{e}(k) + Bs(k+1) \tag{6.44}$$

where $A = \begin{bmatrix} 0 & 1 & 0 & \cdots & 0 \\ 0 & 0 & 1 & \cdots & 0 \\ \vdots & & \ddots & & \vdots \\ 0 & \cdots & \cdots & 0 & 1 \\ -k_n & \cdots & \cdots & \cdots & -k_1 \end{bmatrix} \in R^{nxn}$, $B = [0, \cdots 0, 1]^T \in R^{nx1}$. Because

$\det(sI - \alpha A) = \alpha^n k_n + \alpha^{n-1} k_{n-1}s + \cdots + \alpha k_1 s^{n-1} + s^n$ [58], we select $K = [k_1 \cdots k_n]^T$ such that $\sqrt{2}A$ is stable ($\alpha = \sqrt{2}$). A stable $\sqrt{2}A$ can make the following Lyapunov equation have positive definite solutions for P and Q

$$2A^T P A - P = -Q \tag{6.45}$$

where $P = P^T > 0$, $Q = Q^T > 0$.

Define the following Lyapunov function

$$V(k) = \frac{1}{\sigma^2} \mathbf{e}^T(k) P \mathbf{e}(k) \tag{6.46}$$

where P is a solution of (6.45). Using (6.44) we calculate $\Delta V(k)$

$$\Delta V(k) = \frac{1}{\sigma^2} \mathbf{e}^T(k+1) P \mathbf{e}(k+1) - \frac{1}{\sigma^2} \mathbf{e}^T(k) P \mathbf{e}(k)$$
$$= \frac{1}{\sigma^2} \mathbf{e}^T(k) \left(A^T P A - P \right) \mathbf{e}(k) + \frac{2}{\sigma^2} \mathbf{e}^T(k) A^T P B s(k+1) + \frac{1}{\sigma^2} B^T P B s^2(k+1)$$

We define $K_1 = [1, k_1 \cdots k_n]^T$, from (6.41) $s(k+1) = K_1^T \mathbf{e}(k+1)$, $s(k) = K_1^T \mathbf{e}(k)$. From (6.45) and $s(k+1) = -\sigma sign\,[s(k)] + \beta e_i(k+1)$, $\|A\| = \|B\| = 1$, and using (6.43)

$$\Delta V(k) \le -\frac{1}{\sigma^2} \|\mathbf{e}(k)\|_Q^2 - \frac{2\,[\sigma\,\|K_1\| - \beta H]}{\sigma^2} \|P\|\,\|\mathbf{e}(k)\| + \|P\| \left(1 + \frac{\beta H}{\sigma}\right)^2$$

From condition (6.38)

$$\Delta V(k) \leq -\frac{1}{\sigma^2} \|\mathbf{e}(k)\|_Q^2 + \|P\| \left(1 + \frac{\beta H}{\sigma}\right)^2$$

From [63] we known $V(k)$ is bounded, so $e(k)$ is bounded. Summarizing from 1 to T and using that $V(T) > 0$ and that $V(1)$ is a constant:

$$V(T) - V(1) \leq \sum_{k=1}^{T} -\lambda_{\min}(Q) \mathbf{e}^T(k)\mathbf{e}(k) + \|P\| \left(1 + \frac{\beta H}{\sigma}\right)^2$$

$$\lim_{T \to \infty} \frac{1}{T} \sum_{k=1}^{T} \lambda_{\min}(Q) \mathbf{e}^T(k)\mathbf{e}(k) \leq \lim_{T \to \infty} \frac{1}{T} \left(V(1) + \|P\| \left(1 + \frac{\beta H}{\sigma}\right)^2\right)$$

thus (6.39) is satisfied. By the definition $\mathbf{e}(k) = [e(k - n + 1) \cdots e(k)]^T$ we have that the tracking error $e(k)$ is bounded. ∎

6.5   Experimental Results

The proposed Fuzzy Discrete Sliding mode control(FDSMC), standard discrete sliding mode control(DSMC) and Discrete PID controller are compared. For PID Controller gains selected are as follows

$$K_{px} = 1800, K_{py} = 2000, K_{p\theta} = 2200, K_{dx} = 160$$
$$K_{dy} = 220, K_{d\theta} = 300, K_{ix} = 2000, K_{iy} = 2300, K_{i\theta} = 3500$$

All these controllers are designed to work within the range of AMD and TA. For DSMC and FDSMC. The value of σ are chosen to be $\sigma = 3$ for the AMD and $\sigma = 0.17$ for the TA. The conditions for the selecting the values of σ are from the viewpoint of Theorem. 2. These parameters are selected in such a way that satisfactory chattering and vibration attenuation are achieved. The performance validation of these controllers are implemented by the vibration control with respect to the seismic execution on the prototype. The value of $\eta(k)$ is chosen to be 0.9. The position and velocity inputs related to the fuzzy systems are normalized in such a manner that $z(k) \in [-1, 1]$. Number of experiments carried out reveals that 6 rules for $\hat{f}$ and 4 rules for $\hat{g}$ are sufficient to sustain minimal regulation errors. The Gaussian membership function is utilized for this operation. Three membership function are used to extract the linguistic variables from the floor position and velocity. As both the dampers are placed on the second floor, so the position and velocity data from the second floor are utilized. The vibration of the shake table uses the Northridge earthquake signal.
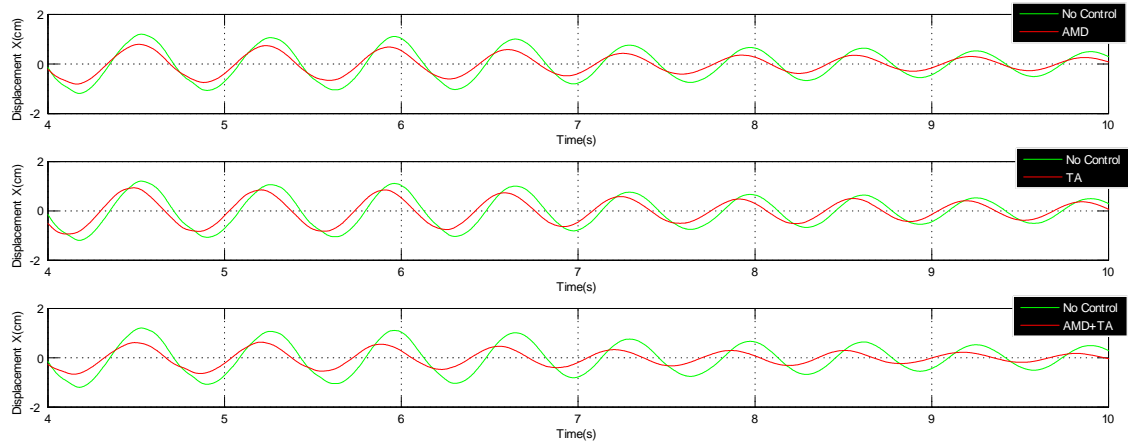
Figure 6.1: PID control of the second floor in the X direction.
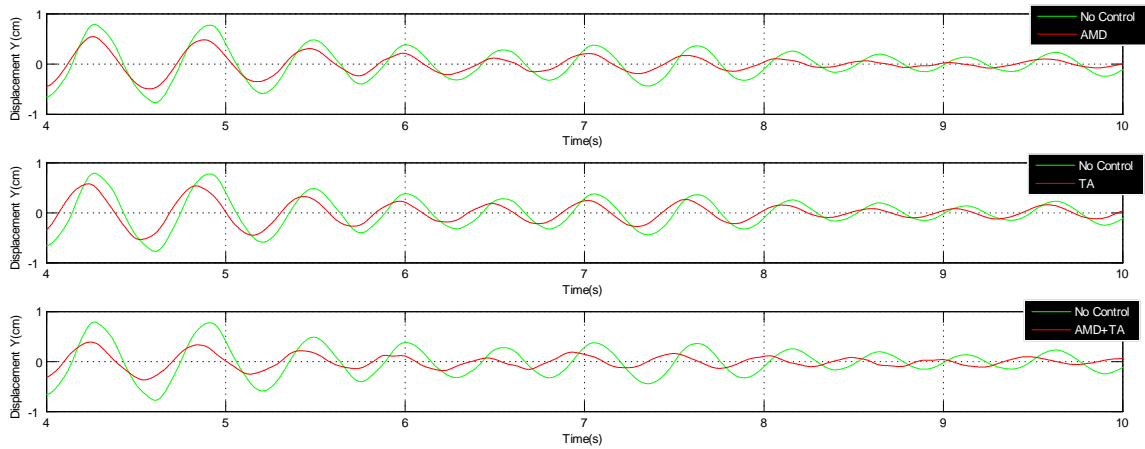
Figure 6.2: PID control of the second floor in the Y direction.

Figure 6.3: PID control of the second floor in the θ direction.

Figure 6.4: Discrete sliding mode control of the second floor in the X direction.

Figure 6.5: Discrete sliding mode control of the second floor in the Y direction.

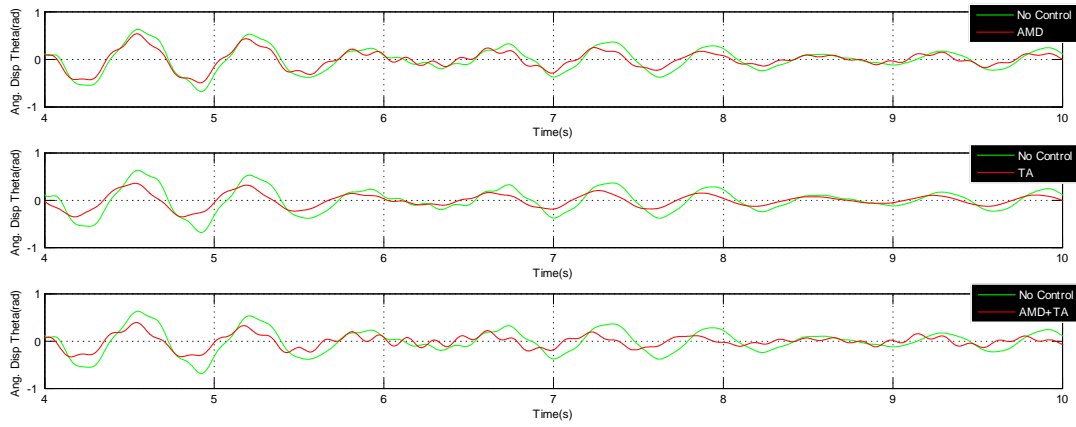Figure 6.6: Discrete sliding mode control of the second floor in the θ direction.
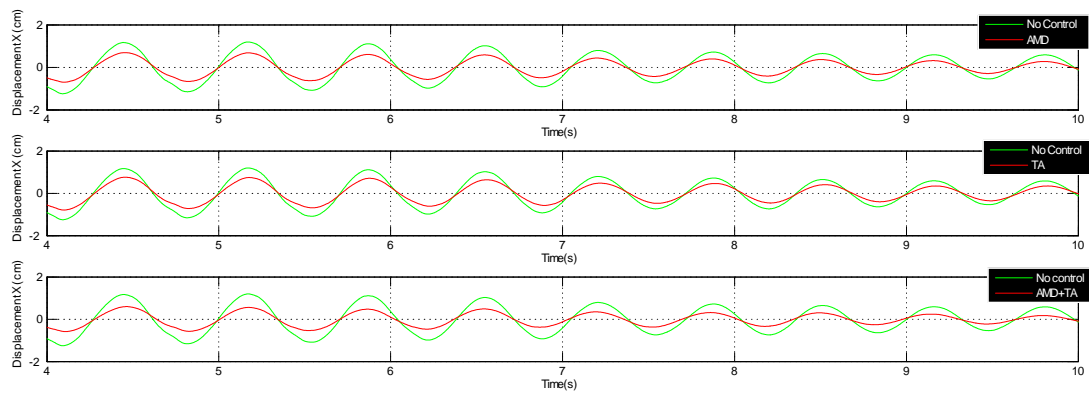
Figure 6.7: Fuzzy discrete sliding mode control of the second floor in the X direction.
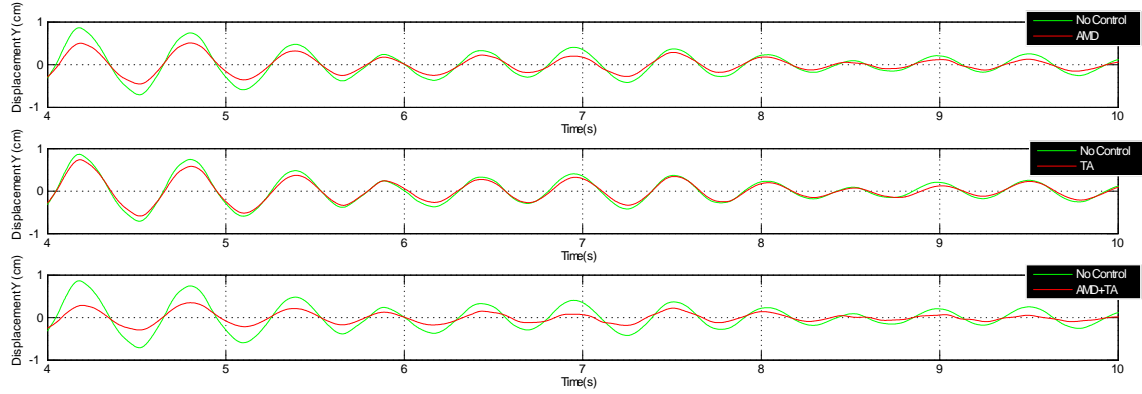

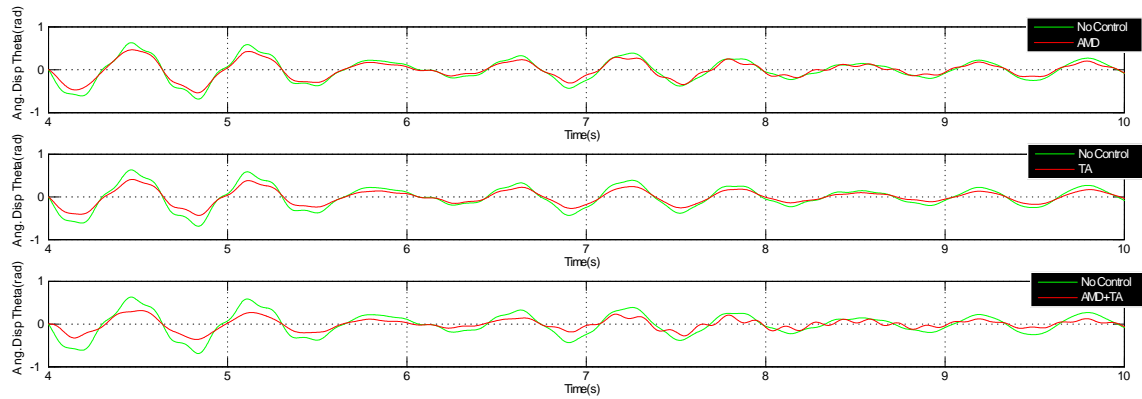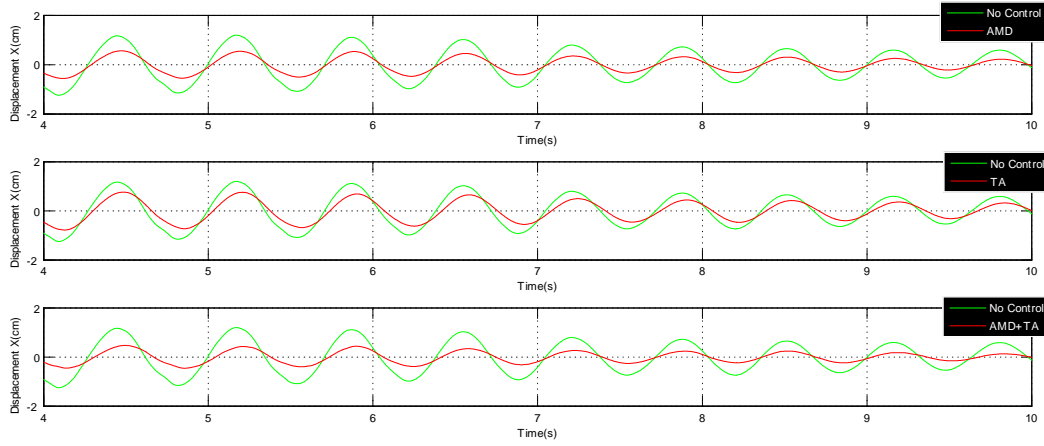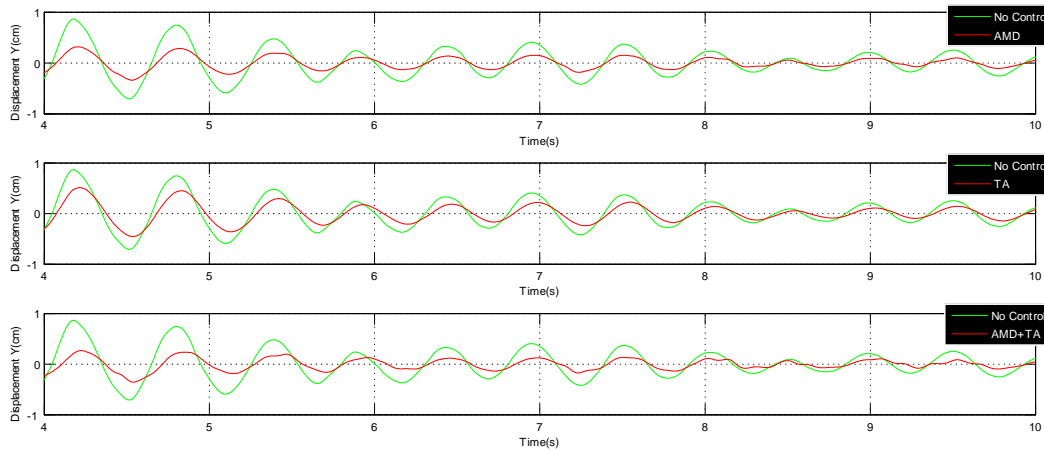Figure 6.8: Fuzzy discrete sliding mode control of the second floor in the Y direction.
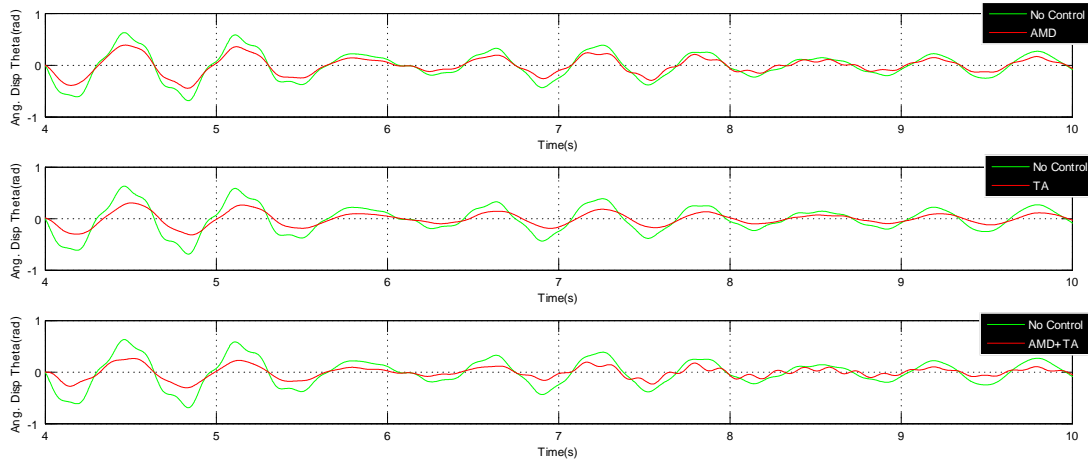
Figure 6.9: Fuzzy discrete sliding mode control of the second floor in the θ direction.
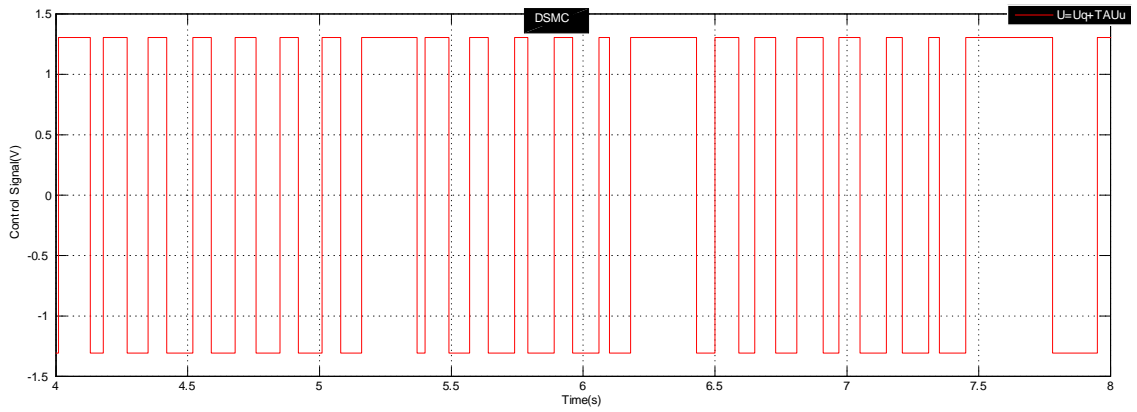
Figure 6.10: Control signal of discrete sliding mode control
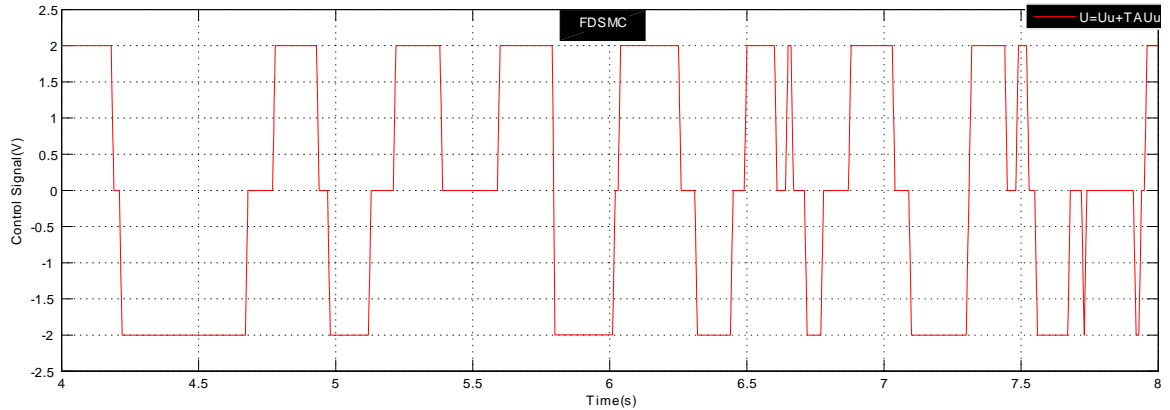
Figure 6.11: Control signal of fuzzy discrete sliding mode control

We compare our controllers in three cases: 1) without any active control (No Control); 2) with the torsion actuator (TA); 3) with both the active mass damper and the torsion actuator (AMD+TA). Figure 6.1 - Figure 6.9 displays the action of the PID control, DSMC and FDSMC to curb the vibration along $X-$direction, $Y-$direction and θ-direction. The control signal of DSMC and FDSMC are displayed in the Figure 6.10 and Figure 6.11 respectively. For clarity of the results, the vibration responses are displayed for the period of $4s$ to $10s$,whereas the control signals are scaled from the time period of $4s$ to $8s$. The average vibration displacement are calculated by the mean squared error as

$$MSE = \frac{1}{N} \sum_{k=1}^{N} x\left(k\right)^2$$

where $x\left(k\right)$ is the displacement of the floor, N is the total data number.

Table 1 - Table 4 represents the quantitative analysis of vibration control along $X-$direction, $Y-$direction and θ-direction. Here $\downarrow$ sign indicate decrease.

Table 1. Average vibration displacement by AMD+TA

	PID control	% $\downarrow$ error	DSMC	% $\downarrow$ error	FDSMC	% $\downarrow$ error	No control
X-direction	0.2216	70.5	0.1854	75.3	0.1545	79.4	0.7514
Y-direction	0.0648	50.9	0.0436	66.9	0.0388	70.6	0.1320
θ-direction	0.0588	49.9	0.0402	65.7	0.0312	73.4	0.1174

Table 2. Average vibration displacement with PID control

	with AMD	% ↓ error	with TA	% ↓ error	No control
X-direction	0.2937	60.9	0.4501	40.9	0.7514
Y-direction	0.0760	44.6	0.0838	36.5	0.1320
θ-direction	0.0713	39.2	0.0593	49.4	0.1174

Table 3. Average vibration displacement with DSMC

	with AMD	% ↓ error	with TA	% ↓ error	No control
X-direction	0.2388	68.2	0.4118	45.2	0.7514
Y-direction	0.0577	56.2	0.0779	40.9	0.1320
θ-direction	0.0637	45.7	0.0429	63.4	0.1174

Table 4. Average vibration displacement with FDSMC

	with AMD	% ↓ error	with TA	% ↓ error	No control
X-direction	0.1995	73.4	0.3847	48.8	0.7514
Y-direction	0.0511	61.2	0.0715	45.8	0.1320
θ-direction	0.0599	48.9	0.0399	66.1	0.1174

It is observed from the results that PID controller has slower response time in comparison to the FDSMC. We can see that all PID, DSMC and FDSMC controllers gives efficient performance with AMD and TA, because both horizontal actuator and torsional actuator act simultaneously. The vibration attenuations along X-direction and Y-direction are much better than θ-direction, because the active vibration control is achieved by the position of the actuator and the torque direction of the actuator. FDSMC controller is better than both PID and DSMC controllers in the vibration attenuation in all three directions. The active control of structures is improved by adding the fuzzy compensation.

6.6   Summary

In this chapter, the equation of motion related to the controlled building structures is converted into the form of discrete-time control system. The discrete sliding mode control along with fuzzy control techniques are blended to achieve superior vibration control considering bidirectional seismic forces. In the control signal (6.36), the time varying gain helps reducing the chattering better in comparison to the standard DSMC. A two-floor structure associated with one horizontal actuator and one torsional actuator for active vibration control

is proposed. The stability of the proposed controller has been established using Lyapunov stability theory. The theoretical analysis shows the effectivity of the proposed controllers. The experimental results show that PID, DSMC and FDSMC controllers works well with horizontal actuator and torsional actuator. The FDSMC controller in combination with both horizontal actuator and torsional actuator are considered to be the most efficient in mitigation of vibration along X-direction, $Y-$direction, and $\theta-$direction.

Chapter 7

Conclusions

There has been a large amount of increased research in structural vibration control in the past few decades. A number of control algorithms and devices have been applied to the structural control applications. Linear controllers were found to be simple and effective. More advanced controllers have improved the performance and robustness. Even though this field is well developed, there is still room for further research considering lateral-torsional vibration.

In this thesis, an active vibration control system for building structures was developed. Three different control algorithms were developed for the structure vibration attenuation. In the first case, classical PD/PID control techniques were used to mitigate the vibration of the structure under the bidirectional forces. The stability of the controller is validated using Lyapunov candidate. In the second phase, the PD/PID control is combined with type-2 fuzzy. The PD/PID control is used to generate the control signal to attenuate the vibration and the type-2 fuzzy logic is used to compensate the uncertain nonlinear effects present in the system. The PD/PID gains are selected such that the system is stable in Lyapunov sense. An adaptive technique was developed for tuning the fuzzy weights to minimize the regulation error. This controller shows very good vibration attenuation capability. However, its design needs some level of system knowledge. As a result another controller has been proposed, which can work with a parametrically uncertain system. Here the popular sliding mode controller has been used. So a novel fuzzy discrete sliding mode controller (FDSMC) is proposed in order to attenuate structural vibration along all three components under the grip of bidirectional earthquake forces. The analysis is based on the lateral-torsional vibration under the bidirectional waves. The proposed fuzzy discrete-time sliding mode control (FDSMC) also facilities in reducing chattering due to its time-varying gain. We prove that the closed-loop system with sliding mode control and fuzzy identifier are uniformly

stable by utilizing Lyapunov stability theorem. The proposed algorithms were experimentally verified in a lab prototype. Also the controllers, especially the FDSMC, can function with nonlinear and uncertain systems like the real building.

From the experimental analysis, it has been observed that type-2 fuzzy PID controller outperformed all other controllers. But the computational cost of the controller was big. PD/PID controller also successfully attenuated the building vibration. So the PD/PID controller is highly recommended due to its simple nature. The nature of movement of sliding mode controller is similar to that of structural movement. So this type of controller can be effectively use for vibration mitigation which is evident from the experimental results. So from computational cost and performance point of view, the discrete sliding mode controller is considered to be the most reliable one. The development of novel torsional actuator offers the superior mitigation of vibration along θ component which a significant contribution in the area of torsional vibration mitigation. Its is observed that both horizontal actuator(AMD) and torsional actuator (TA) in combination works effectively and offers efficient vibration control.

Chapter 8

Appendix: Experimental Setup

The experimental setup was established to carry out necessary experiments. The main components of the experimental set up are listed as follows

8.1 Shake Table I-40

The Shake Table I-40 (STI-40) (Quanser made) system is illustrated in Figure 8.1, where two shake table are used to generate bidirectional motion. A heavy load, bench-scale, single-axis shaker, this table features a wide surface that can easily hold a number of structures and accommodate complex as well as simple experiments. These factors, along with its convenient portability, make the Shake Table particularly useful in teaching and research labs. It's ideal for research purposes because it is easy to use, accessible, and portable. It can accurately mimic seismic activity and test building seismic performance. QUARC's open architecture control software, working with MATLAB/Simulink, makes it easy to control several tables at the same time. Flexibility is high due to various integral components. The stage is mounted on a high-quality, low backlash linear guide with a total travel of $40.0mm$ (i.e., $20.0mm$) and is driven using a ball-screw drive mechanism. Using the high torque direct drive motor, the stage loaded with a $1.5kg$ mass can be accelerated up to $1.0g$ (i.e., $9.81m/s^2$). The high-resolution encoder enables the system to obtain a linear stage position resolution of $1.22m$. The main devices needed to run the shake table is a power amplifier (e.g., VoltPAQ), a data acquisition (DAQ) device (e.g., Quanser Q2-USB), and a PC running the QUARC control software. This system can be used to simulate earthquakes. The dimensions of the top stage is $43.2 \times 10.2cm2$. The DC motor used for the Shake Table I-40 is the Magmotor S23 Brushed Servo Motor with a stack length of 100. The linear position of the stage is obtained
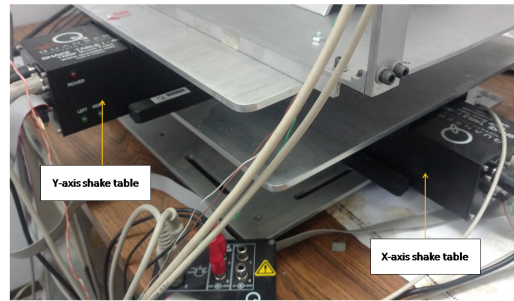
Figure 8.1: Bidirectional shake table arrangement

using a high-resolution rotary optical encoder coupled to the linear screw of the linear guide. Specifically, it is a US Digital E3-2048-250-N-H-D-B encoder. When used in quadrature mode, the encoder outputs 8192 counts per revolution of the shaft. Using this encoder, the effective linear position resolution of the top stage is $1.22m$. The top stage of the Shake Table I-40 is mounted on the Misumi LX3010C-B1-T3056.4-150 single-axis actuator. It is a covered single-axis linear guide with a rail length of $150mm$ and has a lead-screw pitch of $10mm$. The Left or Right limit switch gets triggered when the top stage moves close to the left or right mechanical range. These sensors are used to stop the controller when the table exceeds its stroke. They are also used to calibrate the stage to its center, mid-stroke position [114].

8.2   VoltPAQ-X2 amplifier

The VoltPAQ (Quanser made) is a linear power amplifier designed to run Quanser experiments. The amplifier has been illustrated in the Figure 8.2. The VoltPAQ-X2 can power two loads. The VoltPAQs replaces the UPM line of power amplifiers. Every VoltPAQ-X2 consists of the following components and features:

1. Amplifier capable of supplying around $24V$ and $4A$ continuous per channel.
2. Current sensing capability for each channel.
3. User ability to enable/disable individual amplifiers.
4. Automatic thermal shut-down to prevent damage to amplifier.
5. Over-heating/over-current fault indication output.
6. E-stop.

Figure 8.2: VoltPAQ-X2 amplifier

Amplifier Specifications Value are listed as:

Output voltage no load: $-23.3V$ to $+21.8V, 2A$ load:$-22.3V$ to $+20.8V$,continuous current output per channel $\pm\ 4A$,voltage gain $3V/V$,current Sense $1A/V$,amplifier command voltage range $\pm\ 10V$ [101]

8.3   Q2 USB data acquisition device

Quanser ground-breaking USB data acquisition technology delivers reliable real-time performance via a USB interface. Q2-USB data acquisition device offers an extensive range of hardware features and software support capabilities. Quanser DAQ technology combined with standard connector interfaces ensure easy and quick access to signals. With low I/O conversion times and easy connectivity, the Q2-USB is ideal for teaching control concepts, as you can achieve up to $2kHz$ closed-loop control rate. This control rate is superior to any other commercially available USB-DAQ technology. When combined with Quanser power amplifier and control design software, the Q2-USB provides a convenient rapid prototyping and Hardware-In-The-Loop (HIL) development environment. With a wide range of inputs and outputs, you can easily connect and control a variety of devices instrumented with analog and digital sensors, including encoders - all with one board. A Q2-USB is shown in Figure 8.3. The main features of Q2 USB are [106]

1. Optimized for real-time control performance with Quanser QUARC and RCP Toolkit control software or custom code.

2. USB 2.0 high-speed interface.

3. Compatible with Windows 7.

Figure 8.3: Q2-USB data acquisition

4. Multiple Q2-USB units can be used simultaneously.

5. Robust metal data acquisition device case.

8.4   Inteco RT-DAC/USB

The RT-DAC/USB2 is a multifunction analog and digital I/O board dedicated to real-time data acquisition and control in the Windows 95/98/NT/2000/XP environments. The board contains a Xilinx FPGA chip. All boards are built as the OMNI version. It means the boards can be reconfigured to introduce a new functionality of all inputs and outputs without any hardware modification. The default configuration of the FPGA chip accepts signals from incremental encoders and generates PWM outputs, typical for mechatronic control applications and is equipped with the general purpose digital input/outputs (GPIO), A/D and D/A converters, timers, counters, frequency meters and chronometers [62]. The RT-DAC/USB is illustrated in Figure 8.4

The RT-DAC/USB2 setup contains:

- RT-DAC/USB2 board.

- Two 40-pin ribbon cables (only one cable when the digital version is distributed).

- USB cable.

- 9V-12V DC / 4W stabilized power supply.

The block diagram of the RT-DAC/USB2 board is shown in Figure 8.5
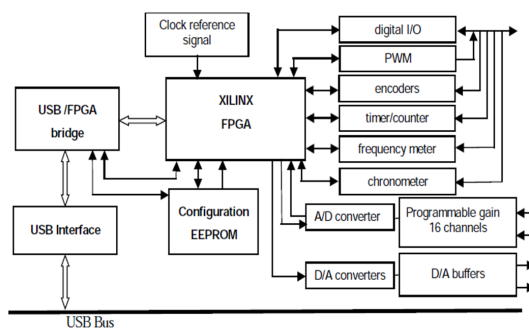
Figure 8.4: RT-DAC/USB

Figure 8.5: Block diagram of RT-DAC/USB2

Figure 8.6: Biaxial accelerometer

8.5   Biaxial XL403A accelerometer

Measurement Specialities XL403A biaxial analog accelerometer have the temperature working range of $-40°C$ to $+85°C$ and offers high precise measurements. The outputs are DC coupled. The other attributes are it is fully scaled,temperature compensated and referenced. The improved accuracy are achieved by minimizing the variations between temperature and aging effects. A view of biaxial accelerometer is shown in Figure 8.6. The important features of these type of accelerometer are [142].

- High precision and linearity considering vast range of temperature.
- Meant for rugged and tough environment.
- Small size.
- Built in power supply regulation feature.
- Instillation is easy.

8.6   Two floor structure

The two floor structure is displayed in Figure 8.7 . The material of the structure is stainless steel. The length of the floors in X and Y directions are 54 cm and 32 cm respectively. The total height of the structure from the shake table is 120 cm having a distance gap of 60 cm each between ground floor, first floor and second floor respectively. The weight of each floor is $3.5Kg$. Both the actuator are placed on the top floor.
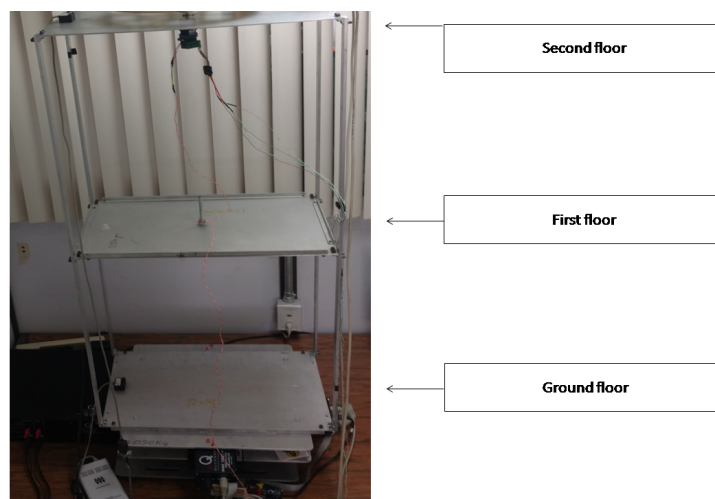
Figure 8.7: Two floor structure on bidirectional shake table

8.7 Horizontal actuator (AMD)

Active mass damper (AMD) is used for lateral vibration attenuation. AMD is a linear servo actuator (STB1108, Copley Controls Corp). The total length of the actuator is $34\ cm$. The schematic view of the AMD can be seen in Figure 8.8. ServoTube delivers the speed of a belt-drive system with the clean reliability of a linear forcer at a price unprecedented in the industry. Familiar form factor, integral position feedback and large air gap make installation simple. The ServoTube forcer components consist of an IP67 rated forcer and a sealed stainless steel thrust rod enclosing rare-earth magnets. Four models deliver a continuous force range of $9{\sim}27N$ ($2{\sim}6lb$) with peak forces up to $92N$ ($21lb$). A range of Thrust Rods are available for travel lengths up to $372mm$. The patented magnetic design of ServoTube generates $12micron$ repeatability and $350micron$ accuracy from a non-contact, integral position sensor. No external encoder is required. Position output is industry standard $1V$ pk-pk sin/cos signals. The tubular forcer has superior thermal efficiency, radiating heat uniformly. High duty cycles are possible without the need for forcer-air or water cooling [124].

8.8 Torsional actuator (TA)

Torsional actuator is a circular disc which is used for torsional vibration attenuation. The torsional actuator power is provided by $5V$ DC motor. The disc is made of aluminum which is of diameter $30\ cm$. The schematic view of TA with motor can be seen in Figure 8.9.

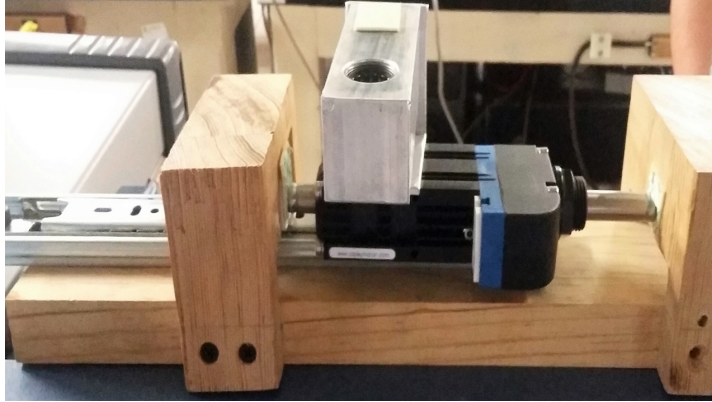Figure 8.8: Horizontal Actuator (AMD)

Figure 8.9: Torsional actuator with motor

Bibliography

[1] Adeli, H., and Saleh, A, Optimal control of adaptive/smart bridge structures, *Journal of Structural Engineering* , Vol.123, Issue No.2, pp.218 –226, 1997.

[2] Adeli, H. and Jiang, X., Dynamic fuzzy wavelet neural network model for structural system identification, *Journal of Structural Engineering*, Vol.132, Issue No.1, pp.102–111, 2006.

[3] Agrawal, A. K., and Yang, J. N., Compensation of time-delay for control of civil engineering structures, *Journal of Earthquake Engineering and Structural Dynamics*, Vol. 29, Issue No.1, pp.37–62, 2000.

[4] Ahlawat , A. S. and Ramaswamy, A. , Multiobjective optimal FLC driven hybrid mass damper system for torsionally coupled, seismically excited structures, *Earthquake Engineering & Structural Dynamics*, Vol. 31, Issue No.12, pp.2121–2139, 2002.

[5] Alavinasab, A., Moharrami, H., and Khajepour, A., Active control of structures using energy-based LQR method, *Computer-Aided Civil and Infrastructure Engineering*, Vol.21, Issue No.8, pp.605-611, 2006.

[6] Ali, S. F., and Ramaswamy, A., Optimal fuzzy logic control for MDOF structural systems using evolutionary algorithms, *Engineering Applications of Artificial Intelligence*, Vol. 22, pp. 407–419, 2009.

[7] Alkhatib, R. and Golnaraghi, M. F., Active Structural Vibration Control: A Review, *The Shock and Vibration Digest*, Vol.35, Issue No.5, pp.367–383, 2003.

[8] Amini, F., and Tavassoli, M. R., Optimal structural active control force, number and placement of controllers, *Engineering Structures*, Vol.27, Issue No.9, pp.1306–1316, 2005.

[9]   Anderson, J. C., and Naeim, F.,*Basic structural dynamics*, Wiley , Los Angeles, California, 2012.

[10] Angeles-Cervantes, J. M., and Alvarez-Icaza, L., 3D identification of seismically excited buildings with sensors arbitrarily placed, *American Control Conference*, pp.3807-3812, Minneapolis, Minnesota, USA, 2006.

[11] Angeles-Cervantes, J. M., and Alvarez-Icaza, L., 3D Identification of buildings seismically excited, 16th IFAC World Congress, Czech Republic, Vol.16, 2005.

[12] Arfiadi, Y., and Hadi, M. N. S., Passive and active control of three-dimensional buildings, *Earthquake engineering & structural dynamics*, Vol.29, Issue No.3, pp.377-396, 2000.

[13] Bani-Hani, K., and Ghaboussi, J., Nonlinear Structural Control Using Neural Networks, *Journal of Engineering Mechanics*, Vol. 24, Issue No. 3, pp.319-327, 1998.

[14] Bartoszewicz, A., Discrete-time quasi-sliding mode control strategies, *IEEE Transactions on Industrial Electronics*, Vol. 45, pp. 633–637, 1998.

[15] Bathaei, A., Zahrai, S. M., and Ramezani, M., Semi-active seismic control of an 11-DOF building model with TMD+MR damper using type-1 and -2 fuzzy algorithms,*Journal of Vibration and Control*, 2017.

[16] Bernhard, B. and Mulvey, C. J., A constructive proof of the Stone-Weierstrass theorem, *Journal of Pure and Applied Algebra,* Vol.116, Issue No.1–3, pp.25-40, 1997.

[17] Cai, G. and Huang, J., Discrete-time variable structure control method for seismic-excited building structures with time delay in control, *Earthquake Engng Struct. Dyn.*, Vol. 31, pp.1347-1359, 2002.

[18] Camp, C., Pezeshk, S., and Cao, G., Optimized Design of Two-Dimensional Structures Using a Genetic Algorithm, Journal of Structural Engineering, Vol.124, Issue No.5, pp.551–559, 1998.

[19] Chang, J. C. H. , Soong, T. T. , Structural control using active tuned mass damper, *Journal of Engineering Mechanics,* Vol.106, Issue No.6, pp.1091-1098, 1980.

[20] Chia-Ming Chang, Billie F. Spencer Jr. and Pengfei Shi, Multiaxial active isolation for seismic protection of buildings, *Structural Control and Health Monitoring*,Vol.21, pp.484-502, 2014.

[21] Cheng,F.Y.,*Matrix analysis of structural dynamics: Applications and earthquake engineering*, CRC press, New York, 2000.

[22] Choi, K. M., Cho, S. W., Kim, D. O., and Lee, I. W., Active control for seismic response reduction using modal-fuzzy approach, *International Journal of Solids and Structures*, Vol.42, Issues No.16-17, pp.4779–4794, 2005.

[23] Chopra, A. K., *Dynamics of Structures*,Prentice-Hall International Series, 2011.

[24] Chandiramani, N.K. and Motra, G.B., Lateral-Torsional Response Control of MR Damper Connected Buildings, I*nternational Mechanical Engineering Congress and Exposition*, Vol.4B ,San Diego, California, USA, 2013.

[25] Christenson, R.E., Spencer Jr, B. F., Hori, N., and Seto, K., Coupled building control using acceleration feedback, *Computer-Aided Civil and Infrastructure Engineering*, Vol.18, Issue No.1, pp.4–18,2003.

[26] Collins, R. , Basu, B. , Broderick, B. , Control strategy using bang–bang and minimax principle for FRF with ATMDs, *Engineering Structures, Vol.*28, Issue No.3 pp.349–356, 2006.

[27] Constantinou, M. C., and Symans, M. D., Seismic response of structures with supplemental damping, *The Structural Design of Tall Buildings*, Vol.22, Issue No.2, pp.77–92, 1993.

[28] Correnza, J. C, Hutchinson, G. L. and Chandler, A. M. , Effect of transverse load-resisting elements on inelastic earthquake response of eccentric-plan buildings, *Earthquake Engineering & Structural Dynamics*, Vol.23, Issue No.1, pp75-89, 1994.

[29] Crossley, W. A. , Cook, A. M. , Fanjoy, D. W. , and Venkayya, V. B. , Using the two branch tournament genetic algorithm for multiobjective design, *AIAA Journal*, Vol.37, Issue No.2, PP.261-267, 1999.

[30] Cruz, E., and Cominetti, S., Three-Dimensional buildings subjected to bidirectional earthquakes. Validity of analysis considering unidirectional earthquakes, *12th World Conference on Earthquake Engineering*, 2000.

[31] Dai, J., Fuzzy Logic Based Control and Simulation Analysis for Nonlinear Structure, *Second International Conference on Computer Modeling and Simulation*, Sanya, Hainan, China, 2010.

[32] Das, D., Datta, T. K., and Madan, A, Semiactive fuzzy control of the seismic response of building frames with MR dampers, *Earthquake Engineering and Structural Dynamics*, Vol.41, pp. 99–118, 2012.

[33] Datta, T. K., A state-of-the-art review on active control of structures, *ISET Journal of Earthquake Technology*, Vol. 40, Issue No. 1, pp.1-17, 2003.

[34] De Cock K, De Moor B, Minten W, et al. (1997) A tutorial on PID-control. Katholieke Universiteit Leuren Department of Electrical Engineering ESAT-SISTA /TR.

[35] Desu, N.B., Deb, S. K. and Dutta, A., Coupled tuned mass dampers for control of coupled vibrations in asymmetric buildings, *Structural Control and Health Monitoring*, Vol.13, Issue No.5, pp.897–916, 2006.

[36] Donaldson, B., *Introduction to structural dynamics*, Cambridge University Press, United Kingdom,2006.

[37] Du, Y. and Lin, Z., Sequential optimal control for serially connected isolated structures subject to two-directional horizontal earthquake, *Control and Automation (ICCA),* pp.1508 - 1511, Xiamen, 2010.

[38] Du, H., and Zhang, N., H_∞ control for buildings with time delay in control via linear matrix inequalities and genetic algorithms, *Engineering Structures*, Vol.30, Issue No.1, pp.81-92, 2008.

[39] Duc, N. D., Vu, N. L., Tran, D. T., and Bui, H. L., A study on the application of hedge algebras to active fuzzy control of a seism-excited structure, *Journal of Vibration and Control*, Vol.18, Issue No. 14, pp. 2180-2200, 2012.

[40] Fisco, N. R., and Adeli, H., Smart structures: part I – active and semi-active control, *Scientia Iranica*, Vol.18, Issue No.3, pp. 275–284, 2011.

[41] Fisco, N. R., and Adeli, H.,Smart structures: part II – hybrid control systems and control strategies, *Scientia Iranica*, Vol.18, Issue No.3, pp.285–295, 2011.

[42] Forrai, A., Hashimoto, S., Funato, H., and Kamiyama, K. , Structural control technology: System identification and control of flexible structures, *Computing and control engineering Journal*, Vol.12 , Issue No. 6 , pp.257 - 262, 2001.

[43] Fu, C., Application of torsional tuned liquid column gas damper for plan-asymmetric buildings, *Structural Control and Health Monitoring*, Vol.18, Issue No.5, pp.492–509, 2011.

[44] Fujinami, T., Saito, Y., Morishita, M. ,Koike , Koike, Y. and Tanida, K., A hybrid mass damper system controlled by H■ control theory for reducing bending–torsion vibration of an actual building, *Earthquake Engineering and Structural Dynamics*, Vol.30, Issue No.11, pp.1639–1653, 2001.

[45] Fur, L-S., Yang T. Y. H., and Ankireddi S., Vibration control of tall buildings under seismic and wind loads, *Journal of Structural Engineering, Vol.122*, Issue No.8, pp.948–957, 1996.

[46] Gao, W., Wang, Y., and Homaifa, A., Discrete-time variable structure control systems, *IEEE Trans. Ind. Electron.*, Vol. 42, pp. 117–122, 1995.

[47] Gattulli, V. , Lepidi, M. and Potenza, F., Seismic protection of frame structures via semi-active control: modeling and implementation issues, *Earthquake Engineering and Engineering Vibration*, Vol.8, Issue No.4, pp.672-645, 2009.

[48] Gawronski, W., Actuator and sensor placement for structural testing and control, *Journal of Sound and Vibration*, Vol.208, Issue No.1, pp.101–109, 1997.

[49] Ghaboussi, J., and Joghataie, A, Active control of structures using neural networks, Journal of Engineering Mechanics, Vol.121, Issue No.4, pp.555–567, 1995.

[50] Guclu, R., Sliding mode and PID control of a structural system against earthquake, *Mathematical and Computer Modelling*, Vol.44, Issues No.1-2, pp.210–217, 2006.

[51] Guclu, R., and Yazici, H., Vibration control of a structure with ATMD against earthquake using fuzzy logic controllers, J*ournal of Sound and Vibration,* Vol.318, Issues No.1-2, pp.36-49, 2008.

[52] Hart, G. C., and Wong, K., *Structural Dynamics for Structural Engineers,* Wiley, 1999.

[53] Hartog, J.P., *Mechanical Vibrations*, McGraw-Hill, New York, 1956.

[54] Heo, J. S., Lee, S. K., Park, E., Lee, S. H., Min. K. W., Kim, H. , Jo, J., and Cho, B. H. ,Performance test of a tuned liquid mass damper for reducing bidirectional responses of building structures, *The Structural Design of Tall and Special Buildings, Vol.18*, Issue No.7, pp.789–805 , 2009.

[55] Ho, C. C., and Ma, C. K., Active vibration control of structural systems by a combination of the linear quadratic Gaussian and input estimation approaches, J*ournal of Sound and Vibration,* Vol.301, Issues No.3-5, pp.429-449, 2007.

[56] Hochrainer, M. J., Adam, C. and Ziegler, F., Application of tuned liquid column dampers for passive structural control, *7th International Congress on Sound and Vibration (ICSV 7)*, Garmisch-Partenkirchen, Germany, 2000.

[57] Holland, J. H., *Adaptation in natural and artificial systems*, MIT press, 1975.

[58] Horn, R. A. and Johnson, C. R., *Matrix Analysis*, Melbourne, Australia: Cambridge University Press, 1985.

[59] Housner, G. W., Bergman, L. A., Caughey, T. K., Chassiakos, A. G., Claus, R. O., Masri, S. F., Skeleton, R. E., Soong, T. T., Spencer Jr., B. F., and Yao, J. T. P., Structural Control: Past, Present and Future, *Journal of Engineering Mechanics*, Vol.123, Issue No.9, pp.897-971, 1997.

[60] Huo, L. ,and Li, H. , Torsionally coupled vibration control of eccentric buildings using liquid dampers,   *Active and Passive Smart Structures and Integrated Systems 2009*, Vol. 7288, 2009.

[61] Ikhouanea, F., Mañosaa, V., and Rodellara, J., Dynamic properties of the hysteretic Bouc-Wen model, *Systems and Control Letters,* Vol.56, Issue No. 3, pp. 197–205, 2007.

[62] IINTECO RT-DAC/USB2 I/O Board, *User's Manual*, Kraków, 2010.

[63] Ioannou, I.A., and Sun, J., *Robust Adaptive Control*, Upper Saddle River, NJ: Prentice-Hall, Inc., 1996.

[64] Iwamoto, K., Yuji, K., Kenzo, N., Koji, Tanida and Itaru, Iwasaki., Output Feedback Sliding Mode Control for Bending and Torsional Vibration Control of 6-story flexible Structure, *JSME International Journal Series C*, Vol.45, Issue No.1, pp.150-158, 2002.

[65] Janardhanan, S., and Bandyopadhyay, B., Multirate feedback based quasi-sliding mode control of discrete-time systems, *IEEE Trans. Autom. Control*, Vol. 52, pp. 499–503, 2007.

[66] Jiang, X. and Adeli, H., Pseudospectra, MUSIC, and dynamic wavelet neural network for damage detection of highrise buildings, *International Journal for Numerical Methods in Engineering*, Vol.71, Issue No.5, pp.606–629, 2007.

[67] Jiang , X., and Adeli, H., Neuro-genetic algorithm for non-linear active control of structures, *International Journal for Numerical Methods in Engineering*, Vol.75, Issue No.7, pp.770-786, 2008.

[68] John, R. I., and Coupland, S., Type-2 Fuzzy Logic: A Historical View. *IEEE Computational Intelligence Magazine,* Vol. 2, Issue No. 1, pp. 57–62, 2007.

[69] Jolly, M. R. , Bender, J. W. , and Carlson, J. D. , Properties and applications of commercial magnetorheological fluids, *Smart Structures and Materials 1998: Passive Damping and Isolation*, Vol. 3327, pp.262-275, 1998.

[70] Kim, J. T., Jung, H. J., and Lee, I. W., Optimal structural control using neural networks, *Journal of Engineering Mechanics*, Vol.126, Issue No.2, pp.201–205, 2000.

[71] Kim , H. and Adeli, H., Hybrid control of irregular steel highrise building structures under seismic excitations, *International Journal for Numerical Methods in Engineering*, Vol.63, Issue No.12, pp.1757–1774, 2005.

[72] Lagaros, N. D, Fragiadakis, M., Fragility assessment of steel frames using neural networks, *Earthquake Spectra*, Vol.23, Issue No.4, pp.735–752, 2007.

[73] Lagaros, N. D., Plevris, V., Papadrakakis, M., Neurocomputing strategies for solving reliability-robust design optimization problems, *Engineering Computations*, Vol.27, Issue No.7, pp.819–840, 2010.

[74] Lagaros, N. D. , and Papadrakakis, M., Neural network based prediction schemes of the non-linear seismic response of 3D buildings, *Advances in Engineering Software*, Vol.44, Issue No.1, pp.92–115, 2012.

[75] Lee, C. S., and Hong, H. P., Statistics of inelastic responses of hysteretic systems under bidirectional seismic excitations, *Engineering Structures*, Vol.32, Issue No. 8, pp.2086-2074, 2010.

[76] Lewis, F. L., Dawson, D. M., and Abdallah, C. T., *Robot Manipulator Control: Theory and Practice*. Second Edition: Marcel Dekker Inc, 2004.

[77] Liang, S. G., Experiment study of torsionally structural vibration control using circular tuned liquid column dampers, *Special Structures*, Vol.13, Issue No.3, pp.33-35, 1996.

[78] Li, H. N., Chang, Z. G. , Song, G. B., and Li, D. S.,Studies on structural vibration control with MR dampers using GA, *American Control Conference*, Vol.6, pp.5478-5482, Boston, Massachusetts, 2004.

[79] Li, Z., and Wang, S., Robust optimal H∞ control for irregular buildings with AMD via LMI approach, *Nonlinear Analysis: Modelling and Control*, Vol.19, Issue No.2, pp.256–271, 2014.

[80] Li, H. N., and Li, X. L., Experiment and analysis of torsional seismic responses for asymmetric structures with semi-active control by MR dampers, *Smart Materials and Structures*, Vol.18, Issue No.7, 2009.

[81] Li, C. , Li, J., and Qu, Y., An optimum design methodology of active tuned mass damper for asymmetric structures , *Mechanical Systems and Signal Processing* , *Vol.*24 , Issue No.3, pp.746–765, 2010.

[82] Li, H-N and Huo , L-S., Seismic response reduction of eccentric structures using tuned liquid column damper(TLCD), *Vibration Analysis and Control -New Trends and Development* , 2011.

[83] Li, H-N and Huo , L-S., Optimal design of liquid dampers for torsionally coupled vibration of structures, *Intelligent Control and Automation, Vol.5, pp.4535-4538.2004.*

[84] Li, Z., Gu, Z., and Deng, Z., Discrete-time fuzzy variable structure control for buildings with delay time in control, *8th World Congress on Intelligent Control and Automation (WCICA)*, Jinan, China, 2010.

[85] Li, Z., and Den, Z., Improving existing "reaching law" for better discrete control of seismically-excited building structures, *Front. Archit. Civ. Eng.*, Vol. 3, Issue No. 2, pp.111–116, 2009.

[86] Liang, Q., and Mendel, J.M., Interval type-2 fuzzy logic systems: theory and design, *IEEE Transactions on Fuzzy Systems,* Vol.8, Issue No.5*, pp. 535-550, 2002.*

[87] Lin, J. L., Tsai, K. C. and Yu, Y. J., Bi-directional coupled tuned mass dampers for the seismic response control of two-way asymmetric-plan buildings, *Earthquake Engineering & Structural Dynamics*, Vol.40, Issue No.6, pp.675–690, 2011.

[88] Lin, TC., Liu, HL., and Kuo, MJ., Direct adaptive interval type-2 fuzzy control of multivariable nonlinear systems, *Engineering Applications of Artificial Intelligence*, Vol.22, Issue No. 3, pp. 420-430, 2009.

[89] Lin, C. C., Chang. C., and Wang, J. Fu., Active control of irregular buildings considering soil–structure interaction effects, *Soil Dynamics and Earthquake Engineering*, Vol.30, Issue No. 3, pp.98–109, 2010.

[90] Lin, J. L. and Tsai, K. C., Seismic analysis of two-way asymmetric building systems under bi-directional seismic ground motions, *Earthquake Engineering & Structural Dynamics,* Vol.37, Issue No.2, pp.305-328, 2008.

[91] Lu, X. and Zhao, B., Discrete-time variable structure control of seismically excited building structures, E*arthquake Engng Struct. Dyn.*, Vol. 30, pp. 853-863, 2001.

[92] Luca, S. G., Chira, F., and Rosca, V. O., Passive active and semi-active control systems in civil engineering, *Constructil Arhitectura, pp.*3-4, 2005.

[93] Maria, G., Selvaganesan, N., Ajith Kumar, B., and Kapoor, S., Dynamic analysis and sliding mode vibration control for a two storeyed flexible building structure, *International Conference on Control Communication & Computing India (ICCC)*, Trivandrum, India, 2016.

[94] McNamara, R. J., Tuned mass dampers for buildings, *Journal of the Structural Division*, Vol.103, Issue No.9, pp.1785–1798, 1977.

[95] Mendel, J. M., *Uncertain rule-based fuzzy logic systems: Introduction and new directions*, Prentice Hall PTR, Upper Saddle River, NJ, 2001.

[96] Nerves, A. C., and Krishnan, R., Active control strategies for tall civil structures, *International Conference on Industrial Electronics, Control, and Instrumentation*, Vol.2, pp.962–967, Orlando, Florida, 1995.

[97] Nguyen, T. H., Kwok, N. M. , Ha, Q. P. , Li, J. and Samali, B., Adaptive sliding mode control for civil structures using magnetorheological dampers, *International Symposium on Automation and Robotics in Construction, 2006.*

[98] Nigdeli, S. M., and Boduroglu, M. H., Active tendon control of torsionally irregular structures under near-fault ground motion excitation, *Computer-Aided Civil and Infrastructure Engineering*, Vol.28, Issue No. 9, pp.718–736, 2013.

[99] Nigdeli, S. M., Effect of feedback on PID controlled active structures under earthquake excitations, *Earthquakes and Structures*, Vol.6, Issue No.2, pp.217-235, 2014.

[100] Obe, O. I., Optimal actuators placements for the active control of flexible structures, *Journal of Mathematical Analysis and Applications*, Vol.105, Issue No.1, pp.12–25, 1985.

[101] VoltPAQ-X2/X4, User Manual, Quanser inc., 2010.

[102] Park, W., Park, K. S., and Koh, H. M., Active control of large structures using a bilinear pole-shifting transform with H_∞ control method, *Engineering Structures*, Vol. 30, Issue No.11, pp.3336-3344, 2008.

[103] Park, K. S., Koh, H. M., and Ok, S. Y., Active control of earthquake excited structures using fuzzy supervisory technique, *Advances in Engineering Software*, Vol. 33, Issue No. 11-12, pp. 761–768, 2002.

[104] Paul, S., Yu, W., and Li, X., Recent advances in bidirectional modeling and structural control, *Shock and Vibration* 2016, 17 pages, 2016.

[105] Paul, S., and Yu, W., A method for bidirectional active control of structures, *Journal of Vibration and Control*, First published date: May-16-2017.

[106] Q2-USB data acquisition device, http://www.quanser.com/products/q2-usb.

[107] Reigles,D. G., and Symans, M. D., Supervisory fuzzy control of a base-isolated benchmark building utilizing a neuro-fuzzy model of controllable `fluid` viscous dampers, *Structural Control and Health Monitoring*, Vol.13, Issues No.2-3, pp.724-747, 2006.

[108] Roldán C, Campa FJ, Altuzarra O, et al. (2014) Automatic identification of the inertia and friction of an electromechanical actuator. In: New Advances in Mechanisms, Transmissions and Applications, Volume 17 of the series Mechanisms and Machine Science, pp.409-416.

[109] Saiful Islam, A. B. M, Hussain, R. R., Jameel, M., et al., Non-linear time domain analysis of base isolated multi-storey building under site specific bi-directional seismic loading, *Automation in Construction*, Vol. 22, pp.554-566, 2012.

[110] Saragih, R., Designing Active vibration control with minimum order for flexible structures. In:IEEE International Conference on Control and Automation, pp. 450-453, 2012.

[111] Sarpturk, S.Z. , Istefanopolos, Y., and Kaynak, O., On the stability of discrete-time sliding mode control systems, *IEEE Transactions on Automatic Control*, Vol. 32, pp. 930–932, 1987.

[112] Sepúlveda, R., Castillo, O., Melin, P., Rodríguez-Díaz, A., and Montiel, O., Experimental study of intelligent controllers under uncertainty using type-1 and type-2 fuzzy logic, *Information Sciences*, Vol. 177, Issue No. 10, pp. 2023–2048, 2007.

[113] Seto, K., A structural control method of the vibration of flexible buildings in response to large earthquake and strong winds. In:Proceedings of the 35th Conference on Decision and Control ,vol. 1, pp. 658-663, 1996.

[114] Shake Table I-40, *User Manual*, STI-40, Quanser Inc., 2012.

[115] Shariatmadar, H., Golnargesi, S., and Akbarzadeh-T, MR., Vibration control of buildings using atmd against earthquake excitations through interval type-2 fuzzy logic controller, *Asian Journal of Civil Engineering*, Vol. 15, Issue No. 3, pp.331-328, 2014.

[116] Shook, D. A., Roschke,P. N., Lin, P.Y., and Loh, C. H., GA-optimized fuzzy logic control of a large-scale building for seismic loads, Engineering Structures, Vol.30, Issue No.2, pp.436-449, 2008.

[117] Shook, D. A., Roschke, P. N., Lin, P. Y., and Loh, C. H., Semi-active control of a torsionally-responsive structure, *Engineering Structures,* Vol.31, Issue No.1, pp.57-68, 2009.

[118] Singh, M. P. , Singh, S. and Moreschi, L. M., Tuned mass dampers for response control of torsional buildings, *Earthquake Engineering and Structural Dynamcs*, Vol.31, Issue No.4 pp.749–769, 2002.

[119] Soleymani, M., Abolmasoumi, A.H, Bahrami, H., Khalatbari-S, A., Khoshbin, E., and Sayahi, S., Modified sliding mode control of a seismic active mass damper system considering model uncertainties and input time delay, *Journal of Vibration and Control,* First published date: July-06-2016.

[120] Sontag, E. D., and Wang Y., On characterizations of the input-to-state stability property, *Systems and Control Letters*, Vol. 24, Issue No. 5, pp.351-359, 1995.

[121] Soong,T. T., *Active Structural Control: Theory and Practice*, Addison-Wesley Pub, New York, 1999.

[122] Soong, T. T., and Spencer, B. F., Supplemental energy dissipation: State-of-theart and state-of-the-practice, *Engineering Structures*, Vol.24, Issue No.3, pp.243–259, 2002.

[123] Spencer, B. F., and Nagarajaiah, S., State of the art of structural control, *Journal of Structural Engineering*, Vol.129, Issue No.7, pp.845–856, 2003.

[124] MODELS STB1104-1116 SERVOTUBE COMPONENT, *User Manual*, Copley Motion Systems LLC.

[125] Suresh, S., Narasimhan, S., and Nagarajaiah, S., Direct adaptive neural controller for the active control of nonlinear base-isolated buildings, *Structural Control and Health Monitoring*, Vol.19, Issue No.3, pp.370–384, 2011.

[126] Symans, M. D., & Constantinou, M. C., Semi-active control of earthquake induced vibration,*World conference on earthquake engineering*, 1996.

[127] Tang, Y., Active control of SDF systems using artificial neural networks, *Computers and Structures*, Vol.60, Issue No.5, pp.695–703, 1996.

[128] Taskin, A. and Kumbasar, T., An Open Source Matlab/Simulink Toolbox for Interval Type-2 Fuzzy Logic Systems, *IEEE Symposium Series on Computational Intelligence*, 2015.

[129] Thenozhi, S., and Yu. W., Advances in Modeling and Vibration control of building structures, *Annual Reviews in Control,* Vol. 37, Issue No. 2, pp.346-364, 2013.

[130] Thenozhi, S., and Yu. W., Stability analysis of active vibration control of building structures using PD/PID control, *Engineering Structures,* Vol. 81, Issue No. 7, pp.208-218, 2014.

[131] Tso W.K., and Zhu, T. J., Design of torsionally unbalanced structural systems based on code provisions I: ductility demands, *Earthquake Engineering & Structural Dynamics*, Vol.21, Issue No.7, 1992.

[132] Utkin, V. I., *Sliding modes in control and optimization*, Springer-Verlag, Berlin, 1992.

[133] Ignacio J. Vial,Juan C. de la Llera, Jose L. Almazan and Víctor Ceballos, Torsional balance of plan-asymmetric structures with frictional dampers: Experimental results, *Earthquake Engineering & Structural Dynamics,* Volume 35, Issue 15, pages 1875–1898, December 2006.

[134] L. X.Wang, *Adaptive Fuzzy Systems and Control*, Upper Saddle River, NJ: Prentice-Hall, 1994.

[135] Wu, B. ,Ou, J. P.,Soong, T. T. , Optimal placement of energy dissipation devices for three-dimensional structures, *Engineering Structures*, Vol.19, Issue No. 2, pp.113–125, 1997.

[136] Wu, W. H.,Wang, J. F.,and Lin, C. C., Systematic assessment of irregular building–soil interaction using efficient modal analysis, *Earthquake Engineering & Structural Dynamics*, Vol.30, Issue No. 4, pp.573–594, 2001.

[137] Wu, D., On the Fundamental Differences between Type-1 and Interval Type-2 Fuzzy Logic Controllers. *IEEE Trans. Fuzzy Syst.*, Vol. 10, Issue No. 5, pp. 832- 848, 2012.

[138] Wu, D., and Mendel, J.M.: Enhanced Karnik-Mendel algorithms, *IEEE Trans. Fuzzy Syst.* Vol. 17, Issue No. 4, pp. 923–934, 2009.

[139] Wu, D., Twelve considerations in choosing between Gaussian and trapezoidal membership functions in interval type-2 fuzzy logic controllers, *IEEE International Conference on Fuzzy Systems*, Brisbane, QLD, pp. 1-8, 2012.

[140] Wu, D., and Nie, M., Comparison and practical implementation of type reduction algorithms for type-2 fuzzy sets and systems, *IEEE Int. Conf. Fuzzy Systems*, Taipei, Taiwan, 2011.

[141] Wu, D., Approaches for reducing the computational cost of interval type-2 fuzzy logic systems: Overview and comparisons, *IEEE Trans.Fuzzy Syst.*, Vol. 21, No. 1, pp. 80–99, 2013.

[142] XL403A Acceleroemeter, *User Manual*, Measurement Specialities, 2013.

[143] Xu. K., and Igusa, T., Dynamic characteristics of multiple substructures with closely spaced frequencies, *Earthquake Engineering and Structural Dynamics*, Vol. 21, Issue No.12, pp.1059–1070, 1992.

[144] Yang, J., Li, J. B., and Lin, G., A simple approach to integration of acceleration data for dynamic soil–structure interaction analysis, *Soil Dynamics and Earthquake Engineering*, Vol.26, Issue No.8, pp.725–734, 2006.

[145] Yanik, A. , Pinelli, J. P., Gutierrez, H., Control of a three-dimensional structure with magneto-rheological dampers, *11th International Conference on Vibration Problems*, Z. Dimitrovová et al. (eds.),Lisbon, Portugal, 2013.

[146] Yao, J. T. P., Concept of Structural Control, *Journal of the Structural Division*, Vol.98, Issue No.7, pp.1567-1574, 1972.

[147] Yi. F., and Dyke, S. J., Structural control systems: Performance assessment, *American Control Conference*, Vol.1, Issue No.6, pp.14-18, 2000.

[148] Yi, F., Dyke, S. J., Caicedo, J. M., and Carlson, J. D., Experimental Verification of Multi-Input Seismic Control Strategies for Smart Dampers, *Journal of Engineering Mechanics*, Vol.127, Issue No.11, pp.1152–1164, 2001.

[149] Yoshida, O., Dyke, S. J., Giacosa, L. M. and Truman, K. Z., Experimental Verification on Torsional Response Control of Asymmetric Buildings Using MR Dampers, *Earthquake Engineering and Structural Dynamics*, Vol.32, Issue No.13, pp.2085–2105, 2003.

[150] Yoshida, O. and Dyke, S. J., Response Control of Full-Scale Irregular Buildings Using Magnetorheological Dampers, *Journal of Structural Engineering*, Vol.131, Issue No.5, pp.734–742, 2005.

[151] Zadeh, L. A., Fuzzy sets, *Information and Control*, Vol.8, Issue No.3, pp.338–353, 1965.

[152] Zemp, R., Llera, J. C. and Almazán, J. L., Tall building vibration control using a TM-MR damper assembly, *Earthquake Engineering and Structural Dynamics*, 2011, Vol.40, Issue No.3, pp.339–354, 2011.

[153] Zhang, J., and Roschke, P. N., Active control of a tall structure excited by wind, *Journal of Wind Engineering and Industrial Aerodynamics*, Vol.83, Issue No.1-3, pp. 209–223, 1999.

[154] Zhang, J. , Zeng, K. , Jiang, J., An optimal design of bi-directional TMD for three dimensional structure*, Computational Structural Engineering* , pp.935-941, 2009.

[155] Zhao, B. and Gao, H., Torsional vibration control of high-rise building with large local space by using tuned mass damper, *Advanced Materials Research*, Vols.446-449, pp.3066-3071, 2012.